AN ELECTROLYTIC METHOD TO FORM ZIRCONIUM HYDRIDE PHASES IN ZIRCONIUM ALLOYS WITH MORPHOLOGIES SIMILAR TO HYDRIDES FORMED IN USED NUCLEAR FUEL

A Thesis

by

SAMUEL HOUSTON KUHR

Submitted to the Office of Graduate Studies of
Texas A&M University
in partial fulfillment of the requirements for the degree of

MASTER OF SCIENCE

August 2012

Major Subject: Nuclear Engineering

An Electrolytic Method to Form Zirconium Hydride Phases in Zirconium Alloys with Morphologies Similar to Hydrides Formed in Used Nuclear Fuel

AN ELECTROLYTIC METHOD TO FORM ZIRCONIUM HYDRIDE PHASES IN ZIRCONIUM ALLOYS WITH MORPHOLOGIES SIMILAR TO HYDRIDES FORMED IN USED NUCLEAR FUEL

A Thesis

by

SAMUEL HOUSON KUHR

Submitted to the Office of Graduate Studies of
Texas A&M University
in partial fulfillment of the requirements for the degree of

MASTER OF SCIENCE

Approved by:

Chair of Committee,	Sean M. McDeavitt
Committee Members,	Lin Shao
	Pavel V. Tsvetkov
Head of Department,	Yassin A. Hassan

August 2012

Major Subject: Nuclear Engineering

ABSTRACT

An Electrolytic Method to Form Zirconium Hydride Phases in Zirconium Alloys with Morphologies Similar to Hydrides Formed in Used Nuclear Fuel. (August 2012)

Samuel Houston Kuhr, B. B. A., Texas A&M University

Chair of Advisory Committee: Dr. Sean M. McDeavitt

An electrolytic cell was designed, built, and tested with several proof-of-concept experiments in which Zircaloy material was charged with hydrogen in order to generate zirconium hydride formations. The Electrolytic Charging with Hydrogen and a Thermal Gradient (ECH-TG) system has the ability to generate static 20°C to 120°C temperatures for a H_2SO_4 and H_2O bath for isothermal experiment conditions. This system was designed to accommodate a molten salt bath in future experiments to achieve higher isothermal temperatures. Additionally, the design accommodates a cartridge heater which, when placed on the inside of the sample tube, can be set at temperatures up to 350 °C and create a thermal gradient across the sample. Finally, a custom LABVIEW VI, L2.vi, was developed to control components and record data during experimentation. This program, along with web cameras and the commercial StirPC software package, enabled remote operation for extended periods of time with only minor maintenance during an experiment. While proving the concept for this design, 19 experiments where performed, which form the basis for a future parametric study.

Initial results indicate formations of zirconium hydrides which formed rim structures between 8.690 +/- 0.982 μm to 12.365 +/- 0.635 μm thick.

These electrolytically produced rims were compared with hydrides formed under a previous vapor diffusion experiment via Scanning Electron Microscope (SEM) imaging and Energy Dispersive X-ray Spectroscopy (EDS) analysis. While the existing vapor diffusion method formed gradients of zirconium hydride, it failed to produce the gradient in the correct direction and also failed to create a hydride rim. The successful use of the ECH-TG system to create said rim, and some of the methods used to direct that rim to the OD of the tube can be used for future work with the vapor diffusion method in order to create zirconium hydrides of the correct geometry.

The procedures and apparatus created for this project represent a reliable method for creating zirconium hydride rim structures.

DEDICATION

To my wife and my children

ACKNOWLEDGEMENTS

I would like to thank my committee chair, Dr. McDeavitt, and my committee members, Dr. Shao and Dr. Tsvetkov, for their guidance and support throughout the course of this research.

Thanks also to my friends and colleagues and the department faculty and staff for making my time at Texas A&M University a great experience. Kyle Cummins helped form the original idea for the apparatus and launched me into the world of electrochemistry. William Sames, Ryan Brito, Nick Meli, and Nick Brennan provided helpful advice and assistance with the experiments and analysis. Luke Kuhr put many hours into making the system remotely controllable and building the LABVIEW VI program L2.vi, thus allowing safe experimentation overnight. Adam Parkinson, Grant Helmreich, Brian Barnhart, Chad Garcia, and Marie Arrieta all provided thoughtful suggestions and useful information when challenges arose. With all of your help, you all really made this possible in such a short time frame. I am very grateful for your generosity.

I also want to extend my gratitude to the Department of Energy, which provided funding for this project.

Finally, thanks to my mother and father for their encouragement and their foresight to pay for my undergraduate degree. You both gave me a great opportunity many kids don’t have, and I appreciate your sacrifices to give me that education. Most importantly, thanks to my children for their unceasing wonder at the world around us, and to my beautiful wife for her patience, love, and self-less support.

NOMENCLATURE

BCC Body Centered Cubic

DHC Delayed Hydride Cracking

EDS Energy Dispersive X-ray Spectroscopy

HCP Hexagonal Close-Packed

HTC High Temperature Cathodic Charging

SCFH Standard Cubic Feet per Hour

SEM Scanning Electron Microscope

VAC Volts Alternating Current

XRD X-Ray Diffraction

TABLE OF CONTENTS

Page

Page

LIST OF FIGURES

Page

LIST OF TABLES

Page

CHAPTER I

INTRODUCTION

With an ever increasing need for energy, the United States and the nations of the world are making major public and private investments in energy production. In order for nuclear power to remain a viable option, the sound long-term management of used nuclear fuel must be established. Nuclear facilities produce safe, clean, and reliable power. The used fuel assemblies must either be recycled or stored for an extended period due to their latent energy, radiotoxicity, and complex properties. Recycling and permanent disposal options are currently under development and are the subject of social and political debate. On the other hand, short term extended storage solutions are already in place at 55 sites [1] in the US. The integrity of used fuel during storage is very important. There are many synergistic phenomena active during storage that impact the integrity used fuel storage systems. These range from degradation mechanisms that challenge the external canister to internal mechanisms that may enable fuel rupture and internal contamination release. The work reported here is part of a larger research effort funded by the U.S. Department of Energy's Nuclear Energy University Programs designed to study and model prominent degradation mechanisms relevant to used fuel storage. More specifically, this work contributes to the program effort to understand the phenomenon known as Delayed Hydride Cracking (DHC) through the establishment of a

_____

This thesis follows the style of Journal of Nuclear Materials.

lab-scale system to electrochemically insert hydrogen into Zircaloy tubes with a representative morphology to enable future surrogate separate effects testing on the hydride feature.

The objective of this research was to develop the equipment and procedures to hydride (e.g., form hydrogen compounds such as ZrH_2 within a solid metal) Zircaloy-4 tubing in a manner that generates nearly representative microstructures similar to the hydride phases present in used nuclear fuel cladding. Hydrides form in zirconium-based cladding alloys during in-reactor service. The formation mechanism is as a consequence of the oxidation of zirconium in water. The reaction, $2H_2O + Zr \rightarrow ZrO_2 + 4H$, results in the release of hydrogen at the surface of the cladding.[2] Previous researchers observed that between 5% and 20% of this hydrogen is absorbed into the cladding.[3] The entrance of hydrogen into the alloy matrix induces localized concentrations of zirconium hydride platelets which form oriented circumferentially around the Zircaloy-4 tubing. These platelets are then thought to contribute to crack propagation and accelerate the crack growth as illustrated in Fig. 1.

After service in a reactor and an intermediate storage period in a spent fuel pool, used fuel is moved into a dry canister for extended storage. At this time, the expected duration for extended storage is undefined since the final destination for the used fuel is still being deliberated as a national and multi-national issue. However, over an extended storage period between, 30 to 300 years, it has been theorized with some evidence [4][5] that the internal hydride phases will redistribute in situ in response to the thermal, stress, and radiation influences in environment. This redistribution has the potential to

challenge the integrity of the used fuel as the hydride phases are brittle and prone to cracking and the re-orientation places the phases in a maximum state of stress.[6]

Hydride formations in Zircaloy-4 cladding will orient circumferentially while in the reactor core. Previous research showed that tensile stresses applied to these rods will cause the hydrides to re-orient radially. [2] This was an undesirable orientation because, if the hydride platelets unify and forms a break in the Zircaloy-4 cladding, it leads to an increased possibility of major cladding failure. Such a break, while in service, would release uranium fuel and fission products into the reactor core and the reactor would need to be shut down in order to replace the broken rod. The formation of hydrides was, and still is, actually one of the primary restraints on nuclear fuel lifetime in a reactor. [4]

Current practices keep the fuel in the reactor for up to 6 years [3], but after this time, the fuel must be removed and stored. Nuclear facilities are currently licensed to store radioactive waste for up to 100 years, however the original designs of nuclear facilities only expected to keep fuel on site for 20-30 years before sending it to a permanent disposal site.[3] The Department of Energy was working on such a site at Yucca Mountain for the past 25+ years, however recent administrative changes under President Obama, have shut down the Yucca Mountain project.[7] With the closure of this project, nuclear reactor sites have no place to offload their spent fuel. The Department of Energy is now working with researchers to identify long term storage options such as dry cask storage.[7] As of Dec 2010, 44 sites in the United States used dry cask storage to store more than 13,500 metric tons of used nuclear fuel.[8]

In dry cask storage used nuclear fuel, which has been stored for at least 5 years in a spent fuel pool, is moved out of the pool into a cask which is stored on the nuclear facility premise. These casks are generally made of a metallic inner compartment and surrounded by a concrete outer shell. They are placed on thick concrete pads and all the water is drained from the casks leaving natural air convection to cool the used fuel assemblies. Temperatures inside the casks can reach up to 400°C (752°F) under normal operating conditions.[8] These high temperatures are ideal for Hydrogen diffusion through Zircaloy-4 cladding and can result in hydride restructuring.[4][9] Currently the NRC considers the Dry Storage Cask, Fig. 5 and 6, as the primary containment for the nuclear fuel.[10] However, the shift to large scale, "long term storage" necessitates a consideration of the fuel assembly inside of the cask. Of primary concern is the structural integrity and mechanical strength of the Zircaloy-4 fuel cladding. When a permanent storage facility/option is made available, will the fuel assemblies be able to maintain their structure while being transported, re-positioned, and handled by crews moving them from their current location?

Delayed Hydride cracking, creep, and stress corrosion cracking all contribute to deterioration of the Zircaloy-4 cladding.[8] The primary concern in this regard centers around the amount of hydrogen which is still in the fuel cladding and the orientation of those hydrides which will play a critical role in crack propagation in the Zircaloy-4 tubes.[11] In an effort to understand the hydride formations and quantify the probability of crack formations, it is important to study the hydrides formed in used fuel rods, Fig 1. Used fuel rods however are radioactive, "Hot," and can only be accessed with proper

authorization and extremely high-tech and costly equipment and man-power. In an effort to conduct wide scale testing, researchers will take stock Zircaloy-4 and hydride the tubing to form similar geometries and densities of hydrides to those of used nuclear reactor fuel cladding.

Recreating this hydride geometry in a laboratory setting has been attempted with vapor diffusion, electrolytic processes, and auto-claving techniques to varying degrees of success.[9][12][13][14][15] After analyzing the different models, it was determined that an electrolytic process would be developed and compared to the vapor diffusion method.[9] These preliminary results indicate that the electrolytic process is capable of creating a 8.690 +/- 0.982 μm to 12.365 +/- 0.635 μm rim of dense zirconium hydrides around the OD of a Zircaloy sample with as little as 3 hours of charging at 0.5 A/cm^2. When combined with the gradients found in the samples hydride with the vapor diffusion method, it is plausible that a hydride formation, similar to that of used nuclear fuel, could be created in virgin samples of Zricaloy.

The following Chapters present on overview of the relevant literature for DHC and hydride formation methods (Ch. 2), describe the evolution of the electrochemical system designed and established for this work (Ch.3), present the demonstration experimental results (Ch.4), and discuss the meaning of the results and discuss needs for continued development (Ch. 5).

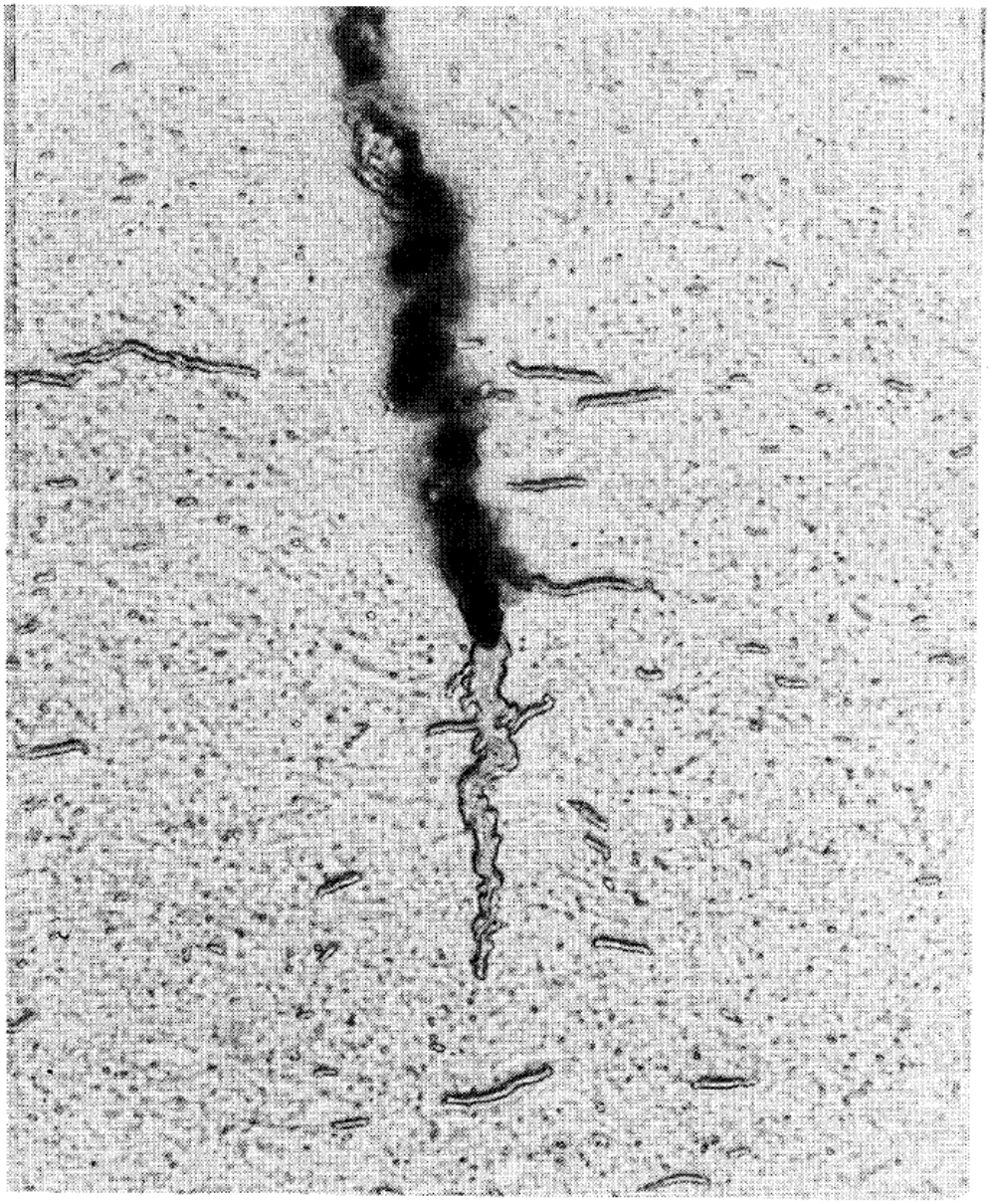

Figure 1 Hydride formation at a crack tip in Zr-2.5 Nb due to the local buildup of stresses (photo from D. Rogers, AECL/Chalk River) [2]

CHAPTER II

BACKGROUND

This chapter provides an overview of the cladding materials and nuclear fuels (Section 2.1), the basic science behind hydride formations and delayed hydride cracking (Section 2.2), and methods that have been used to directly charge zirconium alloys with hydrogen (Section 2.3).

2.1 Zirconium Cladding Alloys and Nuclear Fuel

Fuel assemblies must be able to stand up to the harsh environment of a nuclear reactor. Temperatures ranging from 200°C to 400°C, radiation damage, fluid corrosion, and oxidation effects are found inside of the core of a nuclear reactor. Zirconium metal offers several important characteristics which make it a favorable material for use in fuel cladding design including a small neutron absorption cross-section, relatively high mechanical strength, and a tendency to create a self-sealing oxide layer when exposed to water.

When reactors were first designed, stainless steels served as the primary structural material. Soon however, early uses showed that long term exposure to radiation would cause these materials to swell dramatically. When it was discovered that Zircaloy's mechanical strength could compare with that of SS, Table 1, other properties advantages were also discovered. Zircaloy's transparency to neutrons, illustrated in Table 2, is a huge advantage in core design. This transparency keeps the absorption low and gives fast neutrons a window to cross into the moderator, become thermal, and cross

back into the fuel, thus improving the k_{eff} of the core design in thermal reactors. Finally, the oxidation at the surface of the Zircaloy cladding forms a thin layer of oxides which actually prevents further corrosion from oxidation. This self-sealing characteristic of Zircaloy effectively replicates the corrosion resistance sought in stainless steels. These characteristics of Zirconium lead the industry to develop a variety of Zirconium based alloys which are used in nuclear reactors.

Table 1 Mechanical Properties of Zirconium based alloys as compared to stainless steel. [16]

Material	Condition	Direction of test / Temperature	Tensile Strength (MPa)	Yield Strength (MPa)
SS 304	annealed	-----	515	205
SS 304L	annealed	-----	480	170
Zirconium	annealed	Longitudinal / Room	296	138
		Transverse / Room	296	207
Zircaloy-2	annealed	Longitudinal / Room	400	241
		Transverse / Room	386	303
Zircaloy-4	annealed	Longitudinal / Room	400	241
		Transverse / Room	386	303
Zr-2.5Nb	annealed	Longitudinal / Room	448	310
		Transverse / Room	448	344

Table 2 Thermal Neutron Cross sections [barns] for various reactor materials from ATI Wah Chang [17]

Material	Neutron Absorption Cross-section [barns]
Magnesium	0.059
Lead	0.17
Zirconium	0.18
Zircaloy-4	0.22
Aluminum	0.23
Iron	2.56
Austenitic Stainless Steel	3.1
Nickel	4.5
Titanium	6.1
Hafnium	104
Boron	750
Cadmium	2,520
Gadolinium	48,890

2.1.1 Zirconium and Zirconium Cladding Alloys

Zirconium is most commonly used in an α phase HCP structure. The low temperature αZr matrix has a = 0.323 nm and c = 0.515 nm with a c/a ratio of 1.593. When heated to ~865°C the matrix undergoes an allotropic transformation to the β phase BCC matrix before finally melting at 1860 °C. [18] Zircaloy-4 is a cladding material made primarily of Zirconium and doped with elements of Chromium, Tin, Iron, and Oxygen. Several other Ziconium based alloys exist including Zircaloy-2, Zr-2.5Nb, Zirlo, and M5, the makeup of which is illustrated in Table 3. The focus on Zircaloy-4 in this study was primarily due to the vast quantities of Zircaloy-4 clad used nuclear fuel currently in storage.

Table 3 This table shows the comparison between Zircaloy-4, Zircaloy-2, and Zr-2.5Nb which represent several reactor cladding materials. [17]

Name	Zircaloy-2	Zircaloy-4	Zr-2.5Nb
UNS Grade	R60802	R60804	R60904
Tin	1.20-1.70	1.20-1.70	---
Iron	0.07-0.20	0.18-0.24	---
Chromium	0.05-0.15	0.07-0.13	---
Nickel	0.03-0.08	---	---
Niobium	---	---	2.40-2.80
Oxygen	Per P.O.	Per P.O.	Per P.O.
Iron + Chromium + Nickel	0.18-0.38	---	---
Iron + Chromium	---	0.28-0.37	---

The Zircaloy-4 material is cold worked to form tubes and undergoes a number of extrusions. The full process is discussed by Motta.[2] When formed, the Zircaloy-4 crystals orient in a circumferential direction due to the processing techniques, (Fig. 2). This orientation affects the initial location and geometry of hydrides which are seen to form on the longitudinal direction in the tetrahedral positions.[9] A Zircaloy-4 tube is approximately 3.65 meters (144 inches) long and 1.27 cm (0.5 inches) in diameter. These tubes are arranged into assemblies of 14x14 15x15 or 16x16 fuel pins.[7] This assembly is then loaded into the reactor and the nuclear reaction can begin. Various assembly types are illustrated in Fig. 3.

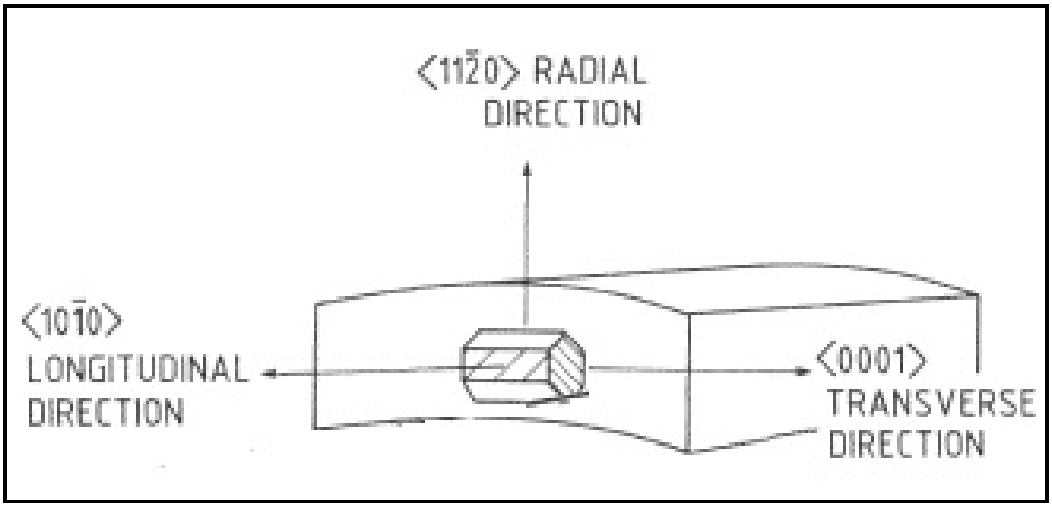

Figure 2 The orientation of Zircaloy-4 crystals is similar to that of this illustration.[2]

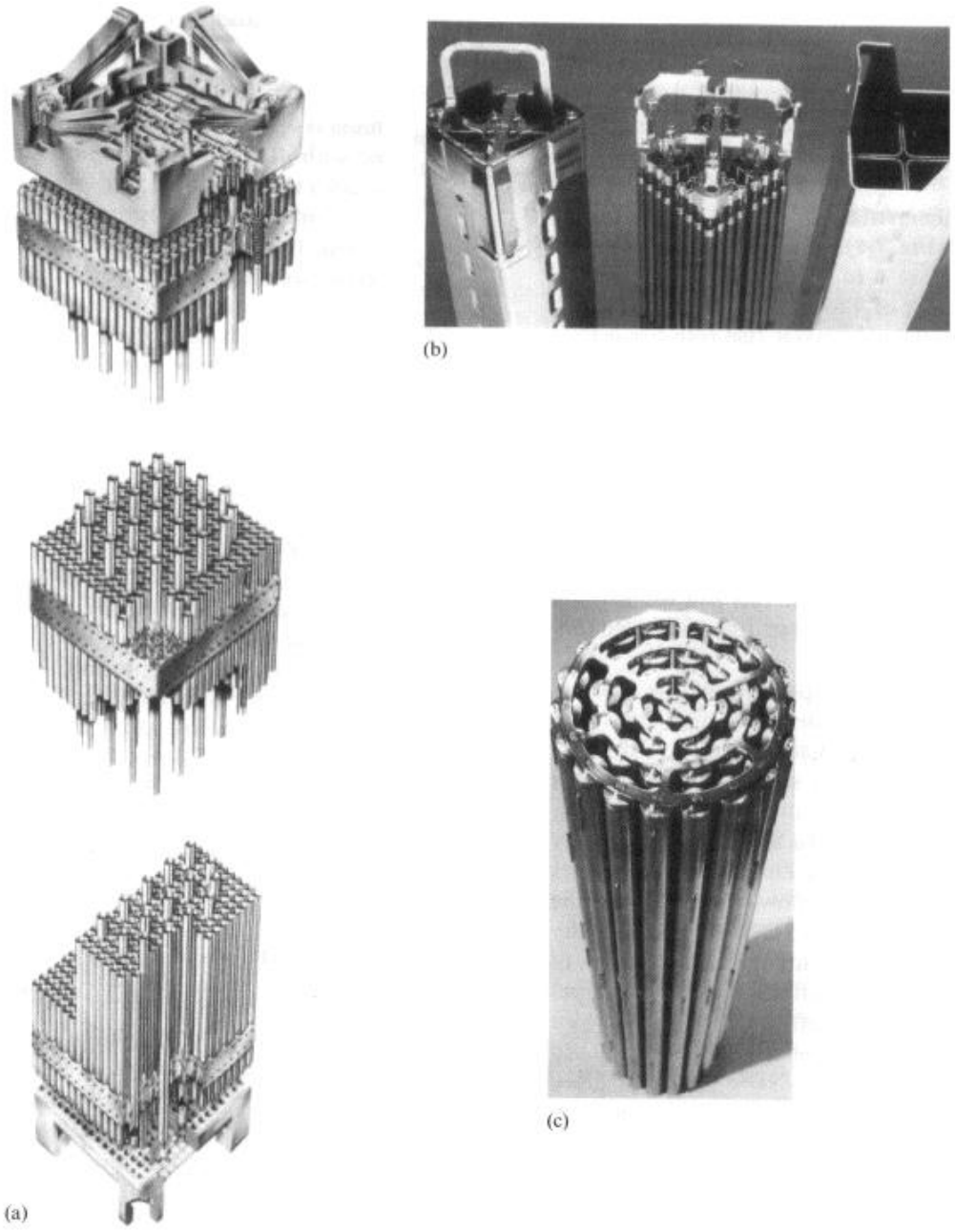

Figure 3 "Fuel cladding and other components made of Zr alloys, used in different reactor types: (a) PWR fuel assembly (courtesy FRAGEMA), (b) BWR fuel assembly and channel (courtesy GEc), (c) CANDU fuel assembly and surrounding pressure tube." [2]

2.1.2 Nuclear Fuel Designs

This work is concerned with the nuclear fuel designs which characterize the vast majority of nuclear fuel today. These designs involve a cladding tube, made of Zircaloy material, which contains pellets of Uranium based nuclear fuel. These tubes are used in nuclear reactors to maintain the fuel in a static orientation and serve not only as a mechanical support, but also as a first line barrier to the escape of fission products and used fuel debris. An illustration of the general concept is shown in Fig. 4 below.

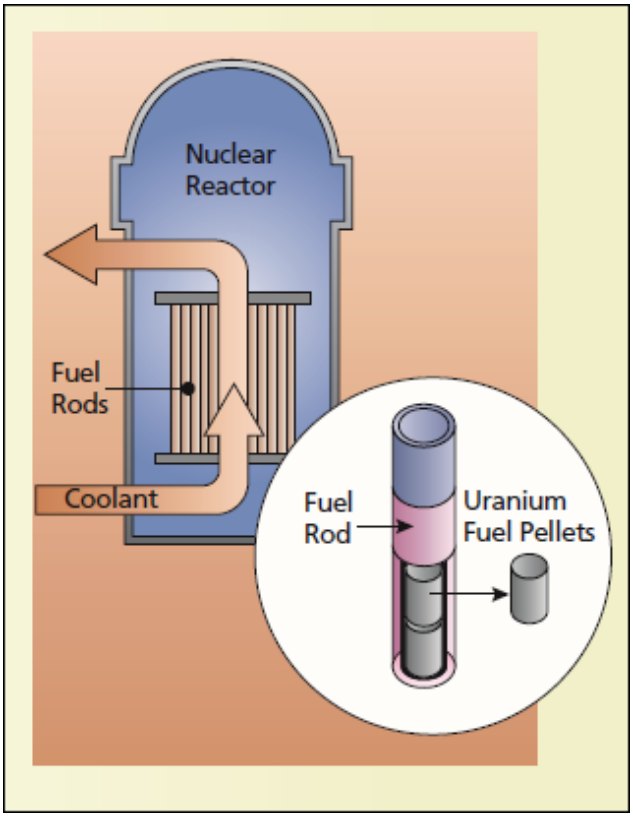

Figure 4 Illustration of fuel cladding (made of Zircaloy-4) in relationship to uranium fuel and overall reactor system. [10]

2.1.3 Used Nuclear Fuel (UNF)

After 5-6 years in a nuclear reactor, the fuel is removed and is generally termed, "Used Nuclear Fuel," or UNF for short.[7] UNF is characterized by a high radioactivity level and significant heat output even after use in the core and it is this material which the Department of Energy is working to safely find permanent disposal solutions.

Used nuclear fuel is currently maintained on site at the 104 reactors around the country as well as at various government labs and facilities. The NRC reports that 65,000 metric tons of UNF are currently stored in spent fuel pools and in dry cask storage.[10] Today, the USA faces a large challenge in handling this radioactive waste. The recent Blue Ribbon Commission on America's Nuclear Future has put forward a number of ideas on how to handle UNF.[7] The default method at the moment will be using dry cask storage to offload fuel from the spent fuel pools to concrete pads on site, as illustrated in Fig. 5 and Fig. 6. These casks are licensed by the NRC for up to 100 years which in many cases will extend beyond the lifetime of the facilities which are usually licensed for 40 to 60 years.[10] Eventually the UNF will need to be consolidated and stored or reprocessed. Both options will require accessing the fuel assemblies inside of the casks.

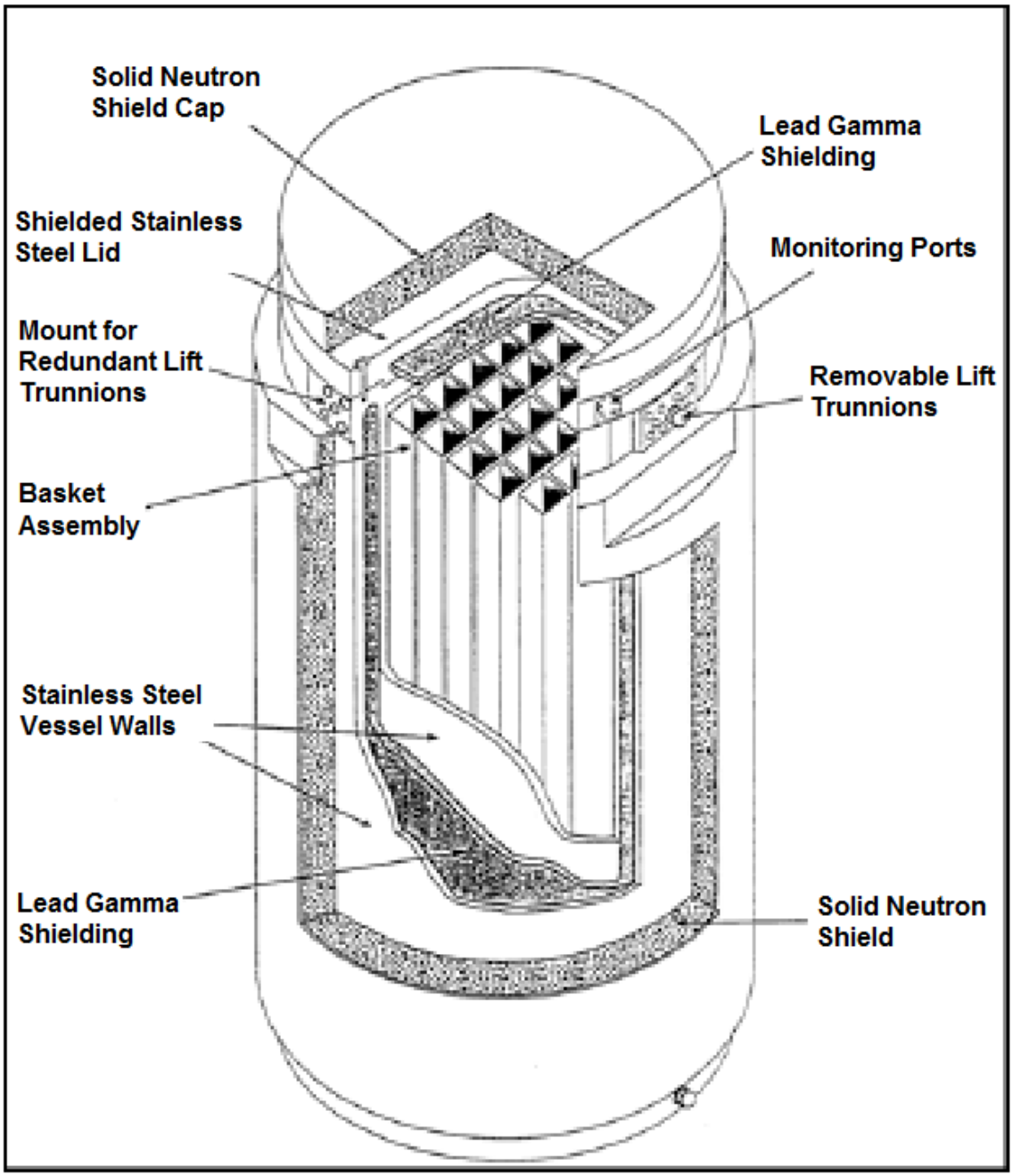

Figure 5 NAC S/T Metal Storage Cask [19]

Figure 6 NAC MPC Dual-Purpose Canister System, CoC #72-1025, Connecticut Yankee ISFSI7 [Hoedeman 2008] [19]

2.2 Hydride Formation and DHC during Dry Storage

2.2.1 Hydride Formation in Cladding during Reactor Operation

While running, the reactor splits Uranium atoms to release energy. This energy evolves primarily as heat and is used to heat water which boils to create steam which turns a turbine and creates electricity. While in the system, Zirconium and water react to release hydrogen via the $2H_2O + Zr \rightarrow ZrO_2 + 4H$.[2] This hydrogen penetrates into the fuel cladding and moves towards the center of the fuel due to diffusion. As the material becomes saturated with hydrogen, hydrogen seeks lattice positions in the

zirconium tetrahedral positions and forms zirconium hydrides. During reactor operation, it is possible for hydrides to contribute to cracking and failure of fuel rods. Operators and fuel manufacturers plan maintenance and refuel operations to reduce the risk of in-core failure.

There are currently two major theories about the actual mechanism driving hydride diffusion.[5] These theories will not be discussed here as this work focused primarily on creating an electrolytic system to develop hydrides. However, use of this system may help inform the previously mentioned theories.

2.2.2 Delayed Hydride Cracking (DHC)

One heavily studied area regarding UNF is the structural stability of the Zircaloy-4 in regards to Delayed Hydride Cracking, DHC, and irradiation damage to the structure. DHC occurs when hydrogen lodges into the Zircaloy-4 material and concentrates into localized areas. This concentration weakens the atomic bonds between metallic atoms and cracks can form in the alloy. These cracks, if oriented radially, lead to fractures in the cladding and possible release of uranium and fission products. Modern reactors are limited by the material properties of the fuel and the cladding. While research has been conducted on understanding DHC at high temperature in a running reactor, little work has been done to understand DHC over the long-term storage of UNF.[4] In fact, several prominent researchers are of the opinion that DHC does not play a factor in long-term

scenarios and should be ignored, while other researchers believe that DHC could pose a potential danger to long-term storage.

When the casks are opened, the transportation issue will be the structural stability of the assemblies themselves. When a crane is attached to the Zircaloy-4 cladding, will the assembly support the tensile and compressive stresses placed on it? The unknown is that these stresses, combined with increased hydride population and delayed hydride cracking will cause the assemblies to break apart while trying to remove them from the casks or during transportation to a new site. Hydride formation and Delayed hydride cracking, DHC, have been studied extensively over the past few decades. [20] However, there have been very few studies to look at the long term (100 year+) affects to the Zricaloy-4 cladding due to hydride buildup and DHC.[8] In order to fill in this missing gap of knowledge, it will be very important to recreate the hydride formations in a laboratory setting which most accurately simulate the formations and morphology of hydrides in UNF.

2.3 Methods for Charging Zirconium Alloys with Hydrogen

From the beginning of hydride analysis, researchers have sought different methods to charge materials with hydrogen. Due to its incredibly small atomic size , hydrogen has a propensity to move quickly and easily through crystal structures. It can lodge easily into the tetrahedral, octahedral, and interstitial sites of most metallic alloys.[9] From the early tests of Attermo[12] with cathodic charging in salt baths, to the

modern methods of vapor diffusion, there have been many permutations of electrolyticly charging[13][14] and vaporously diffusing[9][15] hydrogen into target materials. The challenge is creating morphologies, densities, and geometries of hydrides which mimic those found in the real world application.

2.3.1 Electrolytic Method

Electrolytic methods involving sulfuric acid baths or molten salt baths are used to coat the outside of the sample with hydride. These samples are then place in a furnace for 1 to 4 hours at temperatures ranging from 300 °C to 400 °C. This method also creates homogenous dispersed hydride formations in the material. [12][13][14]

The primary design for this experiment was developed from the design of the apparatus John et. al. created[13], The High Temperature Cathodic Charging (HTC), as depicted in Fig. 7. Initially, the intention was to produce a molten salt bath and to charge the Zircaloy-4 samples around 260 °C. John et. al. had also attempted charging with H_2SO_4 and one particular figure from their research stood out. The ability to create a dense layer of hydride could be accomplished with both the molten salt and with the H_2SO_4 electrolytic system according to Fig. 8. The major difference was how far that hydride layer penetrated into the sample. For the molten salt, at a higher temperature of 260 °C, the penetration was four to five times the depth as the H_2SO_4 charging at 100 °C. For all other components being equal, temperature was the only real difference driving the depth to which hydrogen would distribute into the sample

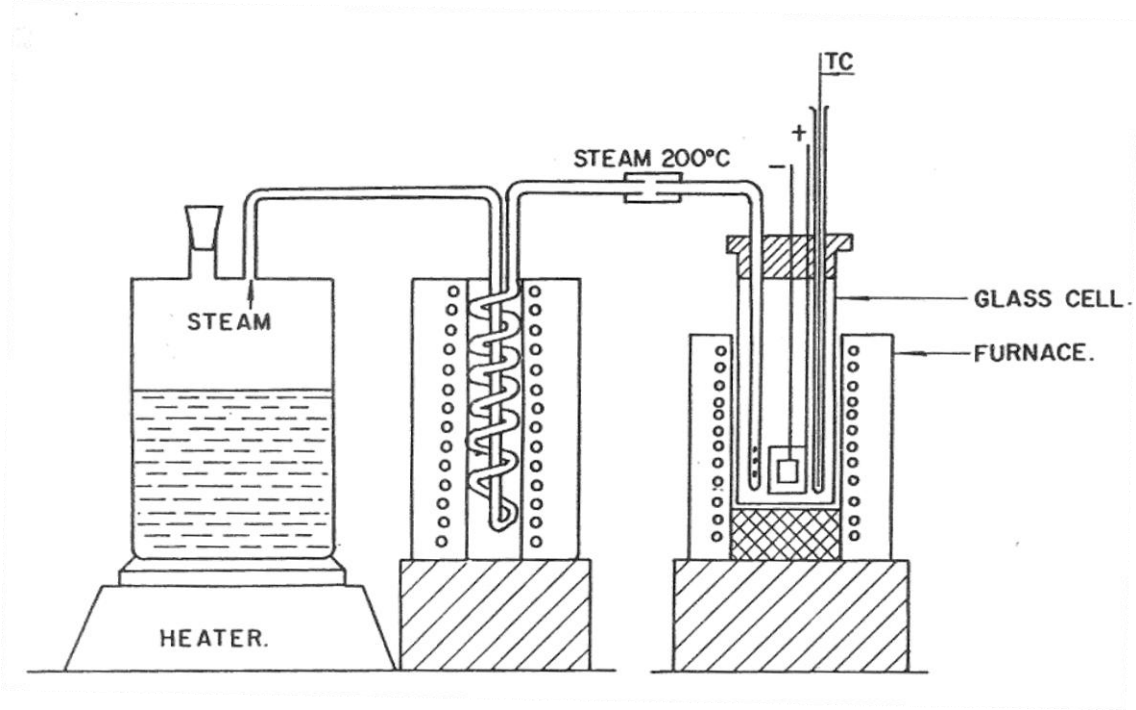

Figure 7 High temperature cathodic charging (HTC) set up design from John et. al. [13]

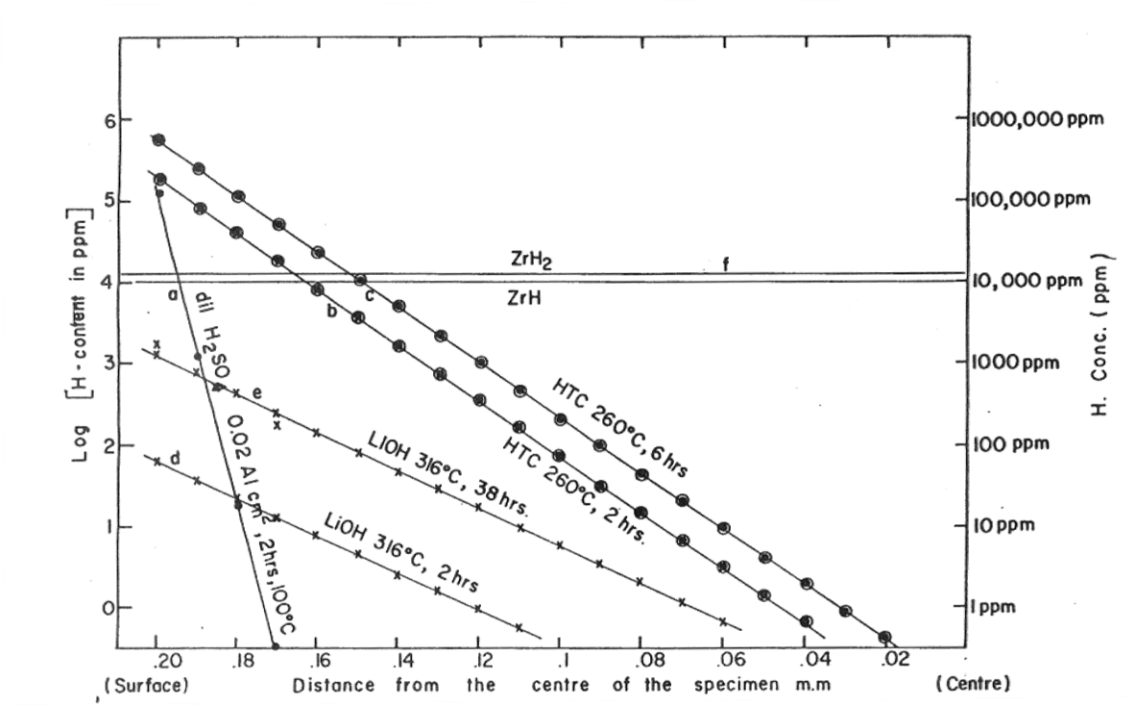

Figure 8 Hydrogen distribution in conventional charging high temperature cathodic charging (HTC) and high temperature autoclaving in LiOH as predicted by theory [13] including charging in H_2SO_4.

A second observation was noted when looking at the thermal profile across a fuel pin of an operating reactor. All experimental results to date had relied on a steady state temperature and diffusion was based on that constant temperature. However, as illustrated in Fig. 9, there exists a temperature gradient between the inner diameter (ID) and the outer diameter (OD) of the Zircaloy-4 cladding in operating reactors. If this ~50 °C delta between the ID of the Zircaloy-4 cladding and the OD of the cladding could be reproduced in the laboratory, then it was hypothesized that an electrolytic system would produce zirconium hydrides in a similar geometry as those found in real cladding.

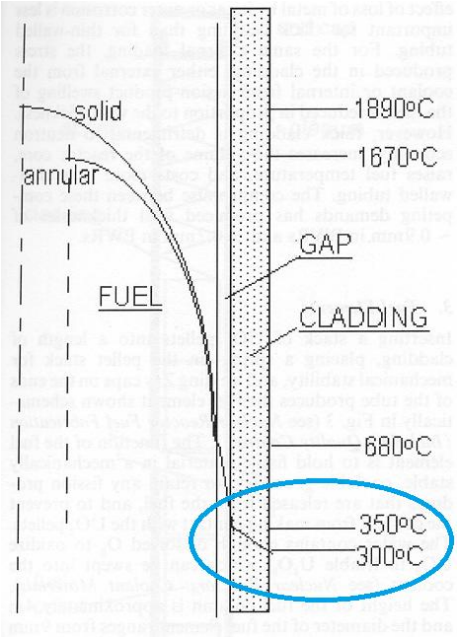

Figure 9 Radial temperature distributions in solid and annular fuel pellets. Linear power: 350 W cm-1; gap thickness: 50 μm; fuel diameter 10 mm; control hole diameter in annular pellet: 2mm; gap gas: 20% xenon; 80% helium. [6]

The High Temperature Cathodic Charging (HTC) design by John et. al. [13] served as the basis for the Electolytic Charging with Hydrogen Operation and a Thermal Gradient (ECH-TG) design for this experiment.

2.3.2 Vapor Diffusion Methods

Vapor diffusion techniques generally involve placing a sample inside of a furnace and flowing a mixture of Hydrogen and Argon around the sample. It has been noted that oxygen and nitrogen have a detrimental effect on hydrogen pickup.

Eliminating these elements often requires a high-vaccum environment and getters, material which captures oxygen or nitrogen before it reaches the sample. [9] The furnace is run between 300°C and 500°C for a variety of times. The results from this type of charging generally create homogenously dispersed hydride formations. With the use of caps on tubes however, some gradient formations can be developed. These formations tend to be extremely thick on one side and very light on the other, failing to give a true smooth gradient of hydrides. Figure 10 shows various morphologies from gas charging methods [6].

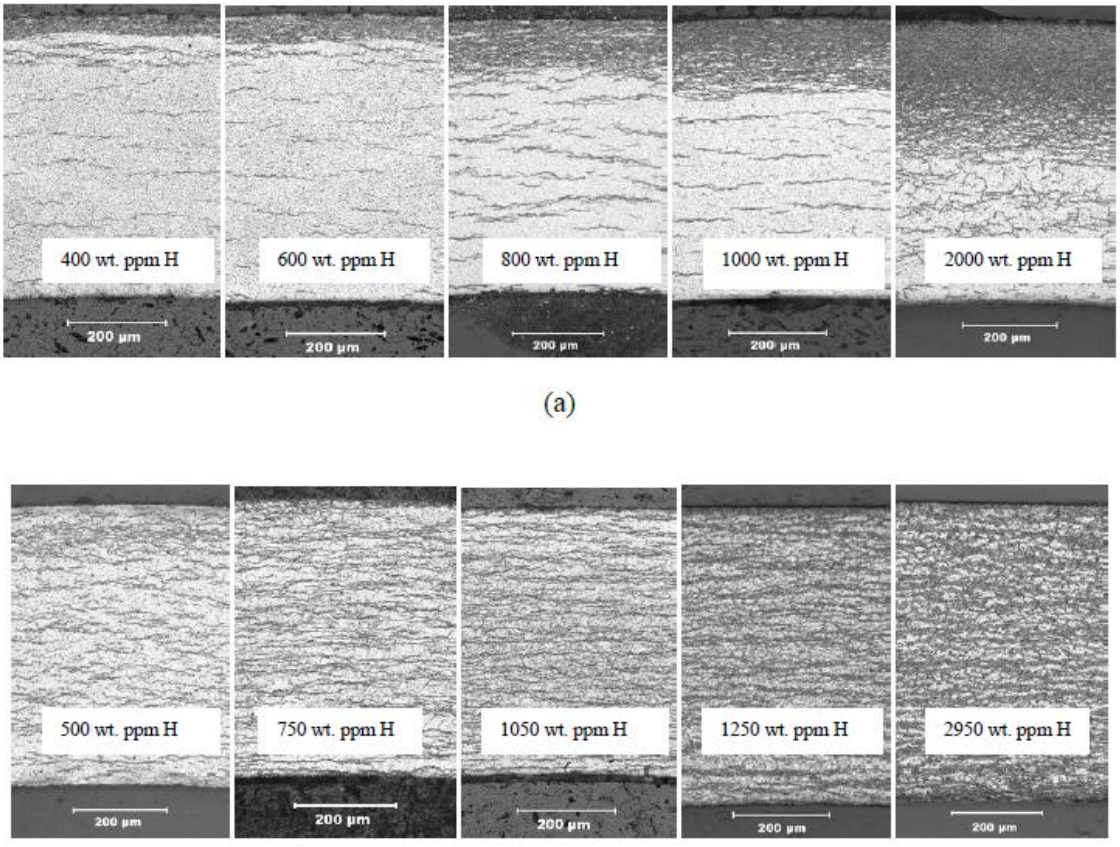

Figure 10 Hydride Morphology from gas charging [5]

Kraemer [21] developed a vapors diffusion apparatus and Parkinson improved on the design. [22] This system was located at Texas A&M University and Fig. 11 presents a schematic of the vapor diffusion device available for this hydride process. While the vapor phase device was not used to generate new samples, the samples from Parkinson's experiments were still available and were analyzed in concert with the newly created samples. These samples were from experiments 89, 91, and 93 (Section 4.2.5) developed for the Master of Science Thesis by Adam Parkinson in 2009. [22]

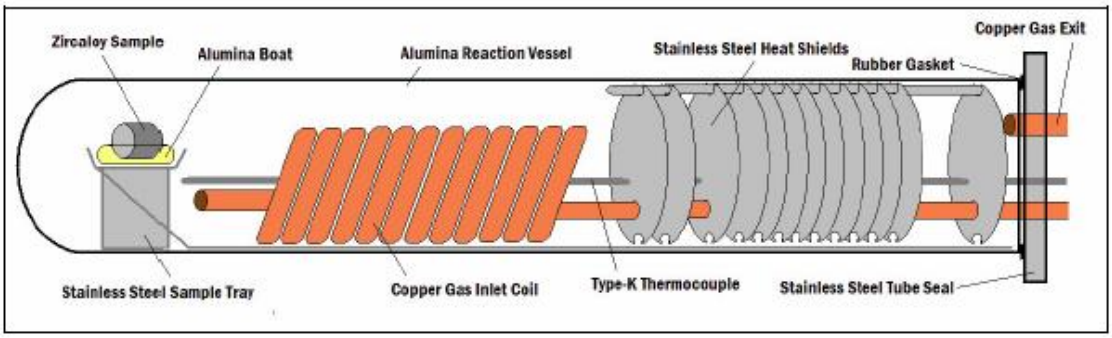

Figure 11 Schematic of Kramer, Parkinson reaction vessel. [22]

2.3.3 Auto-claving Methods

Auto-claving a sample is the third method to implant hydrogen. In this case, hydrogen gas is once again pumped over a sample while the sample is held at a temperature around 300°C and the sample is placed under pressure. [15] Once again, this method creates homogeneously dispersed hydride formations.

2.3.4 Actual UNF Hydride Geometry

For the special geometry of a tube sample, capping the ends of the tube and submitting it to any of the above techniques will generally result in a slight gradient of hydride formations. This slight gradient is an improvement over the homogeneous geometry; however UNF comes out of the reactor with a thicker hydride layer on the outer diameter of the Zricaloy-4 and a strong gradient of material towards the inner diameter. Figure 12 shows an example of hydride precipitates in cladding on high burn-up PWR fuel. [6]

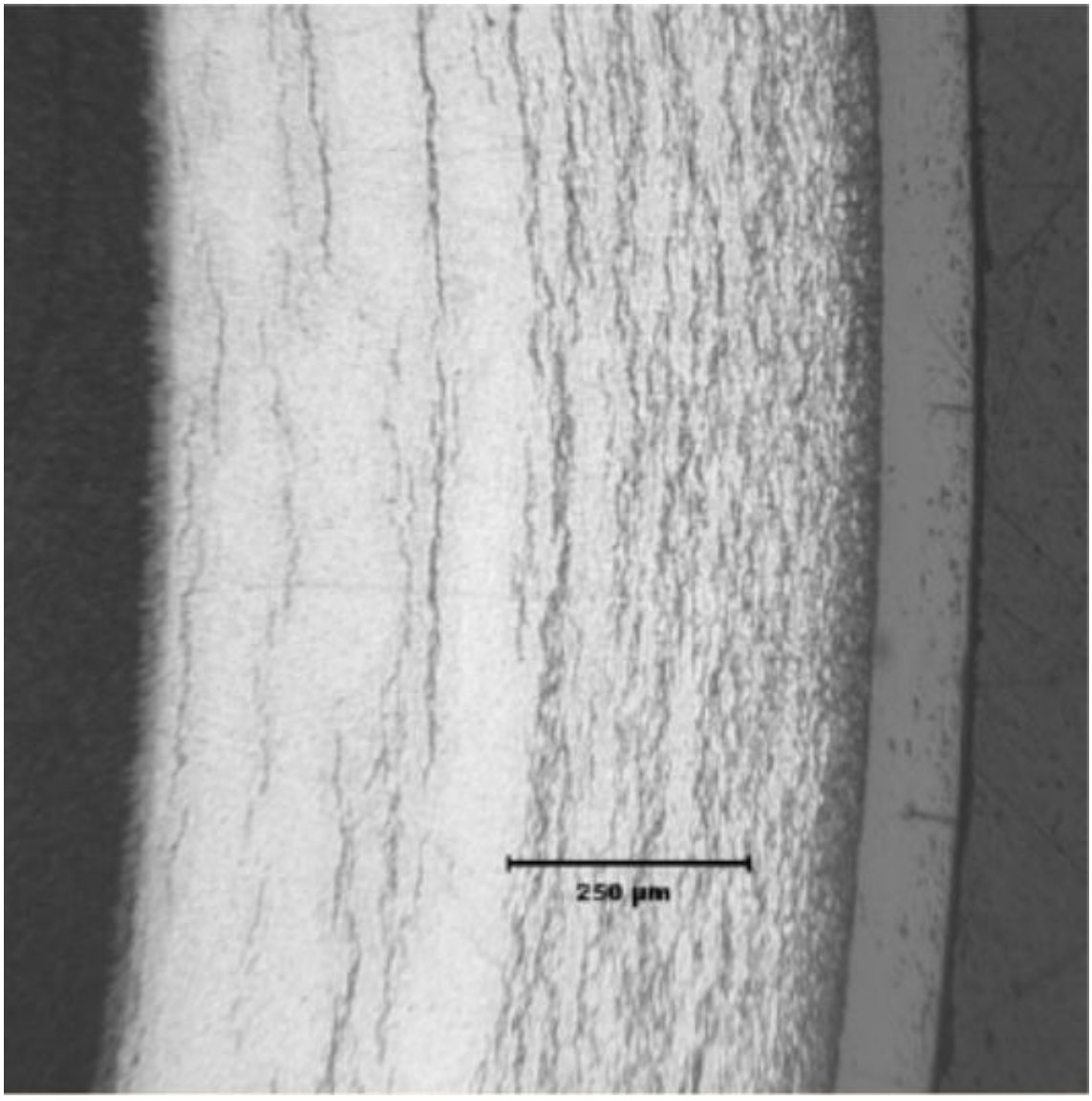

Figure 12 Hydride precipitates in cladding on high-burnup PWR fuel. From R. Daum, ANL. [6]

CHAPTER III

EXPERIMENTAL DESIGN AND PROCEDURE

This Chapter provides an overview of the electrochemical charging system developed for this study. For brevity, the system has been designated as the ECH-TG system, which is an acronym for Electrochemical Charging with Hydrogen using a Thermal Gradient. More specifically, this chapter presents a detailed description of the Electrolytic System Design (3.1), Experiment Procedures (3.2), and Post-test Characterization (3.3).

3.1 Electrolytic System Design

The ECH-TG system design is based on a similar design originally reported by John et. al [13]. The previous High Temperature Cathodic charging (HTC) apparatus was capable of creating hydride rims but a significant modification was created for the current system that was intended to enable the movement of hydrides from the rim into the sample for deeper penetration. In the new ECH-TG system, a sample of Zircaloy-4 tubing is suspended in solution around a hollow tube with a sealed end. A small cartridge heater is place placed inside of the hollow tube along with a thermocouple for temperature measurements. The software package SolidWorks Premium Win 11/12 was employed to design the custom system components and for thermal analysis. Figures 13 and 14 illustrate the initial design and current design of the sample holder, respectively. This long tube houses the cartridge heater and supports the sample on the outside of the

tube. The design permits the heat flux from the cartridge heater to pass through the boron nitride tube and straight to the Zircaloy-4 sample. This boron nitride was initially chosen because of its ceramic properties which included a very high thermal conductivity of 78 W/mK and a very high resistivity of >1013 ohm*cm. These features allowed excellent heat transfer while retarding current flow from the sample to the cartridge heater. For the sample holder the Al_2O_3 rod is 20.32 cm (8 inches) long and the Zircaloy-4 shell is 3.175 cm (1.25 inches) long. In this arrangement, the rod was drawn from spare supply and was too narrow to fit the diameter of the Zircaloy-4 sample. A sleeve of aluminum with a thermal coefficient of 200+ W/mK was used to assist in transferring heat from the Al_2O_3, to the Zircaloy-4 sample. The Viton caps were used to seal the inside of the zircaloy-4 from H_2SO_4 and also protect the aluminum from the bath, which would have degraded the aluminum material.

The Method 2 design was used for experiments M2-03 as described in Section 4.1. The design evolved over the course of the experiments in order to overcome challenges related to the breakdown of the counter electrode, the failures to seal the zircaloy-4 sample from the H_2SO_4 bath, the inconsistent temperature set-points, the tedious data accumulation requiring the operator presence for every experiment (resulting in the creation of a data acquisition program), and perceived inconsistencies in sample analysis due to differences in chemical solutions. The final design was used for experiments M1-30 through M1-36, as described in this chapter.

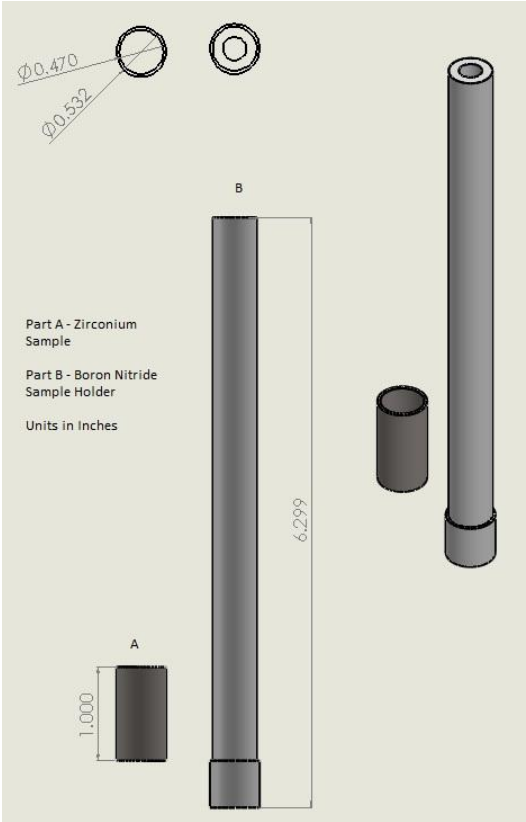

Figure 13 Initial design for sample holder made from Boron Nitride. Unit [in].

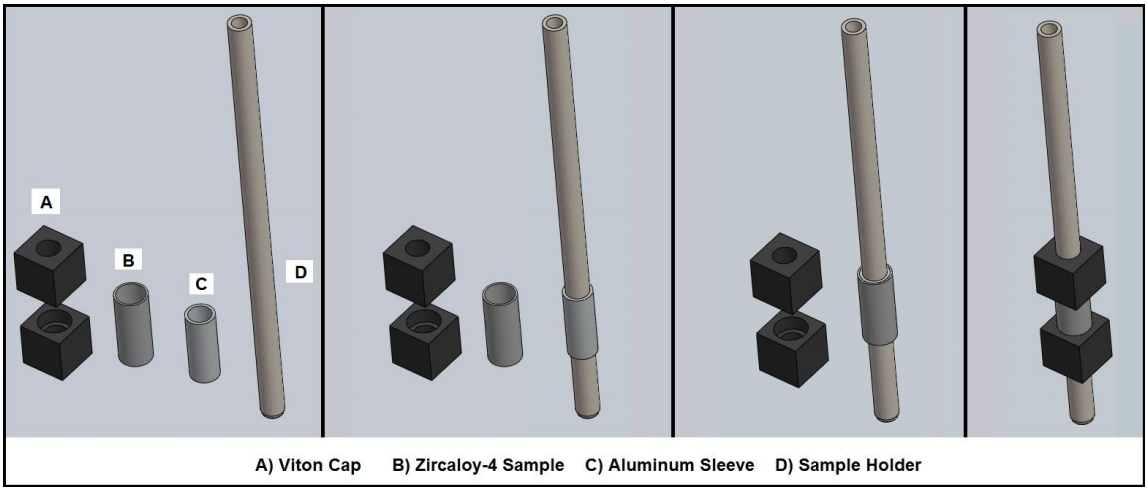

Figure 14 Sample holder assembly for experiments M1-21 to M1-25 and M1-30 to M1-36. The Al_2O_3 rod is 20.32 cm (8 inches) long and the Zircaloy-4 shell is 3.175cm (1.25 inches) long.

Figure 15 ECH-TG assembly with a Zircaloy-4 sample mounted over an aluminum sleeve on the Al_2O_3 sample holder with a Pt counter electrode and Viton caps also pictured.

As seen in Fig. 15, a glass Pyrex Glass beaker served as the main reaction vessel for this experiment. In order to obtain a uniform temperature for the solution, the beaker was placed on a hot plate and a Teflon lid was used to seal the beaker so acid vapors would not escape. Holes for a 3 foot condenser, thermocouples, the sample holder, and the cathode wires were drilled into the top of the Teflon lid. A sulfuric acid and water bath was used as the electrolyte and hydrogen source for the experiment.

The system was controlled and monitored using LABVIEW Student Version 11/12 with a custom virtual instrument created for these experiments. An Omega OM-USB-TC-AI DAQ was used to read temperatures and voltage into the computer at a frequency of 1Hz with accuracy to 1/1000 of a degree a 1mV respectively. Two RS232 connections were used to connect the TDK-Lambda ZUP80-10 Power Supply and the SCILOGEX MS7-H550-Pro 7x7 hotplate stirrer to the computer. This enabled computer control of the hot plate (and thus the temperature) as well as the current or voltage generated by the power supply. See Appendix A for system design schematics, additional system images, and software details.

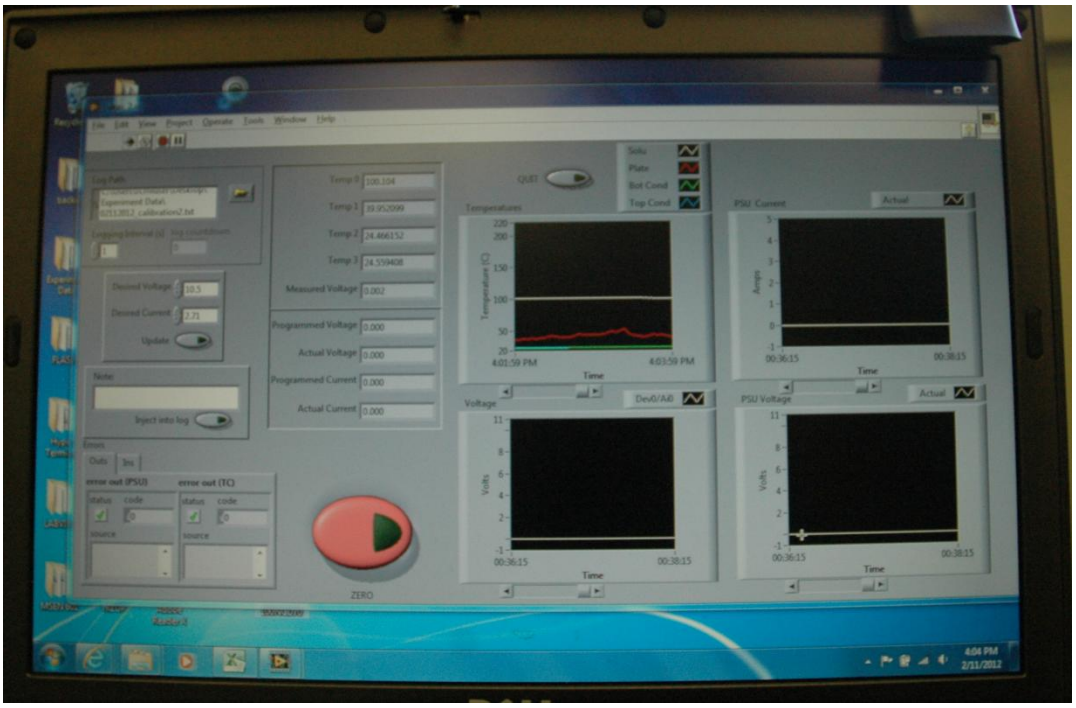

Figure 16 NI LABVIEW Program L2.vi used for controlling experiments and recording voltage, current, and various temperatures. A wiring diagram is attached in Appendix A.

The sample holder designed to hold a Zircaloy-4 shell vertically in the solution is illustrated in Fig. 15. An aluminum oxide tube with one end sealed served to hold the sample and also permitted the cartridge heater to heat the sample from the inside. Viton caps were then used to secure the sample onto the aluminum oxide rod. This rod was hung in the solution so that the sample was suspended above a stir bar. A zirconium wire served as the electrode lead from the sample to the top of the Teflon. Finally, a platinum electrode was suspended in solution so that it surrounded the sample.

The sulfuric acid and water bath was heated to boiling around 120°C. The cartridge heater was then initialized and brought to the designated temperature. The

highest temperature reached was 350°C. The Viton caps started to disintegrate around 200°C, but these pieces were easily fabricated. The breakdown of the Viton served as the limiting factor on the temperatures. The caps were inspected for each experiment and would be re-used of the previous experiment showed little to no signs of acid reaching the ID of the sample. After experiments with a particularly high cartridge heater temperature, over 250°C, the caps were in such a degraded state that they fell apart and had to be replaced.

3.2 Experiment Procedures

The following involves a detailed procedure for the existing ECH-TG system.

1. Sample Preparation (GLOVES ON)
    a. Cut 2.54 cm (1 inch) piece of Zircaloy-4 tube using a diamond saw and sand down the ends to prevent gouging of the Viton caps or Al_2O_3 sample holder
    b. Mass sample, measure dimensions, and label sample
2. Sample Pre-treatment “Pickling” (FULL PPE)
    a. Immerse sample in pickling solution for 5 minutes or until 4-6% mass loss
    b. Immerse sample in large volume of water (6-10 Liters) for 5 minutes and then rinse with water.

c. Mass sample again (once sample is pickled, do not touch it with bare hands and keep it from other contamination by putting it in a clean container)

3. Load sample and prepare vessel (GLOVES ON)
    a. Load sample onto sample holder with aluminum sleeve and viton caps.
    b. Connect a new piece of Zirconium wire (anode wire) to the sample via a tight loop.
    c. Insert sample holder, anode wire, and cathode (Pt electrode) into Teflon lid
    d. Place Teflon lid onto empty Pyrex beaker and place beaker onto hotplate.
    e. Insert thermocouple glass tube and Thermocouple 0 (T0) into opening D of the Teflon lid.
    f. Insert cartridge heater and Thermocouple 2 (T2) into sample holder.
    g. Place magnetic stir-bar into Pyrex beaker via opening E and insert glass funnel into opening E.
    h. Turn on the water flow for the condenser
4. Power on components (GLOVES OFF)
    a. Power on hotplate
        i. Heat should be off (indicated by green LED)
        ii. Stir speed should be off (indicated by green LED)
    b. Power on TDK-Lambda ZUP10-80 Power Supply
        i. The system should be on, but not generating any current

c. Open LABVIEW L2.vi, press run, and indicate output data file name.
    i. Power Supply
        1. Amperage – 0 A
        2. Voltage – 0 V
    ii. Omega DAQ
        1. T0, T1, T2, T3 should all generate initial signals at room temperature
        2. V0 – should be 0
d. Open Dragon-Labs StirPC Software

5. Mix Electrolyte Bath (FULL PPE ON)
    a. Pour 390 ml of distilled water into the ECH-TG via the funnel.
    b. Hotplate stirrer on
        i. Press down on the stir dial to turn on stirring and set speed to 1000 RPM
    c. Measure 210 ml H_2SO_4 (98% concentrated) into graduated cylinder
    d. With an eye on the T0 temperature, slowly pour H_2SO_4 into the ECH-TG via the funnel. This process should take up to 1 minute to complete however it will take longer if too much is added too quickly.
        i. CAUTION – This is a VERY exothermic reaction. The water temperature will go from 25°C to 120°C very quickly. The boiling point of water is 100°C and instantaneous boiling will start to occur as T0 reaches 100°C. This will cause flashes of steam which

will be made of both H_2O and H_2SO_4 which are VERY dangerous to inhale.

e. The graduated cylinder, once emptied, is then placed in a stable location in the fume hood away from the ECH-TG.

f. The Teflon lid is now rotated so that opening E is lined up underneath the condenser, which is now attached at this time.

6. Final Connections

a. Make certain that the condenser is securely attached and that the lid of the system is sitting flat on the top of the Pyrex beaker. It should not wobble or be ajar. If the lid is not sitting flat, vapor will escape into the fume hood and could possibly damage electronic components as well as contaminate other vessels and components in the hood.

b. Power on TDK-Lambda ZUP10-80 Power Supply

i. Connect the BLACK Power supply cable with the anode wire (coming from the sample)

ii. Connect the RED Power supply cable to the Platnium Electrode

iii. DOUBLE CHECK CONNECTIONS.

c. Use the red cable grips to position the Pt electrode into a symmetrical position around the sample.

d. Make sure all thermocouples are providing signals in the expected range.

i. T0 – Solution temperature – 120°C

ii. T1 – Plate temperature – (n/a)

iii. T2 – Cartridge Temperature – 120°C

iv. T3 – Condenser Inlet - < 60°C

7. Stabilize Heat

   a. Dragon-Labs StirPC Software

      i. Program the temperature to 300 °C

      ii. Program the stir-bar to 1000 RPM

   b. Hotplate

      i. Turn off stir-bar rotation by pressing down on the knob but keep hotplate powered on.

   c. LABVIEW L2.VI

      i. Make a note in the comments window that StirPC Software is starting.

      ii. Enter note and quickly initiate the StirPC program

         1. Hotplate should indicate both heat and stirrer are on (green LEDs)

   d. Hotplate

      i. Manually adjust the temperature up to 400 °C on the hotplate. (The actual hotplate has a higher set point than the software allows to be set from the computer.)

   e. Dragon-Labs StirPC Software

      i. The software will record the device temperature as it increases to 400 °C.

f. Wait for the system to equalize the solution and cartridge heater temperatures. Temperature readouts are usually around:
    i. T0 – Solution temperature – 120 °C
    ii. T1 – Plate temperature – (140-160 °C depending on the placement)
    iii. T2 – Cartridge Temperature – 120 °C
    iv. T3 – Condenser Inlet - <60 °C (If ever above 60 °C turn down hotplate. Be careful of vapor discharge from under Teflon rim.)

8. Run Experiment (Temperature Gradient)
    a. If not using Temperature Gradient, skip this section.
    b. Power on the variac
        i. In small increments (5% or less) slowly increase the power on the variac until the cartridge heater reaches desired temperature (T2).
        ii. Temperature increase should be gradual in order to prevent thermal shock to the sample holder and Viton caps.
9. Run Experiment (Voltage)
    a. LABVIEW L2.VI
        i. Set amperage and voltage
        ii. Enter comment that experiment is starting (include experiment parameters)
        iii. Initiate charge
    b. Open Logitech Web Camera Program

i. Position web camera 1 to look at the ECH-TG system

ii. Position web camera 2 to read digital readout from ZUP80-10

c. Remote connect if so desired

d. System can usually run for 12-18 hours without needing attention

i. After 12-18 hours, some of the bath will have escaped due to boiling/vaporization that the condenser was unable to completely condense combined with the breakdown of H_2O into H_2 and O_2 from the electrolytic process.

ii. Using a distilled water bottle, add solution through the top of the condenser until the solution level is returned to the initial level.

iii. Always note under comments what adjustments were made.

10. Ending experiment and cool-down

a. LABVIEW L2.VI

i. Pres the large red "Zero" button on the L2.VI to end the charge from the power supply.

b. ECH-TG

i. Remove the red and black connections from the device immediately. (This prevents any voltaic process from occurring.)

c. Cooling cartridge heater (if Temperature Gradient was not used, skip this section)

i. LABVIEW L2.VI

1. Make a comment noting the start of the cool-down procedure for the cartridge heater.
2. Slowly reduce variac so that the cartridge temperature decreases by approximately 1°C per minute.
3. This was often done with two adjustments per 5 minutes.
4. Reduce variac until it reaches zero power and T2 = T0 = 120 °C.
5. Make a comment noting the end of the cool-down procedure for the cartridge heater.

ii. Variac

1. Turn off variac
2. Leave cartridge heater in sample holder

d. Cooling Hotplate

i. LABVIEW L2.VI

1. T2 is used to gauge the continued cool-down process. This temperature should never decrease faster than 1°C per minute.
2. Make a comment noting the start of the cool-down procedure for the hotplate.

ii. Dragon-Labs StirPC

1. Press “Stop” and “Save” the data file
2. Set temperature to 250 °C and Stirrer to 1000RPM

3. Press “Start”
4. Wait about 20 minutes for temperature to drop gradually
5. Repeat steps 1-4 with setpoints of 150 °C, 100 °C, and 25 °C until the T2 < 70 °C.
6. Once T2 < 70°C, natural convection will cool the solution slower than 1°C per minute. The heat setpoint can be turned off by pressing the heat knob on the hotplate, however the stirbar should continue running in order to facilitate the cooling of the system.

iii. LABVIEW L2.VI

1. Once T2 < 40 °C, the system can be disassembled carefully.

11. Disassembly (FULL PPE- treat everything like H_2SO_4 is on it)

a. Withdraw the cartridge heater and T2 from the sample holder.
b. Disconnect the condenser and turn off the water flow.
c. Carefully lift the ECH-TG off of the hotplate and place it on the fume hood bench top.
d. Very slowly, lift the Teflon lid straight up being careful not to tip it one direction or the other. (Droplets of H_2SO_4 and H_2O are clinging to the underside of the lid). Place the lid on top of an empty beaker.
e. Cover the Pyrex beaker with a beaker cover.

f. Remove the lid with the spare beaker to the sink and thoroughly rinse all parts with water. Be especially careful not to splash water.
g. Disassemble the lid, Pt electrode, viton caps, sample holder, aluminum sleeve and sample and rinse all components separately to remove traces of H_2SO_4.
h. Place sample into clean container.
i. Clean any vessels used and place components of ECH-TG system in storage.

12. Post-Experiment
    a. Mass sample and note any changes in composition (color, thickness etc)
    b. Use a diamond saw to cut sample according to Fig. 21.
13. Imaging preparation
    a. Follow directions given in Appendix C.

3.2.1 Sample Pre-treatment ("Pickling")

The samples of Zircaloy-4 for this experiment came from surplus stock material received from Argonne National Laboratory (Argonne, IL), but the specifications of the alloy were undocumented. Therefore, the composition of the alloy was characterized by Anderson Laboratories (6330 Industrial Loop Greendale, WI 53129 – phone (414) 421-7600)). And Table 4 shows the measured composition compared with nominal values [17] for the composition of Zircaloy-4. This stock supply had been in storage for

over 10 years and so the samples were “pickled” prior to use to revoke surface oxidation and other possible chemical contamination. Pickling is the name for any process that removes stains, organic material, and traces of inorganic materials from the surface of a metal. Using a chemical pickling solution ensured a consistent coverage as compared to sanding the sample clean.

Table 4 This table shows a Zircaloy-4 composition comparison between Wah Change reference and Anderson Laboratory analysis.

	Nominal Composition of Zircaloy-4 [17]	Sample Composition Measured by Anderson Labs Method
Element	Wt % in Zircaloy-4	Wt % in Zircaloy-4
Sn	1.2 - 1.7	1.54
Fe	0.18 – 0.24	0.23
Cr	0.07 – 0.13	<0.01
O	0.12	not tested
Zr	Balance	Balance
Nickel:		< 0.005

The pickling solution (5ml HF (48%), 45ml HNO_3 (70%), and 50ml H_2O) was selected to follow the previous procedure outlined done by John et. al. [13] and the time for pickling was initially held constant at 5 minutes. It would later be determined that the pickling process was not removing the same fraction of material and that longer soak times and/or fresh solutions had to be prepared. Each sample mass and dimensions were measured prior to immersing into the pickling solution for 5 minutes. After 5 minutes, the sample was removed and quickly immersed in a large volume of water to halt the pickling process. The sample was in the water for at least 5 minutes before and then

removed and rinsed with water before drying in air. The post-pickling sample mass was measured and the mass difference recorded: the typical mass loss during a successful pickling procedure was on the order of 4 to 6 percent. After this, the sample was installed into the experiment assembly.

Pickling times for samples were based on an initial 5 minute period in solution followed by another period in order to achieve the 4-6% mass loss. It was noted after several experiments that this pickling solution became saturated with zirconium with repetitive use. Towards the end of this work, the solution was replaced with a fresh solution after a sequence of unsuccessful tests (See Section 4.1.2). It was noted at this time that the mass loss during pickling was 4 to 6 percent for experiments M1-11, M1-12, and M1-13, which all showed a good hydride rim. With a weakened solution, only 1-2% mass loss was measured. In these cases the sample was set to pickle for longer time until at least 4% mass loss was realized. A new bath was then mixed before starting to pickle the next sample.

3.2.2 Electrochemical Charging of Hydrogen

After the sample was mounted onto the sample holder, a freshly cut wire of pure zirconium was cut and connected to the sample. This was typically done with a lasso type configuration. Spot welding is the preferred method of connection; however the equipment was not easily available for this task. Once the sample holder was assembled it was inserted to the Teflon lid (Fig. 17). The Platinum Mesh electrode was also inserted

and the Teflon lid was then placed on top of the empty Pyrex vessel. Platinum was used because its inert properties prevented the absorption of Oxygen into the electrode and permitted for long term use. The mesh geometry was chosen in order to keep costs low while maximizing the cylindrical geometry needed. In electrolytic systems, the surface area of the counter electrode is at least 5 times the size of that of the target anode. Figure 17 illustrates the openings for the Teflon lid and Fig. 18 illustrates the assembled system.

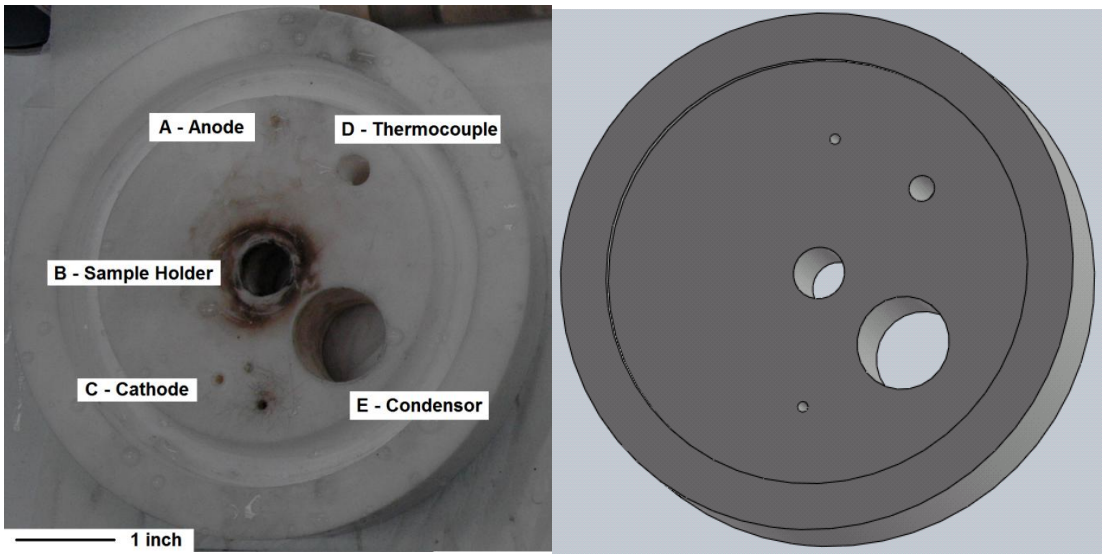

Figure 17 Openings for Teflon lid. Solidworks illustration (left) and actual component (right) are shown.

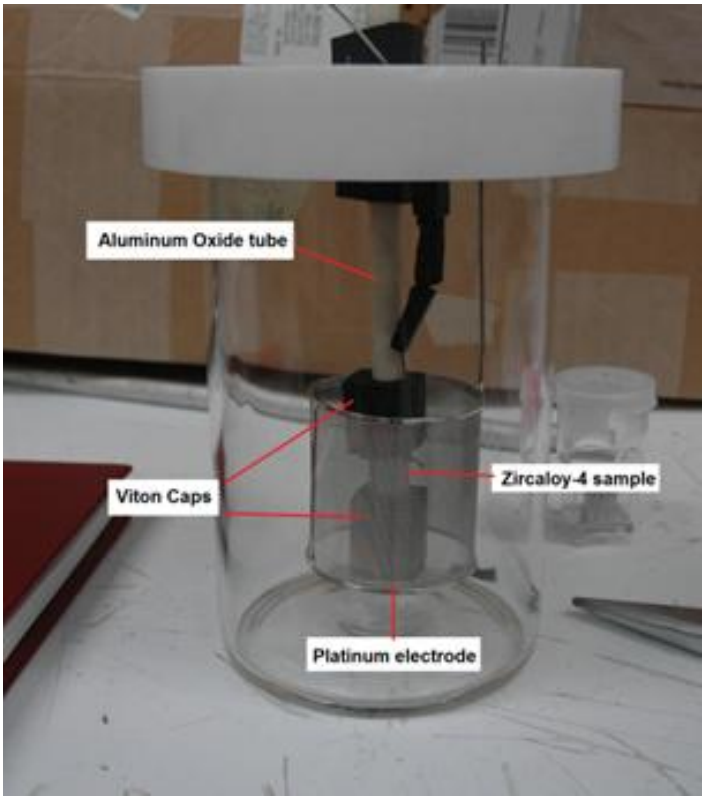

Figure 18 Assembled vessel with sample and without bath.

The assembled experimental vessel was placed on top of the hotplate inside of a fume hood. The use of a fume hood was necessary because the boiling solution produces vapors which were very hazardous. Additionally, in case of any spill or accident, the fume hood would serve as a confined space in which accidents could be controlled. A magnetic stir bar was dropped through the E opening, and its operation during the experiment, via the stirring hotplate (SCILOGEX MS7-H550-Pro 7x7), served to keep the solution uniformly heated. The electrodes from the power supply (TDK-Lambda ZUP80-10) were connected to the electrode and to the zirconium wire. The negative terminal (black wire) was connected to the zirconium lead wire and the positive terminal

(red wire) was connected to the Pt electrode. A closed-end glass tube was inserted into opening D (Fig. 17) and a Type K thermocouple (model) was inserted to the bottom of the tube. Finally, the cartridge heater (Dalton Wattflex 200W 120V 1.5” by 0.25”) and thermocouple were placed down the sample tube. The cartridge heater was inserted to the bottom and then raised ~1 cm (~0.5 in) in order to have the cartridge heater located such that the heat flux would be uniformly distributed into to the sample.

Once these components were in place, the LABVIEW control program was launched. The custom VI required the user to input a specific name for the data output file and starts recording temperature, voltage, and amperage data along with the current date and time. At the same time, the hotplate was turned on and the program (Dragon-Lab StirPC), which controls the hotplate, was turned on. The power supply was powered on, however the charge was kept at zero. While all these programs are turned on, it was important to note that no heat or charge was being delivered to the system. All devices needed to be on in order for the computer to be able to record the temperature and time data which consisted of the components found in Table 5.

Table 5 Current Data Acquisition Matrix.

Logging Program	Device	Data Handle	Data Description
LABVIEW Lukas2.VI	OMEGA OM-USB-TC-AI DAQ	T0 [°C]	Temperature of Solution as taken with a thermocouple in a sealed glass tube
		T1 [°C]	Temperature of the surface of the hotplate as taken with a thermocouple placed directly on the hotplate next to the beaker
		T2 [°C]	Temperature of the interface between the cartridge heater and the Al2O3 sample holder
		T3 [°C]	Temperature of the outside of the lower vapor receiving end of the condenser
		V0 [V]	Measured voltage of the power supply
	TDK-Lambda ZUP80-10	Programmed Current [A]	This indicates the "programmed" value of the current. It has historically been lower than the actual input current in the VI.
		Actual Current [A]	This indicates the measured value of the current. It has historically been lower than the programmed current.
		Programmed Voltage [V]	This indicates the "programmed" value of the voltage, It has historically been lower than the actual input voltage in the VI.
		Actual Voltage [V]	This indicates the measured value of the voltage. It has historically been lower than the programmed voltage.
Dragon-Lab StirPC	SCILOGEX MS7-H550-Pro 7x7	Temperature [°C]	The hotplate internal temperature
		Speed of Spin [1/Min]	The RPM of the stirrer

Table 6 Initial Data Acquisition Matrix.

Logging Program	Device	Data Handle	Data Description
TRACER DAQ	OMEGA OM-USB-TC-AI DAQ	T0 [°C]	Temperature of Solution as taken with a thermocouple in a sealed glass tube
		T1 [°C]	Temperature of the surface of the glass beaker was taken from the outside of the beaker.
		T2 [°C]	Temperature at the center of the cartridge heater was taken.
		T3 [°C]	Temperature of the atmosphere was taken for a control.
		V0 [V]	Measured voltage of the power supply

Once the system was assembled and ready to go, the 600ml electrolytic solution bath was prepared by combing H_2O and H_2SO_4 (98% concentrated) in a 50/50 mixture by weight. This came out to 390 ml of H_2O to 210 ml H_2SO_4. The mixing reaction between water (H_2O) and concentrated sulfuric acid (H_2SO_4) is a highly exothermic reaction, as illustrated in Fig. 19. Proper Protective Equipment (PPE) consisting of close toed shoes, long pants, a thick shirt, a cotton lab coat, a plastic apron, safety glasses, a face-shield, two layers of Nitrile gloves and a third layer of rubber gloves was needed for mixing the chemical solution. A glass funnel was placed in opening E to facilitate pouring the components of the bath into the vessel. It was very important to add the 390 ml of distilled water to the beaker first. Once the water was poured in, the magnetic stirrer was started. A graduated cylinder was then used to measure out 210 ml of H_2SO_4 (98% concentrated) which was slowly and carefully poured into the Pyrex beaker through the funnel. The temperature of the solution was monitored on the LABVIEW program as the sulfuric acid was poured in. If poured slowly, the temperature would rise from 20 °C to 120 °C just as the last drops of acid were poured in. At 120C the bath boiled and the evaporated solution was returned to the liquid bath using a glass condenser (1000mm 24/40 generic brand). All source chemicals where then removed from the area around the experiment and the funnel was removed from opening E. The Teflon lid (Fig. 17) was slowly turned so that the condenser could be securely fit into opening E. With the condenser attached and secured, the water flow to the condenser was turned on. The assembled system is shown in Fig. 20.

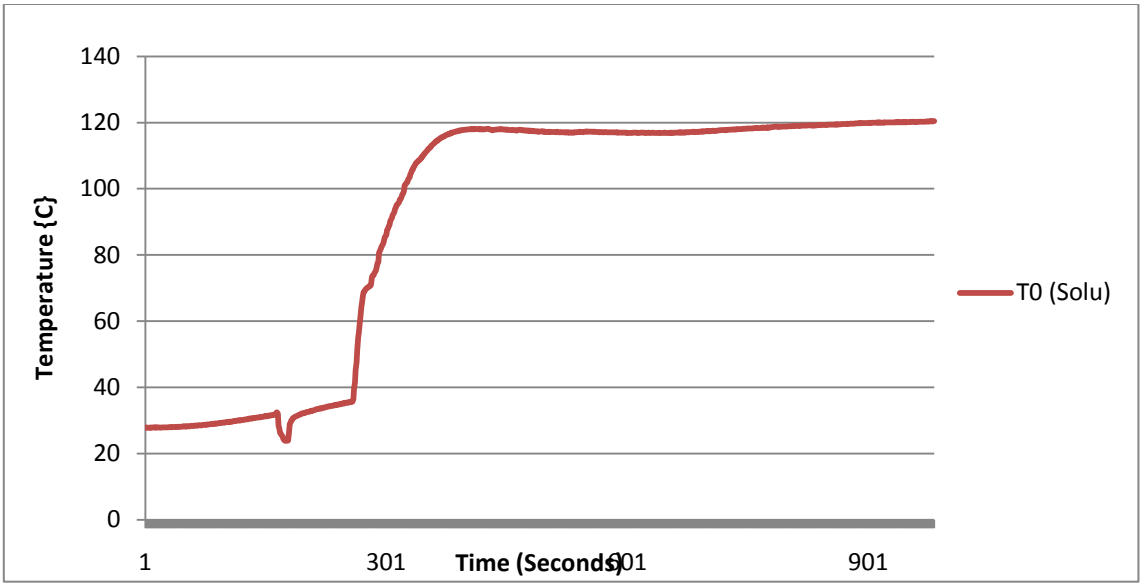

Figure 19 This figure outlines the exothermic nature of the reaction between H_2SO_4 and H_2O. Always add acid to water. The temperature of H_2SO_4 and H_2O solution as 210 ml of 98% concentrated H_2SO_4 is added to 390 ml H_2O.

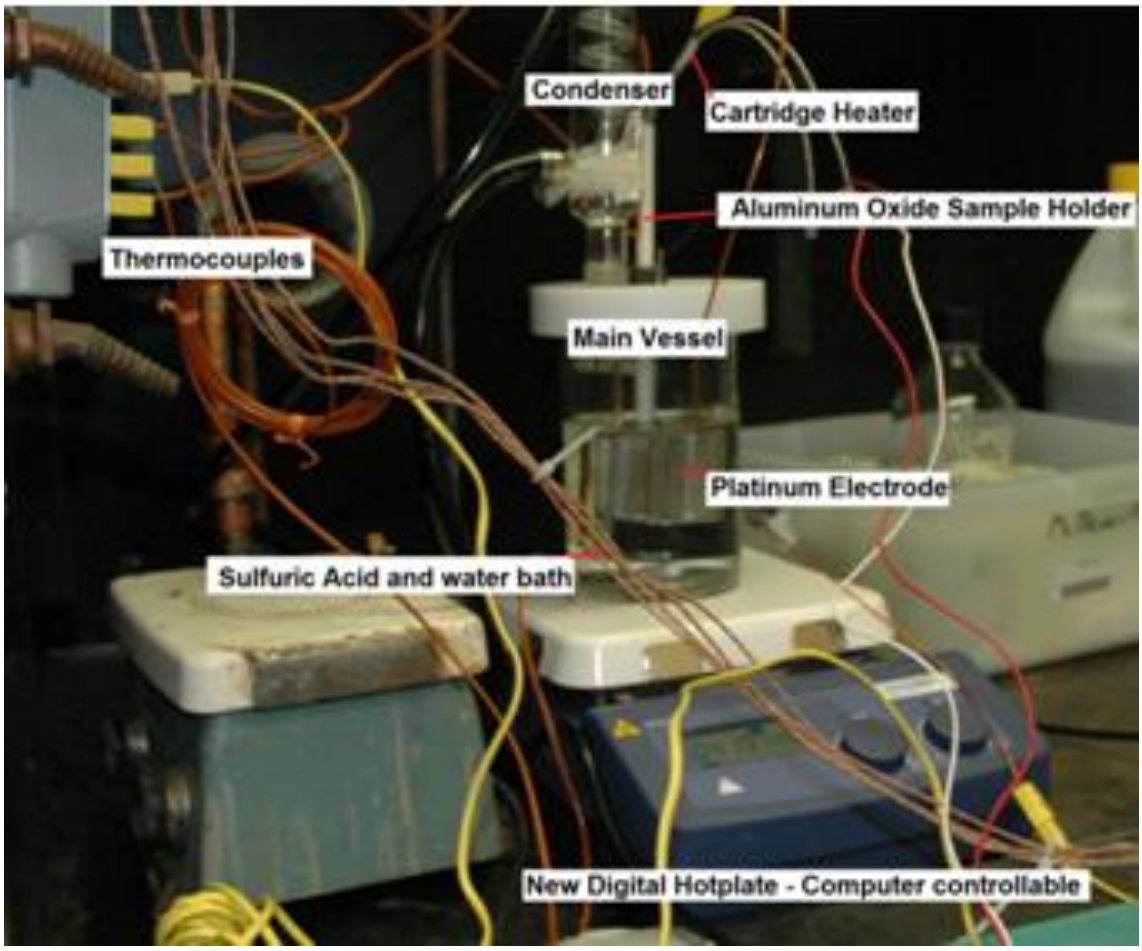

Figure 20 ECH-TG ready for experimentation.

From this point, the system was prepared for the experiment. The hotplate setpoint was increased to 400 °C and the magnetic stirrer rotation rate was set to 1000 RPM using the control system noted in Section 3.1. This created the baseline condition of 120°C boiling acid required for the experiments. The electrochemical potential or current for the system was controlled via the LABVIEW Control Program (Appendix A) and could be programmed up to a voltage of 10V or an amperage of 80A.

The cartridge heater was controlled with set-point controls using a variable voltage transformer (variac), STACO ENERGY Model 3PN1010B. At the end of the experiment the cool down of the system was accomplished by slowly reducing the variac power. After the variac was turned off, then the hotplate temperature would be slowly reduced at 1°C per minute.

Once the system had cooled to at least 40°C, the system was carefully disassembled (while wearing PPE) and the lid was removed with the sample holder and Pt electrode still attached and moved onto an empty beaker. This assembly was then rinsed in running water and disassembled to retrieve the sample.

3.3 Post-test Characterization Procedures

3.3.1 Acid Etching for Imaging

In order to properly identify the zirconium hydrides, an acid etching step was required before taking the sample to be viewed either optically or under an SEM. It was very important to get a good polish on the sample before etching. Without a good polish, it was not possible to see the hydride formations even after etching. The etching solution was made of 0.5 to 1ml of HF (48%), 25 ml HNO_3 (70%), and 25 ml H_2O_2 (30%). The etching technique and details are found in Appendix C.

3.3.2 Sample Imaging

Samples were sectioned, mounted, polished, etched to reveal hydrides, and observed under an electron probe which performed both SEM imagine and EDS analysis. The Zircaloy-4 sample was sectioned with a LECO VC-50 diamond saw into three sections, as illustrated in Figure 21, so that any density changes in hydrides along the axial direction could be analyzed. These samples where then mounted in Epoxy and polished. The polish started at 120 grit and worked down to 1200 grit abrasive paper. Once a mirror like finish was achieved, the sample was taken to be acid etched, before being taken to the microprobe lab.

Samples where then carbon coated and placed in a Cameca SX50 Electron Microprobe equipped with a PGT Energy Dispersive X-ray (EDS) system. This device was used to take SEM images and perform EDS analysis on the samples.

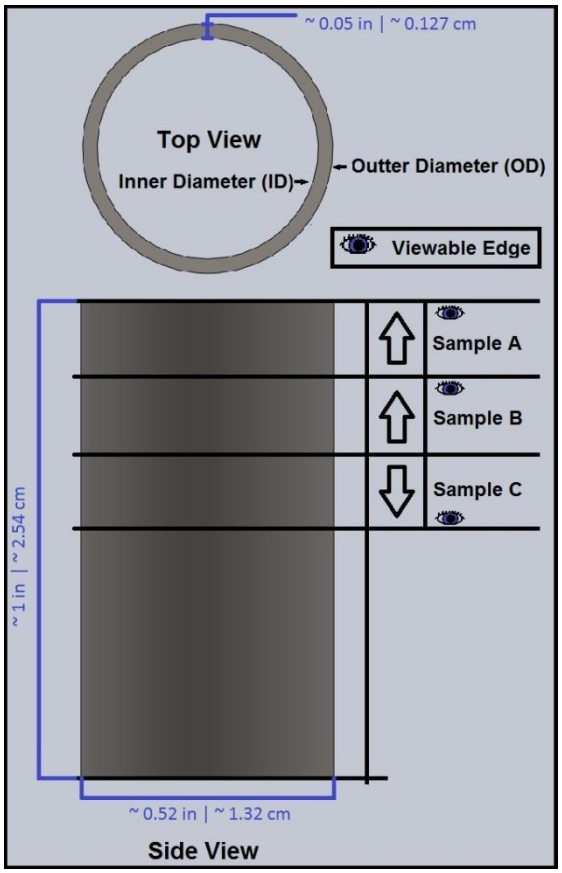

Figure 21 Sectioning Diagram used for Experiments M1-30 to M1-36.

CHAPTER IV

RESULTS

Initial success with forming thin and dense hydride rims was followed by challenges to develop thicker rims which penetrated deeply into the sample. These results followed a series of system alterations which will be covered in this chapter. Figure 22 illustrates a representation of samples after experimentation and before sectioning for imaging. Table 7 presents the complete matrix of experiments performed and the associated changes to system design over the course of system development. These changes to the system resulted in variations of results which are discussed in section 4.1. Section 4.2 discusses the resulting hydride formations or lack thereof.

Figure 22 Samples M1-30, M1-31, M1-32, and M1-33 (from left to right).

Table 7 Master Experiment Chart

Sample # / Experiment Name	Bath Heater	Sample Heater	Sample Holder	Sealed Sample? (y/n)	Cartridge heater (4 or 1.5 inch)	Electrode Material	Data Recording Software	Component broke?
1 / M2-03	hotplate	none	M2 Sample Holder	n	none	Bronze	TRACERDAQ	Bronze electroplated
2 / M1-06	cartridge	none	Aluminum oxide tube with zirc wire down center	n	4	Graphite	TRACERDAQ	
3 / M1-11	cartridge	none	1st BN Tube (AX05)	n	4	Graphite	TRACERDAQ	
4 / M1-12	hotplate	none	1st BN Tube (AX05)	n	4	Graphite	TRACERDAQ	yes - sample holder
5 / M1-13	hotplate	cartridge	2nd BN Tube (AX05)	n	4	Graphite	LABVIEW V1	Failed start - followed up with M1-14
6 / M1-14	hotplate	cartridge	2nd BN Tube (AX05)	n	4	Graphite	LABVIEW V1	
7 / M1-20	hotplate	cartridge	2nd BN Tube (AX05)	partially	4	Platinum	LABVIEW L2	yes - sample holder
8 / M1-21	hotplate	cartridge	Al_2O_3 tube with Al sleeve	y	1.5	Platinum	LABVIEW L2	
9 / M1-22	hotplate	cartridge	Al_2O_3 tube with Al sleeve	y	1.5	Platinum	LABVIEW L2	
10 / M1-23	hotplate	cartridge	Al_2O_3 tube with Al sleeve	y	1.5	Platinum	LABVIEW L2	Sample Reduction
11 / M1-24	hotplate	cartridge	Al_2O_3 tube with Al sleeve	y	1.5	Platinum	LABVIEW L2	
12 / M1-25	hotplate	cartridge	Al_2O_3 tube with Al sleeve	y	1.5	Platinum	LABVIEW L2	
13 / M1-30	hotplate	cartridge	Al_2O_3 tube with Al sleeve	y	1.5	Platinum	LABVIEW L2	
14 / M1-31	hotplate	cartridge	Al_2O_3 tube with Al sleeve	y	1.5	Platinum	LABVIEW L2	
15 / M1-32	hotplate	cartridge	Al_2O_3 tube with Al sleeve	y	1.5	Platinum	LABVIEW L2	
16 / M1-33	hotplate	cartridge	Al_2O_3 tube with Al sleeve	y	1.5	Platinum	LABVIEW L2	
17 / M1-34	hotplate	cartridge	Al_2O_3 tube with Al sleeve	y	1.5	Platinum	LABVIEW L2	
18 / M1-35	hotplate	cartridge	Al_2O_3 tube with Al sleeve	y	1.5	Platinum	LABVIEW L2	
19 / M1-36	hotplate	cartridge	Al_2O_3 tube with Al sleeve	y	1.5	Platinum	LABVIEW L2	Broke sample Holder trying to get sample

An initial experiment matrix was created to explore Method 1 (M1) and Method 2 (M2) for hydriding the Zricaloy-4 samples. The initial numbering system involved an M1 or M2 to signify the method being used, and a number 01 to 10 to represent the parameters that would be followed. This original experiment matrix is provided in Appendix B, but it was never completely executed due to significant failures in the system. These failures where addressed and a new matrix was developed. The second set of planned experiments followed a numbering scheme of M1-1x, where x signified the sequential experiment number. When the counter electrode was changed from graphite to platinum, the new scheme was M1-2x. These M1-2x experiments also involved the use of thermal gradients which were held constant during the experiment. The final set of experiments, designated as M1-3x, involved initially charging the sample without an initial thermal gradient and then changing the thermal gradient while actively charging. This pattern was continued so that data could be easily grouped according to the system configuration at the time of testing.

4.1 Initial Results

Experiment M2-03 (from the initial test matrix in Appendix B) was the first experiment conducted. The boron nitride sample mount had not yet completed so a small piece of graphite was formed into an anode. It was placed inside of the sample using Viton O-rings to separate the sample from the anode. A lead wire made of zirconium was used to connect the anode to the power supply. The experiment was run for 3 hours

at 0.2 A/cm^2. A bronze electrode was fashioned out of 50 mesh bronze gauze which measured about 12 inches by 4 inches and then curled into a cylindrical form and held in place by the walls of the beaker. After removing the electrode, it was discovered that electroplating had occurred in which mass from the electrode was reduced and deposited on top of the carbon anode. Figure 23 shows the resulting deposit from copper electroplating. The bath solution had turned blue and was replaced for the next experiment.

Method 2 experiments were intendeds to drive hydrogen through the wall of the Zircaloy while it traveled in a linear path towards the anode. With this significant failure, it was observed that the charged particles would go around the sample instead of through it. Method 2 was no longer attempted and Method 1 became the focus of the experimentation. A diagram of the anode and sample configuration for Method 2 is shown in Fig. 24. The chemistry required for the electroplating observed in M2-03 was not analyzed as it was quickly decided to move away from the bronze mesh and try other electrode materials. The sample was still included and inspected by electron microscopy, however no hydride formations where discernible.

Figure 23 Copper from the bronze electrode dissolved into solution and electroplated on top of graphite anode.

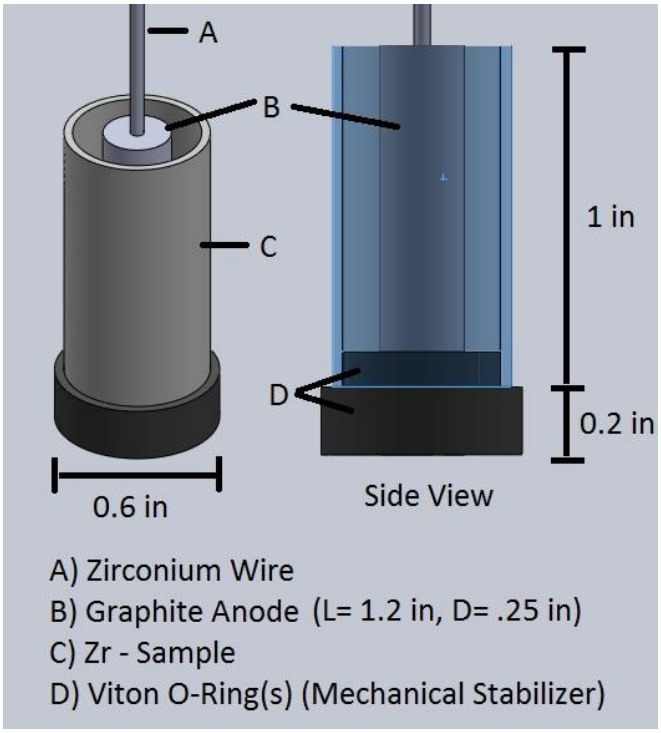

Figure 24 Method 2 sample holder configuration.

Literature pointed to the use of platinum electrodes due to their inert properties and ability to resist oxidation; however the high cost and the relative inexperience of the researcher with fashioning such an electrode required the pursuit of alternative electrodes. After another literature search, graphite was selected as the next electrode. The main challenge with this new electrode was the formation of CO_2 and the subsequent release of carbon into the solution, however it was determined that this was a cheap and readily available material.

The next four experiments, M1-06, M1-11, M1-12, and M1-13 were all performed with the graphite electrode. The initial M1-06 experiment failed to show any hydride formations, however the other three experiments all developed a dense crust of hydrides. ImageJ 1.45s software was used to take 20 measurements across the BSE images from M1-11, M1-12, and M1-13. These measurements were then analyzed to determine that the rims ranged from 8.690 +/- 0.982 μm to 12.365 +/- 0.635 μm and formed uniformly around the sample.

M1-13 and M1-14 used the same sample of material. When M1-13 was started, the graphite electrode was experiencing significant loss of mass from the previous two experiments. The system did not maintain a circuit very easily and the goal of the M1-13 experiment was to run for 24 hours. This electrode wire conducted current for only 6 hours 8 minutes even though the circuit was energized and voltage was available for 7 hours and 6 minutes. The system reached a maximum output at 10.5 V of potential and no measurable amperage was transferred after the initial ~6 hour period. This failure to conduct was due to failure of the graphite electrode to zirconium wire connection and

the resulting broken circuit. With the experiment already assembled, and effectively very little charge through the sample in relation to the 24 hour goal, it was decided to replace the wire and run experiment M1-14 with the same sample as M1-13. All references to M1-13 therefore include the sample from M1-13 which ran for ~6.1 hours at 0.5 A/cm^2 and then ~2.3 hours at 0.25 A/cm^2 under the M1-14 parameters. After the 2.3 hours at the M1-14 parameters the system again failed and the graphite electrode was determined to be insufficient for future runs.

Use of the graphite electrode consistently caused the bath to turn black in color due to the dissolving carbon. Additionally, the experiments could only run for a limited amount of time before the charging counter-electrode failed due to rapid degradation. With the experience of the first 6 experiments, the researcher purchased a Pt electrode for use on the next round of experiments.

Experiments M1-20 through M1-25 were performed using the new Pt electrode and the temperature of the cartridge heater and charge duration were varied as noted in Table 10. Additionally, during these experiments, it was discovered that cooling rates would determine the phase of hydride formed. High cooling rates would result in γ phase ZrH while low cooling rates would result in δ phase $ZrH_{1.66}$.[2] While in earlier experiments the system heating device was switched off and the system allowed to cool by natural convection, a slower cooling process was adopted for the remainder of this project. After each experiment, a 1°C per minute change in temperature was used to cool the samples. Each sample was only charged once before being removed.

The final group of experiments M1-30 through M1-36 where charged according to a matrix of values in an attempt to form a hydride rim and move that rim into the material. This test series was designed to cover a range of low-level temperature gradients and charge times where it was previously suspected that experiments M1-20 through M1-25 had too much off a thermal gradient. Results from the M1-3x set revealed no hydrides when examined by the microprobe. This result was particularly puzzling because even the control, M1-30, which was expected to form the initial hydride rim, failed to materialize

4.1.1 Apparatus Evolution

The initial design called for the test solution to be maintained at 90°C while attempting to bring the cartridge heater up to a temperature between 140°C to 180°C (and thus create a 50°C temperature difference across the sample). However, problems arose from the onset of the experiments. It was challenging to generate a gradient and even with a secondary cooling bath on the outside of the main vessel, the largest delta in temperature was observed to be 5°C.

It was considered that if the H_2SO_4 bath was placed in a boiling condition, and the cartridge heater was brought to a higher temperature, then the desired thermal gradient (~50°C) across the Zircaloy-4 sample could be created. The boiling solution maintained a relatively constant temperature however the vapor would need to be captured and

returned to the bath. This required the addition of the condenser to the top of the Teflon lid in order to preserve the test solution quantity for the duration of the experiment.

. A major challenge was finding materials which would withstand the boiling sulfuric acid environment. H_2SO_4 was an excellent electrolyte, but this strong acid reacts quickly and dissolves many compounds. The sample holder needed to have strong mechanical features, be electrically inert, have a high thermal coefficient, and be able to withstand a hot boiling acid environment, all while being easy to assemble and disassemble for multiple runs and preferably inexpensive to procure.

Aluminum Oxide, Al_2O_3, was initially considered for sample holder material. This material met most of the above requirements except that it was extremely hard to machine. Diamond bits would be needed to fashion and form the pieces and the cost of custom pieces would be high. While reviewing other similar ceramics, the researcher came across several boron nitride compounds. St. GOBAIN – Ceramic Materials, a private company, provided several samples of BN in various compositions and the researcher had two sample holders machined from the BN. These sample holders took on the form in Fig. 25. Figure 26 illustrates the discoloration of the sample holder due to the carbon in situ from the graphite electrode. Figure 27 represents the change in coloration of the sample while using the graphite electrode.

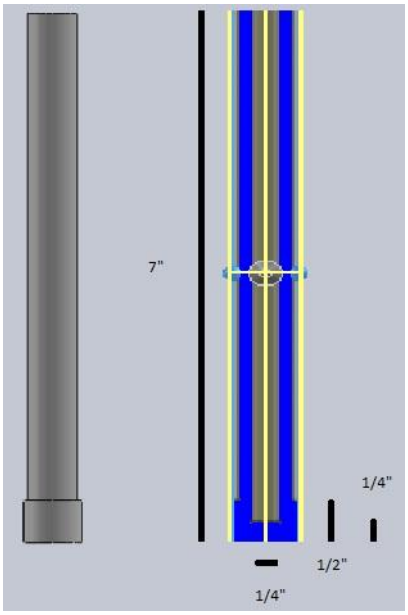

Figure 25 Boron Nitride sample holder dimensions.

Figure 26 Boron nitride tube and sample after experiment M1-06. Discoloration is due to carbon particles which dissolved into solution from the graphite electrode.

Figure 27 Pickled sample of Zircaloy-4 compared with a similar sample after electrolytic process and sectioning with a diamond cutting saw. Samples are approximately 1 inch tall.

For experiments (M1-06, M1-11, and M1-12) the first BN sample holder was used. During the disassembly for the M1-12 experiment, it was observed that the cartridge heater had corrosion during the test and could not be easily withdrawn from the sample holder. When forced from the sample holder, the BN sample holder broke. A second sample holder was used for experiments (M1-13 and M1-20). After these experiments, the second holder also broke in a similar fashion as experienced after experiment M1-12. Consultation with the BN distributor developed the postulation that the environment of H_2SO_4 combined with the 120 °C temperatures for extended period of time was causing micro-fractures that allowed the acid solution to reach the cartridge heater and causing failure. Fig. 28 is an image of the second broken BN with the

cartridge heater firmly lodged inside. Removing the cartridge heater involved pulling on the leads which ultimately lead to significant damage to the unit.

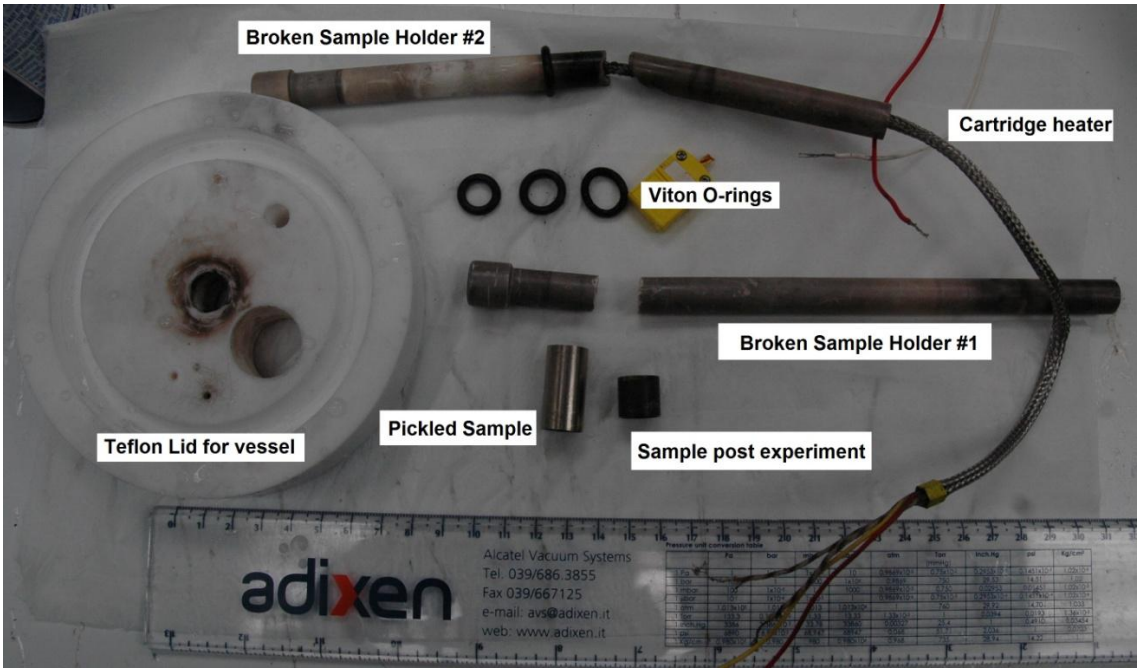

Figure 28 Broken boron nitride sample holders and associated components.

Therefore, a new material for the sample holder And a a better cartridge heater were required. The first cartridge heater, illustrated in Fig. 29 A, from Watlow provided 300W along a 4 inch long ¼ inch diameter cartridge. This was a much larger dispersion of the heat flux than was required for the system because the samples were only 1.27 to 2.54 cm (0.5 to 1 inch) in length. An alternative cartridge heater was purchased (Dalton watt-flex heater) and is shown in Fig. 29 B. This new heaterpacked 200W into a small 3.81 cm (1.5 inch) long 0.635cm (0.25 inch) diameter cartridge. This cartridge heater also came with grooves for a thermocouple to be placed between the heater and the inner

wall of the sample holder providing a much more accurate temperature for later calculations

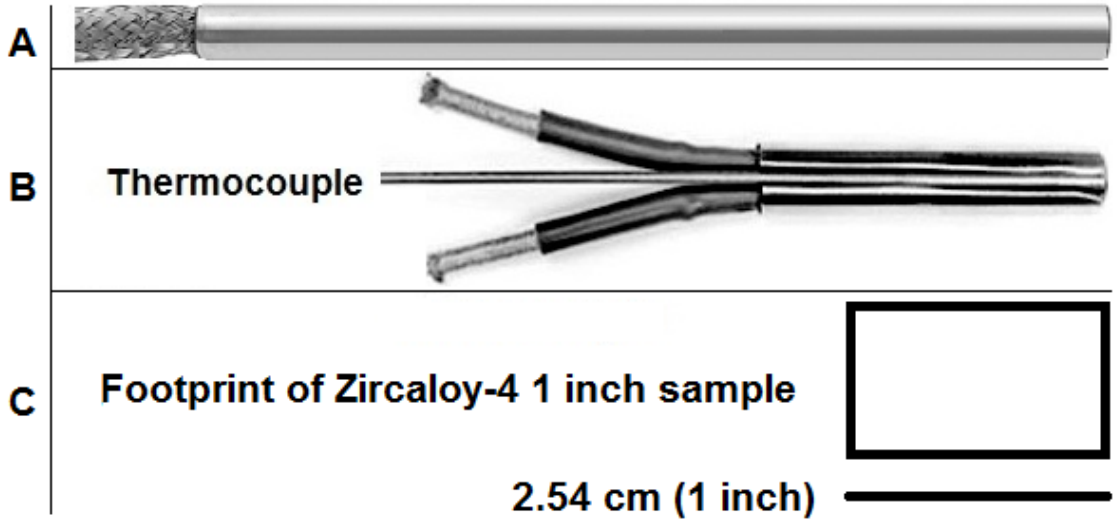

Figure 29 A) Watlow High-Temperature Cartridge Heater with Internal Temperature Sensor Part 8440T135 from McMaster-Carr. Specifications are ¼" diameter, 4" length, 120 VAC, 300 W, 2.5 A. (B) Dalton Watt-Flex heater. Specifications are ¼" diameter, 1 ½" length.

While ordering the new heater it was discovered that fabricated aluminum oxide pieces, in the form of thermocouple covers, very nearly matched the desirable dimensions for a sample holder. Ordering these fabricated parts was necessary because the Al_2O_3 was not easily machine-able like the BN stock which had been previously used to make holders. Three 1.27 cm (0.5 inch) OD, 0.635 cm (0.25 inch) ID, 13.97 cm (5.5 inch) long thermocouple covers formed from Al_2O_3 where procured. Upon arrival however, these thermocouple covers where determined to be out of spec. The cartridge heater was not able to slide down the tube and the outer diameter still needed to be

sanded down to be able to fit the 1.194 cm (0.47 inch) ID of the Zircaloy-4 shells. Diamond sanding strips where purchased and the outer diameter was eventually machined to the correct dimensions. However there was no solution to fix the out of spec internal cavity.

In order to facilitate operation, an Al_2O_3 tube 0.635 cm (0.25 inch) ID, 20.32 cm (8 inch) long and 0.9525 cm (0.3275 inch) OD was used to support the samples. This tube however required the use of an aluminum metal sleeve in order to transfer the thermal energy from the outside of the Al_2O_3 sample holder to the ID of the Zircaloy-4 sample (in retrospect, this may have been a detrimental decision as described in section 5.1). Aluminum has a high thermal conductivity of about 200 W/mK and it was a readily available material which could be manufactured quickly and cheaply. Additionally, with this new sample holder, caps were fashioned out of Viton to inhibit solution egress into the inner diameter of the Zircaloy-4 sample. The need for these caps was two-fold. First, the caps would prevent H_2SO_4 from reaching the aluminum sleeves, which would react and dissolve if in contact with the H_2SO_4. Second, the caps would prevent the hydrogen in solution from interacting with the inner surface of the sample tube. These experiments were designed to limit the surfaces into which hydrogen could enter the sample to the outer diameter.

4.1.2 Chemical Procedure Evolution

Hydride platelets were not observed in the SEM images from experiments M1-2x and M1-3x. Initially, the etching of the samples was considered as a potential cause for this lack of visual evidence of hydride platelets. The etching solution was re-mixed and several control samples were exposed to the etchant for various times and then re-imaged. It was determined that the etching procedure, was generally returning the same results as in initial experiments, however there was a notable loss of fine features. Fine features are defined in this work as the trace hydride structures present in raw, control samples. In contrast, the major features are defined as easily definable dense concentrations of hydride formations. Fine features were not the focus of this work but these acid etching results indicated that the etching procedure was not the reason hydride platelets were not observed.

The pickling solution was then considered. If the samples were not being pickled at the same rate, then perhaps a surface treatment or other contamination on the outer surface of the samples was preventing hydrogen absorption and hydride formation. Examination of the mass loss of dissolved material during pickling (Table 8) revealed that the early experiments M2-03, M1-06, M1-1x, and M1-2x all had a 4 to 6 percent mass change after pickling while the M1-30 through M1 - 34 experiments had a 1 to 2 percent mass change. A fresh pickling solution was mixed and sample M1-35 was inserted for pickling. The researcher noted yellowish brown fumes, illustrated in Fig 30 and 31, coming from the pickling jar (contained in the chemical fume hood) and when the sample was removed it was noted that 28 percent of the mass had been dissolved

(Table 8). It was determined that an exothermic reaction was taking place right after the mixing of the solution and that this energetic state of the pickling solution had dissolved the Zircaloy-4 sample at an increased rate. The sample was still run through the experiment to see if any differences could be examined, however no hydride platelets appeared.

Figure 30 Zircaloy-4 sample in pickling solution shortly after mixing the pickling solution. The exothermic reaction with the Zircaloy-4 is accelerated due to the increased temperature of the solution.

Figure 31 Time-lapse of the vapor emitted from the pickling solution suggesting Nitric Acid was breaking down and releasing Nitrogen gas.

Experiment M1-36 was the final experiment conducted and was an attempt at a very long process to form hydrides. The sample only lost 2 percent of its mass after the 5 minutes of pickling. This sample was then re-pickled for another 5 minutes for a total mass loss greater than 4 percent.

Chemical consistency and procedure were determined to be very critical for accurate outcomes of these experiments. While there were relaxed margins since the formation of bulk hydrides platelets was sought instead of fine features, differences in etching times were not systematically investigated in order to analyze any effect on the overall results.

4.2 Hydrogen Insertion into Zircaloy Samples

Hydrogen insertion into the samples was challenging to observe. The SEM/EDS methods are incapable of observing hydrogen in solution. Etching and image analysis was useful to determine the location and morphology of suspected zirconium hydride platelets. While the EDS method is not able to identify hydrogen in a material, the identification of oxygen and nitrogen is possible. By verifying the absence of other elements, and using a process of elimination, it is reasonable to assume that the platelets visible in SEM are due to hydride formation. Thus, these platelets were analyzed for content, especially focusing on oxygen content, in order to rule out those components as possible causes of the difference in density.

Under Back Scattered Electron (BSE) imaging shown in Figs. 32 to 49, dense features show up as a light shade while darker shades indicate less-dense material. . Zirconium hydrides are less dense than the normal zirconium crystals and so the darker regions signify hydride formations. The absence of oxygen in these darker rims, seen in Figs. 37 - 42, and the process used to form said rims, in combination with the existing techniques and reported results in literature, all contributed to a confidence that the darker rim was in fact zirconium hydride. It was shown that differences in charge and charge time would result in varying thicknesses for the rim structure. These results will form the basis for a future parametric study. Table 8 includes the sample masses at different stages of experimentation, but these results are not consistent and the changes in masses were so small that they fell within the bounds of standard error.

The isothermal insertion of hydrogen generated the only easily identifiable zirconium hydride formations of dense rims on the outer surface, and sometimes the inner surface, of the material. When the samples were properly sealed, only the outer surface would develop the rim structure. These rims varied in thickness according to the charging time and the total current.

Experiment M1-30 was meant to be a standard for the M1-3x experiments. M1-30 was conducted with only a 120°C bath and 3 hours of charging at 0.5 A/cm^2. No thermal gradient was applied and a rim between 9um and 10um was expected. This experiment and experiments M1-31 through M1-34 were all conducted within a short time period and without the opportunity to use the SEM imaging due to high demand for time on the SEM. When viewed at the microprobe session, it was apparent that the

attempt to create a hydride rim with isothermal diffusion had failed to develop a rim of hydrides in the M1-30 experiment as well as the M1-31 to M1-34 experiments. This problem permeated the majority of experiments starting with M1-21 through M1-25 and continuing through experiments M1-30 to M1-35.

In comparison, samples from previous vapor synthesis experiments [21], which used the same source of sample material as the electrolytic experiments, were analyzed using similar methods. In these samples, hydride platelets were distributed within the Zircaloy material and were clearly imaged (Figs. 48 to 49). There was a gradient visible in the vapor diffusion samples; however the gradient was dense on the ID of the tube and thinnest on the OD.

Table 8 Changes in Sample Mass During Experimental Operations (Pickling and Hydrogen Charging)

Sample	Experiment Name	sample before pickling [g]	sample after pickling [g]	Percent Loss to Pickling	Final Mass after H_2 charging	Final mass - Pickled Mass [g]	Percent change from H_2 Charging	Important Notes
1	M2-03	4.8822	4.618	5.41%	4.6179	-0.0001	0.00%	
2	M1-06	4.8822	4.5306	7.20%	4.5308	0.0002	0.00%	
3	M1-11	2.4591	2.3294	5.27%	2.3298	0.0004	0.02%	
4	M1-12	2.1123	0	100.00%	2.2027	See note	See note	information lost regarding pickled mass
5	M1-13	2.2964	2.1949	4.42%		See note	See note	M1-13 and M1-14 are same sample.
6	M1-14				2.1967	0.0018	0.08%	
7	M1-20	2.3639	2.2882	3.20%	2.2883	0.0001	0.00%	
8	M1-21	4.5196	4.3275	4.25%	See note	See note	See note	sample sealed onto aluminum
9	M1-22	4.9451	4.7611	3.72%	See note	See note	See note	sample sealed onto aluminum
10	M1-23	4.8938	4.7758	2.41%	2.3728	-2.403	-50.32%	extreme reduction of material occurred
11	M1-24	4.6476	4.5486	2.13%	4.5487	1E-04	0.00%	
12	M1-25	4.7828	4.6494	2.79%	See note	See note	See note	sample sealed onto aluminum
13	M1-30	5.6014	5.4687	2.37%	5.4686	-0.0001	0.00%	
14	M1-31	5.55	5.4513	1.78%	5.4514	0.0001	0.00%	
15	M1-32	5.6554	5.56	1.69%	5.56	0	0.00%	
16	M1-33	5.7752	5.6903	1.47%	5.6955	0.0052	0.09%	
17	M1-34	6.3157	6.2318	1.33%	6.2394	0.0076	0.12%	
18	M1-35	6.316	4.5453	28.04%	See note	See note	See note	sample sealed onto aluminum
19	M1-36	6.3997	6.1281	4.24%	6.1193	-0.0088	-0.14%	

4.2.1 Control and Initial Experiment Matrix

In order to compare and contrast developed hydrides from native hydrides present in the raw material, sample R1 was included in the first SEM imaging session. R1 was a section of Zircaloy-4 tubing which did not undergo any pickling and was not electrolytically charged. This sample was included in the mount with the M2-03 and M1-06 samples. It was polished, etched and then viewed with SEM imaging. Figure 32 is a full width Back Scattered Electron (BSE) image of R1 in which fine features, very light, widely dispersed hydride platelets, are visible. Figure 33 is a Secondary Electron (SE) image of the same area. These features would be found in other samples and were used as a gauge to identify the quality of the etching process. Clear and distinct fine features represented “great” etches of samples. Variations in etching times and rinsing processes were not tracked during these trials. It was only necessary to get “good” etches on samples which would indicate major hydride formations and orientations.

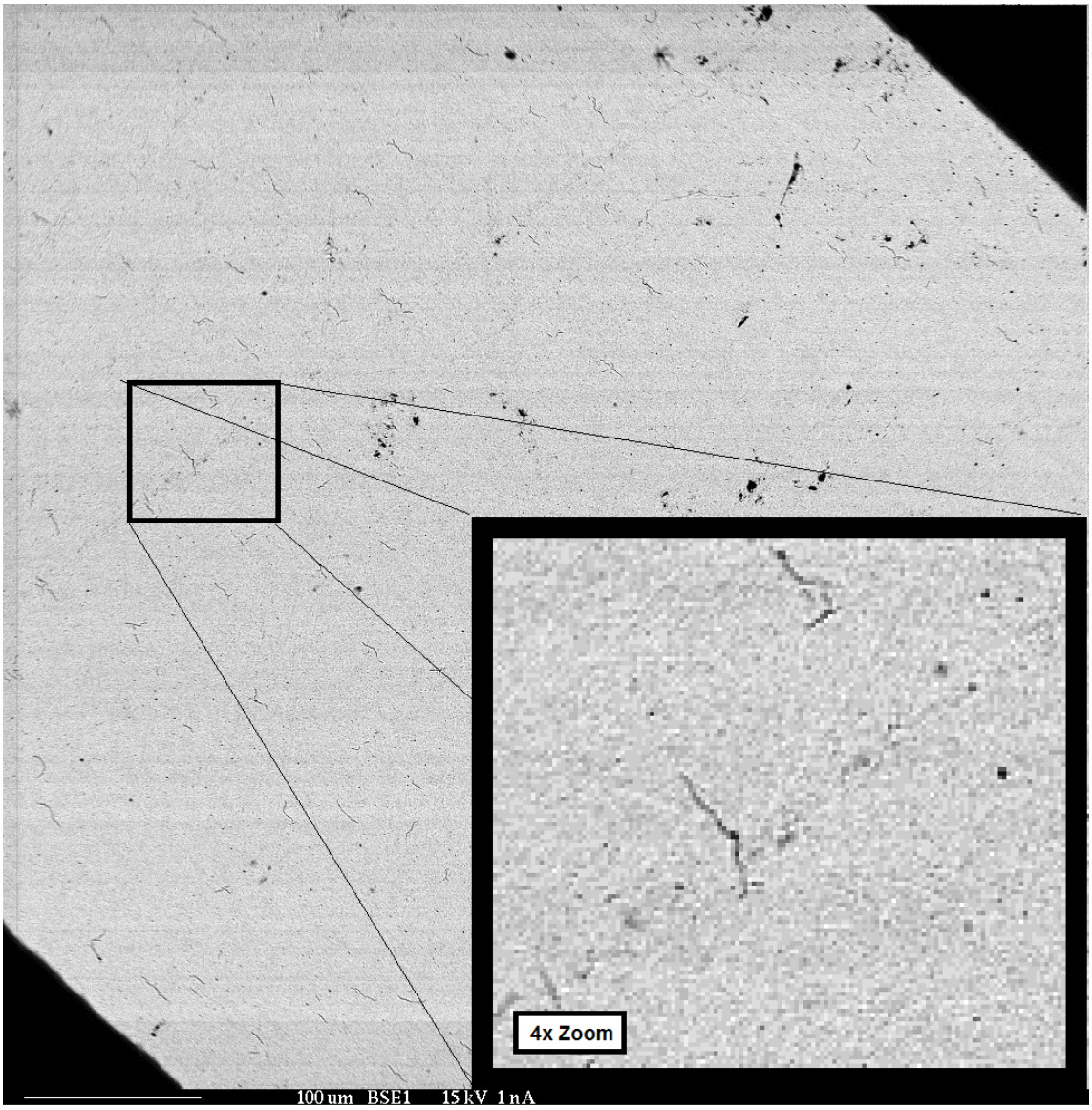

Figure 32 BSE image of the R1 sample indicated small, widely dispersed hydride platelets were artifacts of the fabrication process (Same location as Figure 5a).

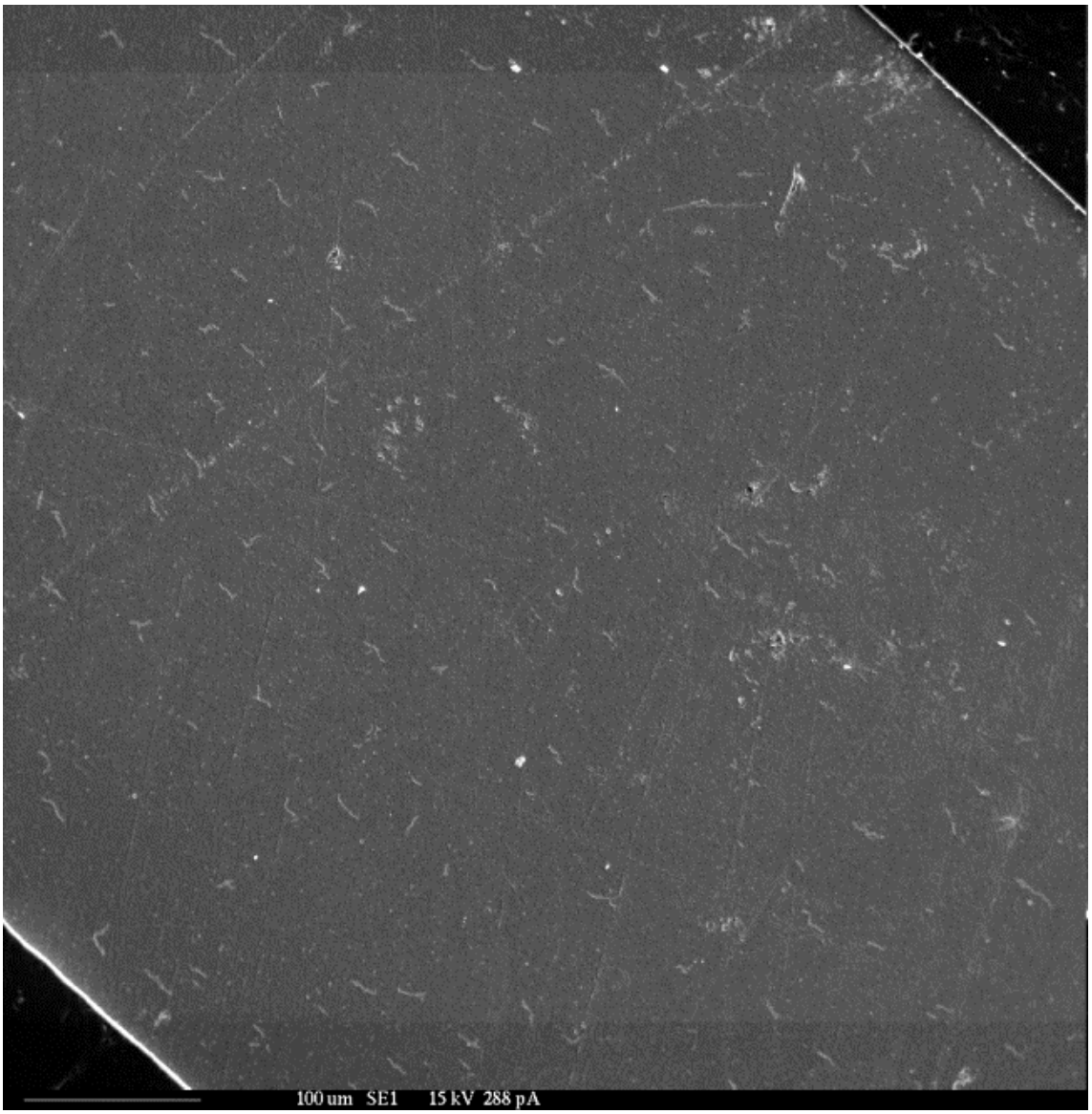

Figure 33 Secondary Electron Image of control Zircaloy-4 sample.

The only sample taken with the Method 2 procedure, M2-03, was imaged along with R1. This experiment was run at 90°C for 3 hours at 0.2 A/cm^2 with a bronze electrode resulting in an electroplating of the anode. This sample underwent the same polish and etch as the R1 sample. Results from the SEM imaging (Fig. 34) showed the

same fine features as identified in the R1 sample. There was no clear distinction between the SEM images of R1 and M2-03

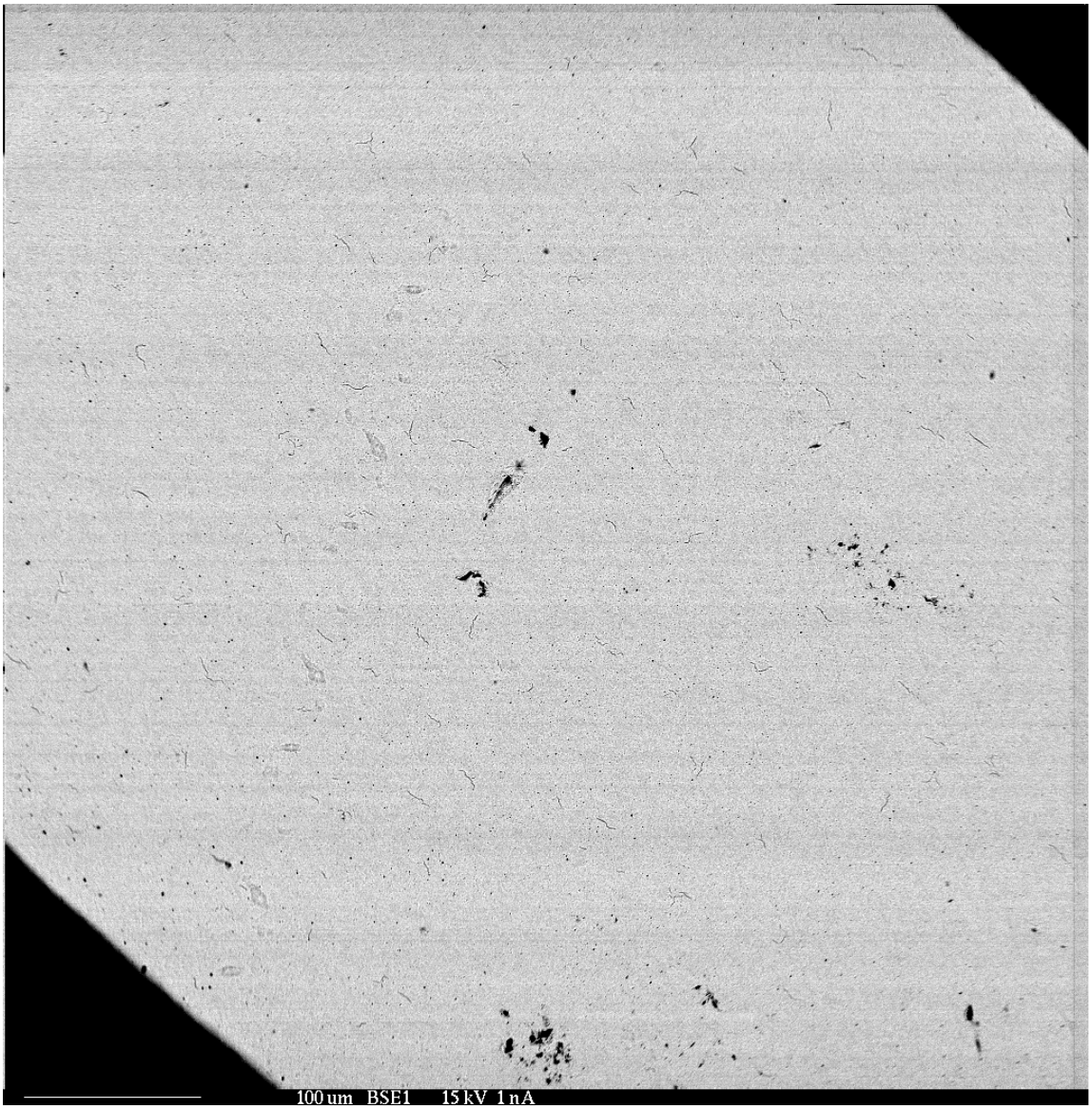

Figure 34 The M2-03 center portion of the sample was showed no distinguishable difference from the R1 sample.

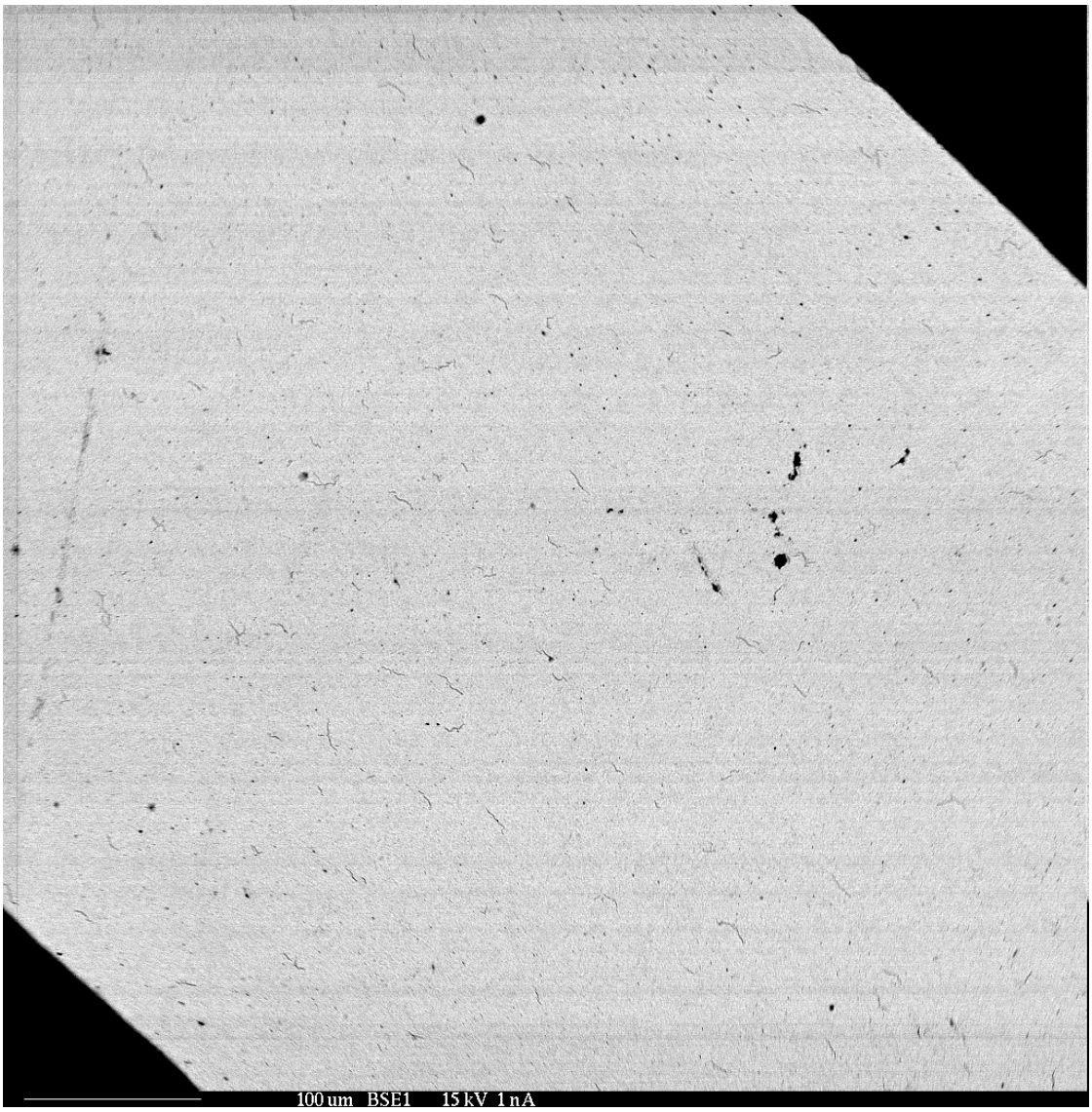

Figure 35 The M1-06 center portion sample was indistinguishable from the R1 sample and lacked any of the expected major hydride formations.

Experiment M1-06 was the first Method 1 experiment conducted with a new graphite electrode to replace the bronze electrode. This experiment ran for 2 hours at 0.4 A/cm^2 in a 90 °C bath. It was also mounted with R1 and M2-03 and imaged at the same

time. Upon inspection (Fig. 35) the same fine features where visible, as seen in R1. The M1-06 sample lacked of any major hydride formations.

4.2.2 Isothermal Insertion of Hydrogen

The first experiment to show a minimal indication of hydride formation was M1-11. This experiment was conducted for 2.7 hours at 1 A/cm^2 in a 90 °C bath in an attempt to maximize the charge applied to the sample. While examining the edge with SEM imaging, it was noted that some of the material was fractured from the surface by the shrinking epoxy. An EDS was taken of the less dense formation to make sure it was not oxidation and an image was taken of this small feature, Fig. 36 and 37. This was the first time hydrides could be confirmed and a later re-polishing of the sample would reveal the hydride rim, (Fig. 38 and 39). The rim was measured using ImageJ software to record 20 measurements of the dark rim features. These measurements where then calculated for a mean value and associated standard deviation.

Thicker hydride rims were formed on the outer diameter rather easily if the ends of the sample were sealed. Rims were also formed on the inner surfaces when the seals were not effective and the sample was completely exposed to solution. Experiments M1-11, M1-12, and M1-13 all developed clear and easily identifiable rims (Figs. 38 to 43). These rims were so dense that the material became brittle enough to be cracked by the drying epoxy which exerted a tensile force normal to the surface of the sample. Once it was clear that rims could be formed, the demonstration focus shifted to electrolytic

charging with a thermal gradient. This proved to be a premature decision, since no further evidence of hydride formation was observed (see Section 4.2.3). Figures 38 through 43 illustrate the rims found in experiments M1-11, M1-12, and M1-13 and Table 9 records the parameters of each experiment.

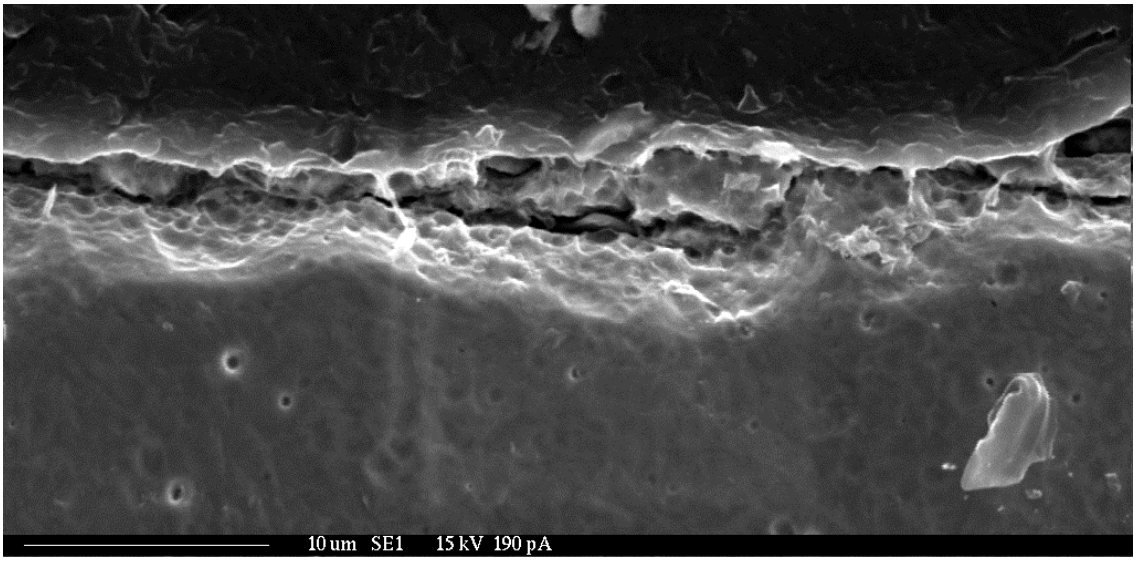

Figure 36 This SE image of M1-11 on 01-18-12 was the first positive sign of zirconium hydride formation. The sample is on the bottom and the epoxy is above the embrittled formation.

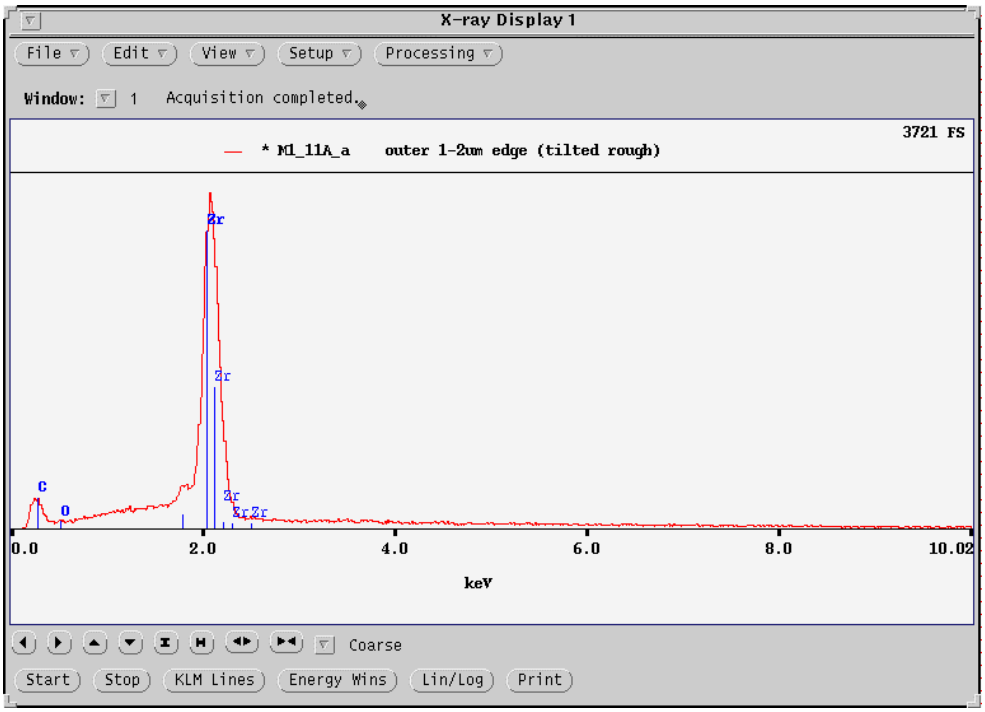

Figure 37 EDS of M1-11A showing no noticeable increase in oxygen in suspected zirconium hydride area.

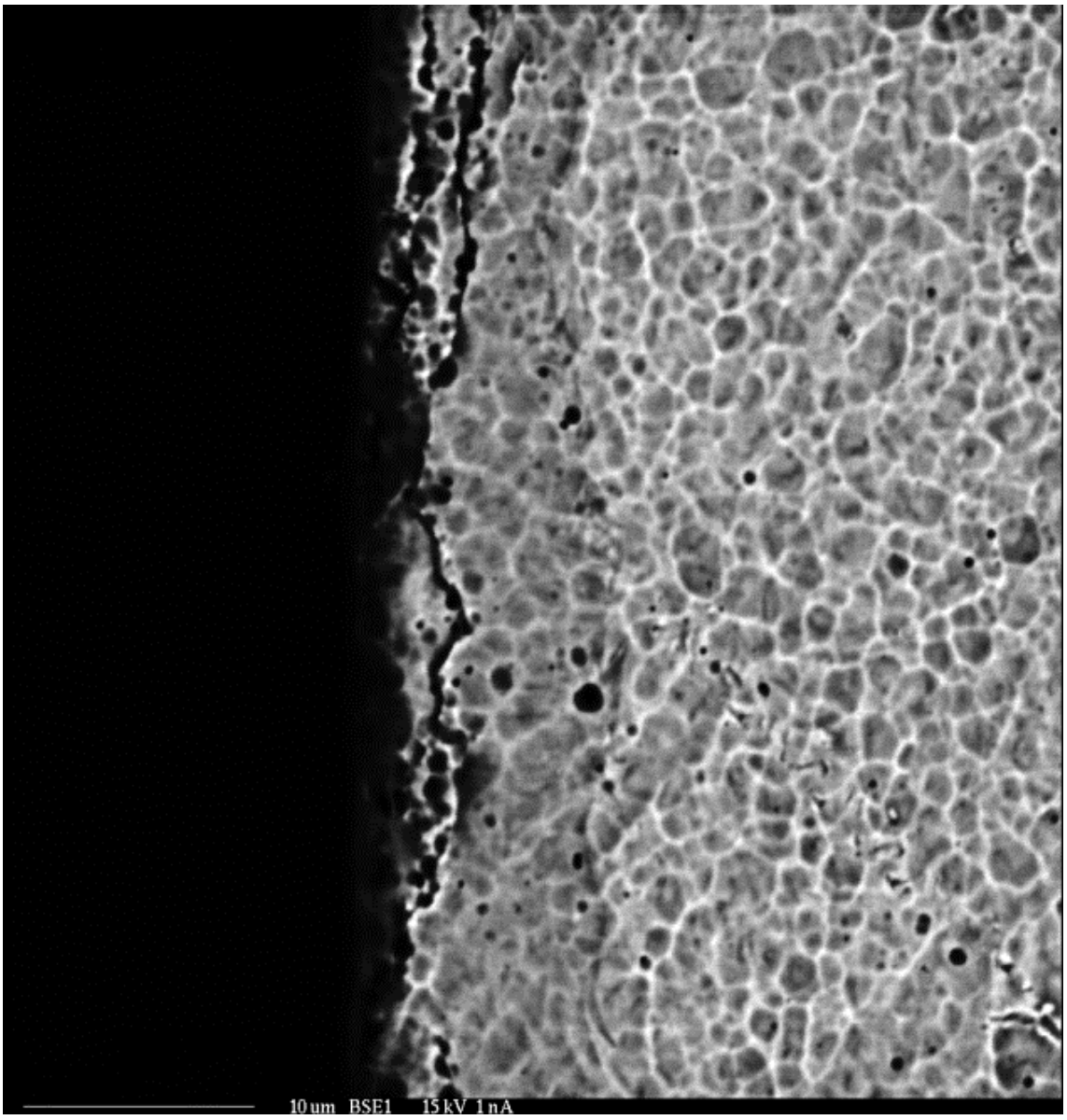

Figure 38 Back Scattered Electron image of 8.69 +/- 0.982 µm hydride rim from Experiment M1-11 which used a 1 A/cm^2 charge over 2.7 hours in a 90°C bath.

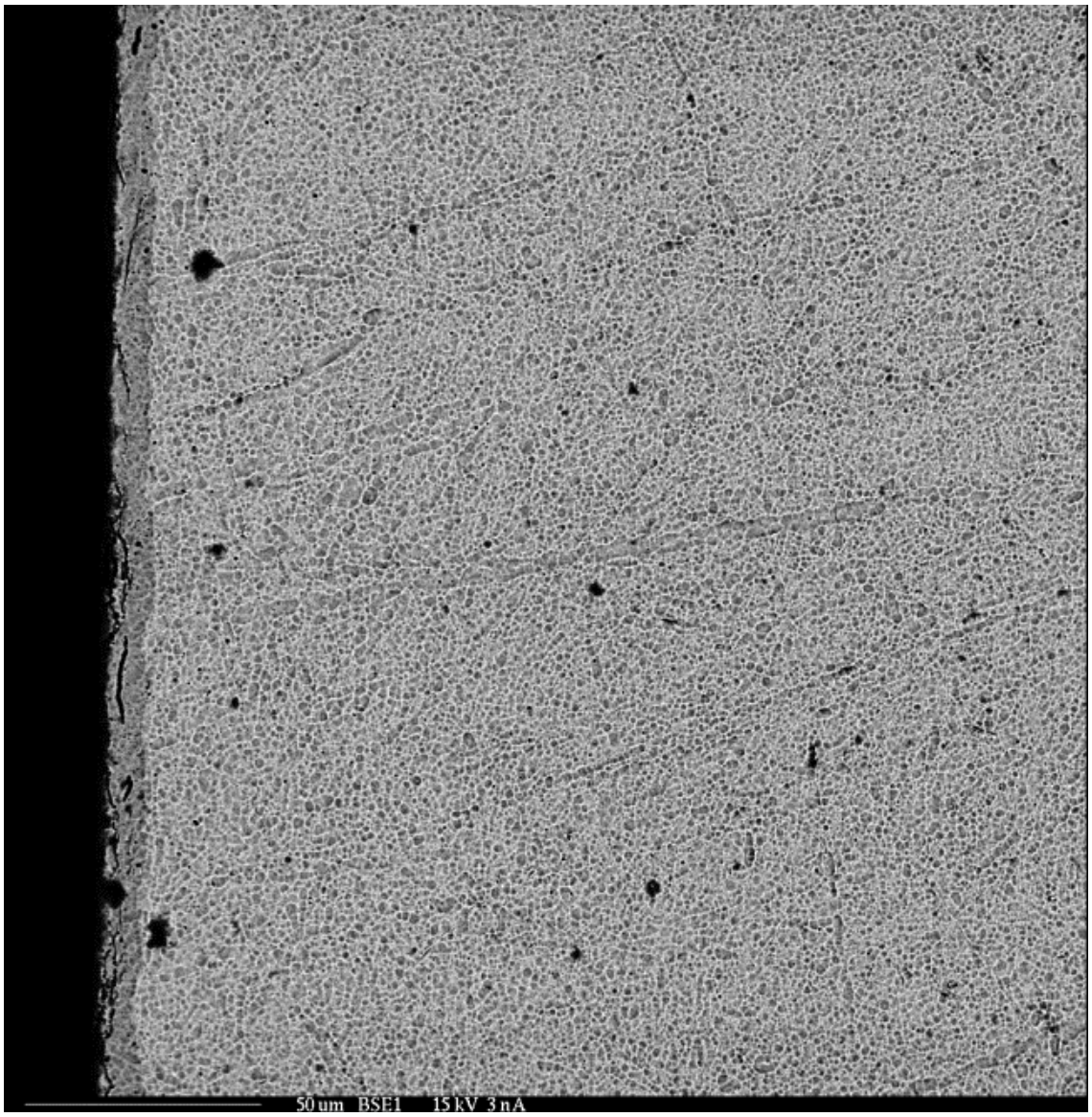

Figure 39 Back Scattered Electron image of hydride rim from Experiment M1-11.

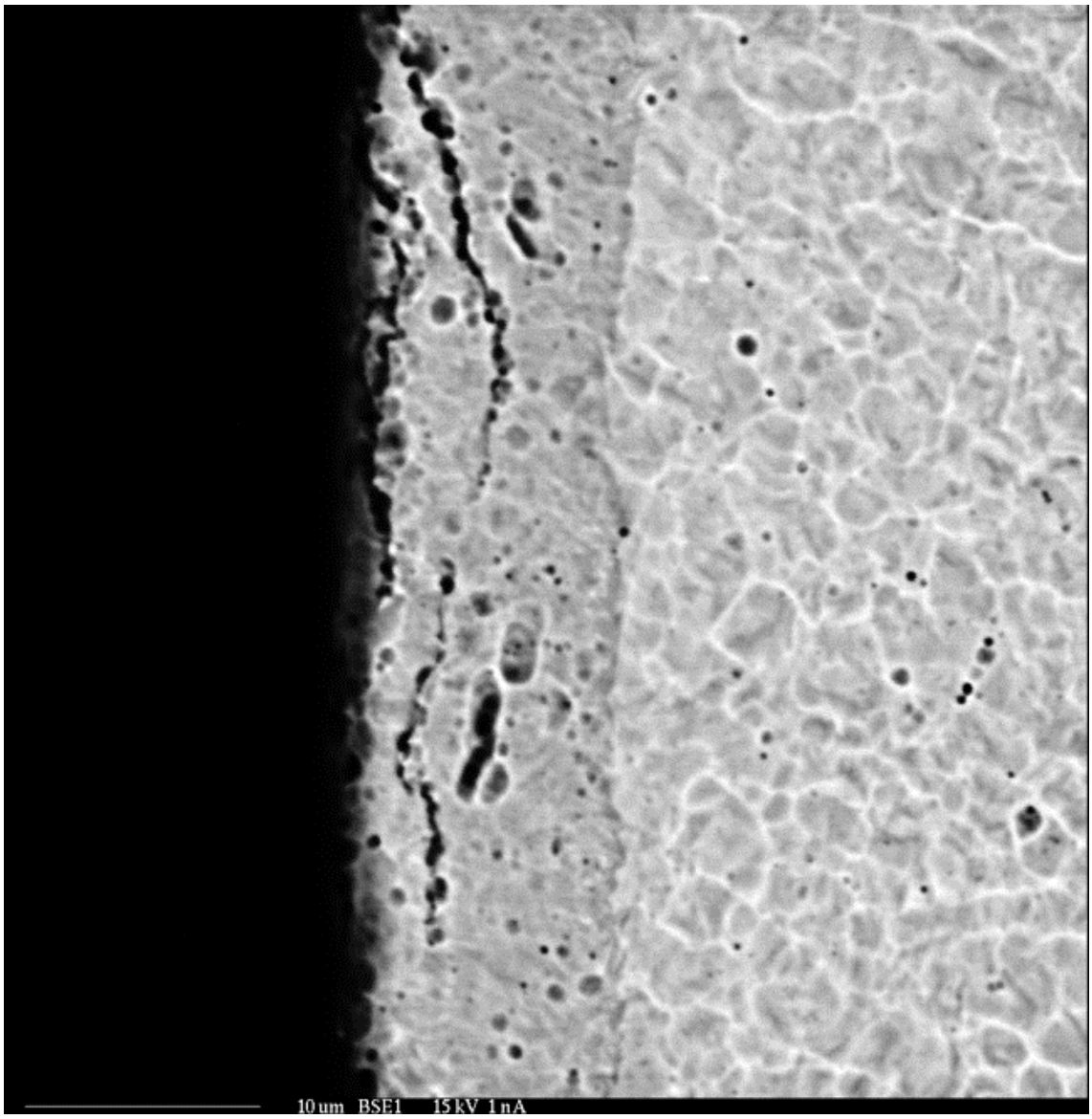

Figure 40 Back Scattered Electron image of 11.023 +/- 0.465 µm hydride rim from Experiment M1-12 which used a 0.5 A/cm^2 charge over 5.8 hours in a 90°C bath.

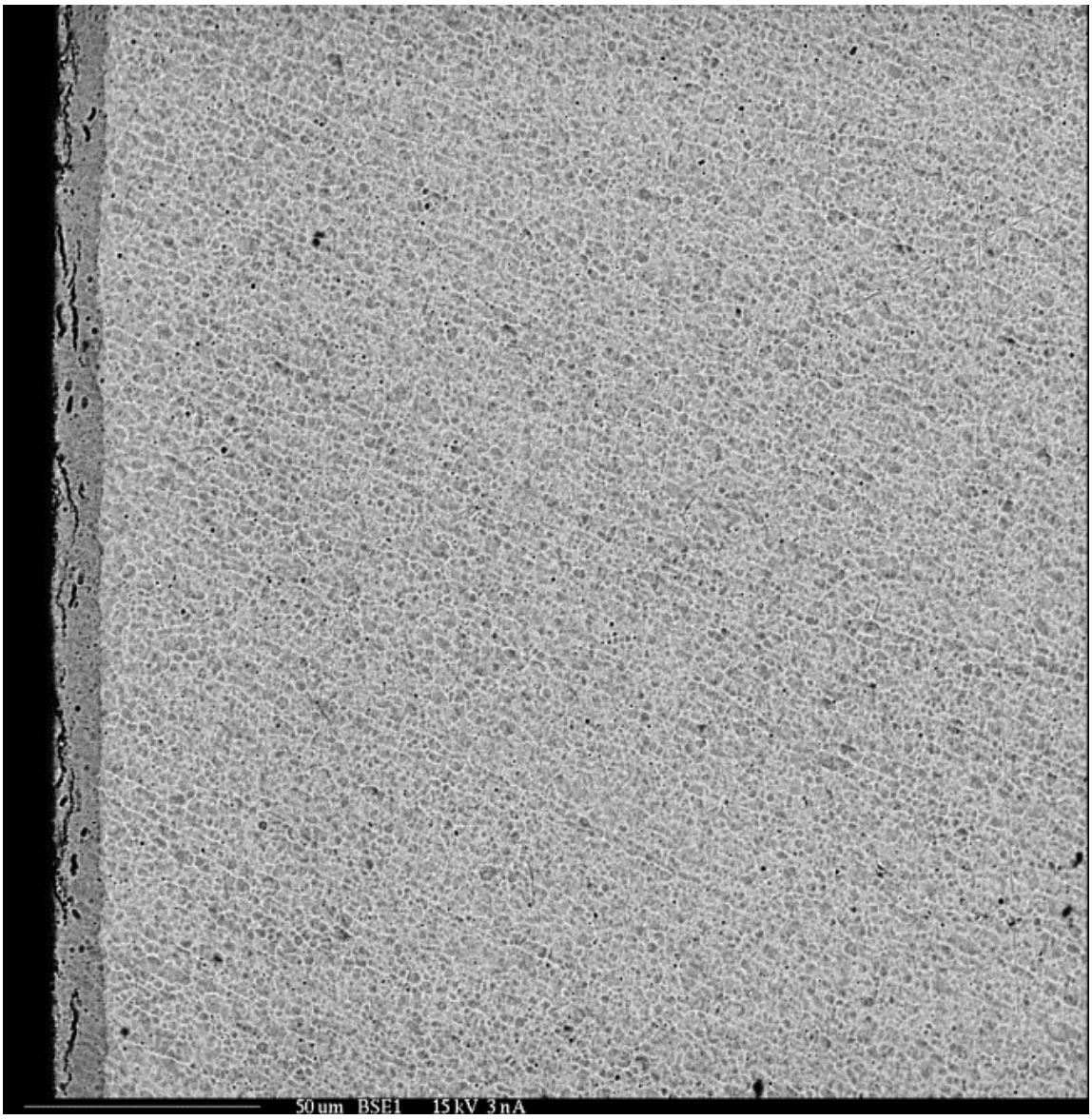

Figure 41 Back Scattered Electron image of hydride rim from Experiment M1-12.

As mentioned in section 4.1, M1-13 and M1-14 experiments where completed on the same sample due to a broken circuit, during experiment M1-13, before the goal charge time of 24 hours was accomplished. M1-13 was conducted at 0.5 A/cm^2 for 6.1 hours in a 124.54 +/- 6.659 °C bath and followed by M1-14 which was conducted at

0.25 A/cm^2 for 2.3 hours at 121.778 +/- 0.213°C This combination of charges and the longest run of 8.4 hours resulted in the thickest rim formation at 12.365 +/- 0.635 µm.

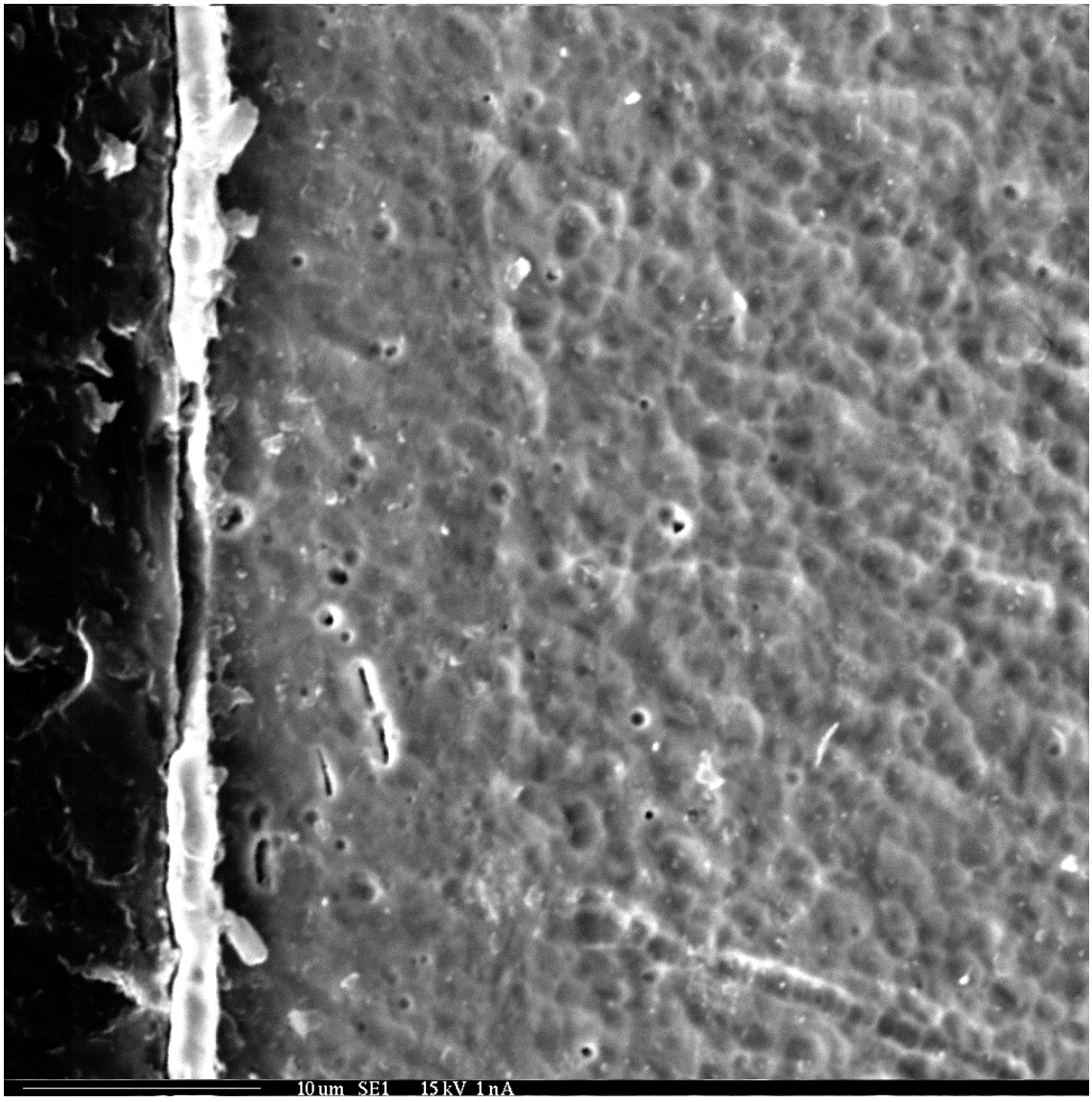

Figure 42 Secondary Electron image of 12.365 +/- 0.635 µm hydride rim from Experiment M1-13 which was conducted along with M1-14 on the same sample resulting in an 8.4 hour charge time in ~120°C boiling bath.

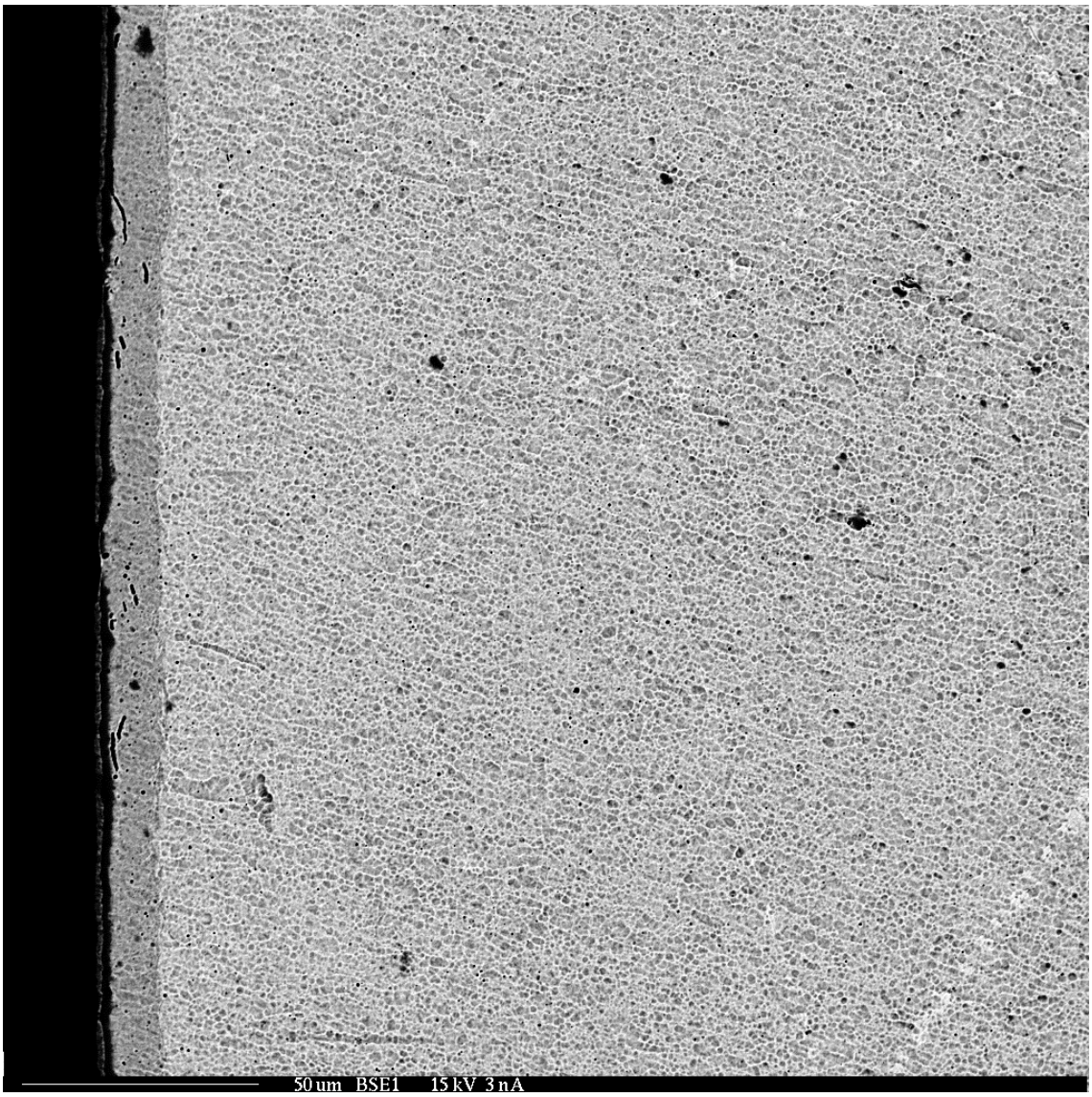

Figure 43 Back Scattered Electron image of hydride rim from Experiment M1-13, OD.

Experiment M1-30 was conducted at 120 °C for 3 hours with a charge of 0.5 A/cm^2 and was intended to serve as a control for the following M1-31 to M1-36 experiments. These experimental parameters place M1-30 in the isothermal category and a rim was expected to form. Figures 44 to 46 show an absence of the hydride rim.

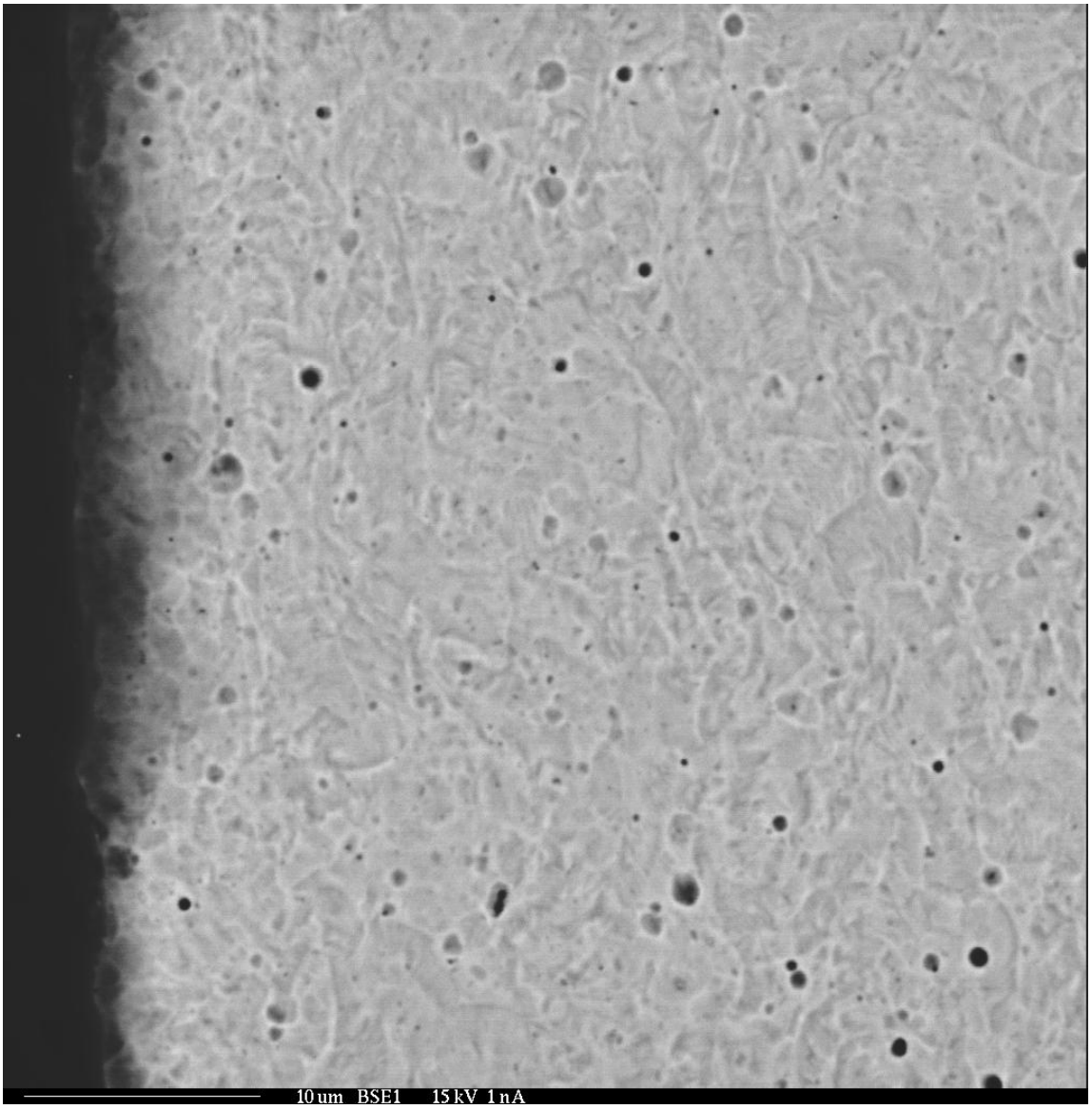

Figure 44 BSE image of Experiment M1-30, outer surface, which was conducted for 3 hours with a charge of 0.5 A/cm^2 in a ~120°C boiling bath. Pore development is more evident than in previous images.

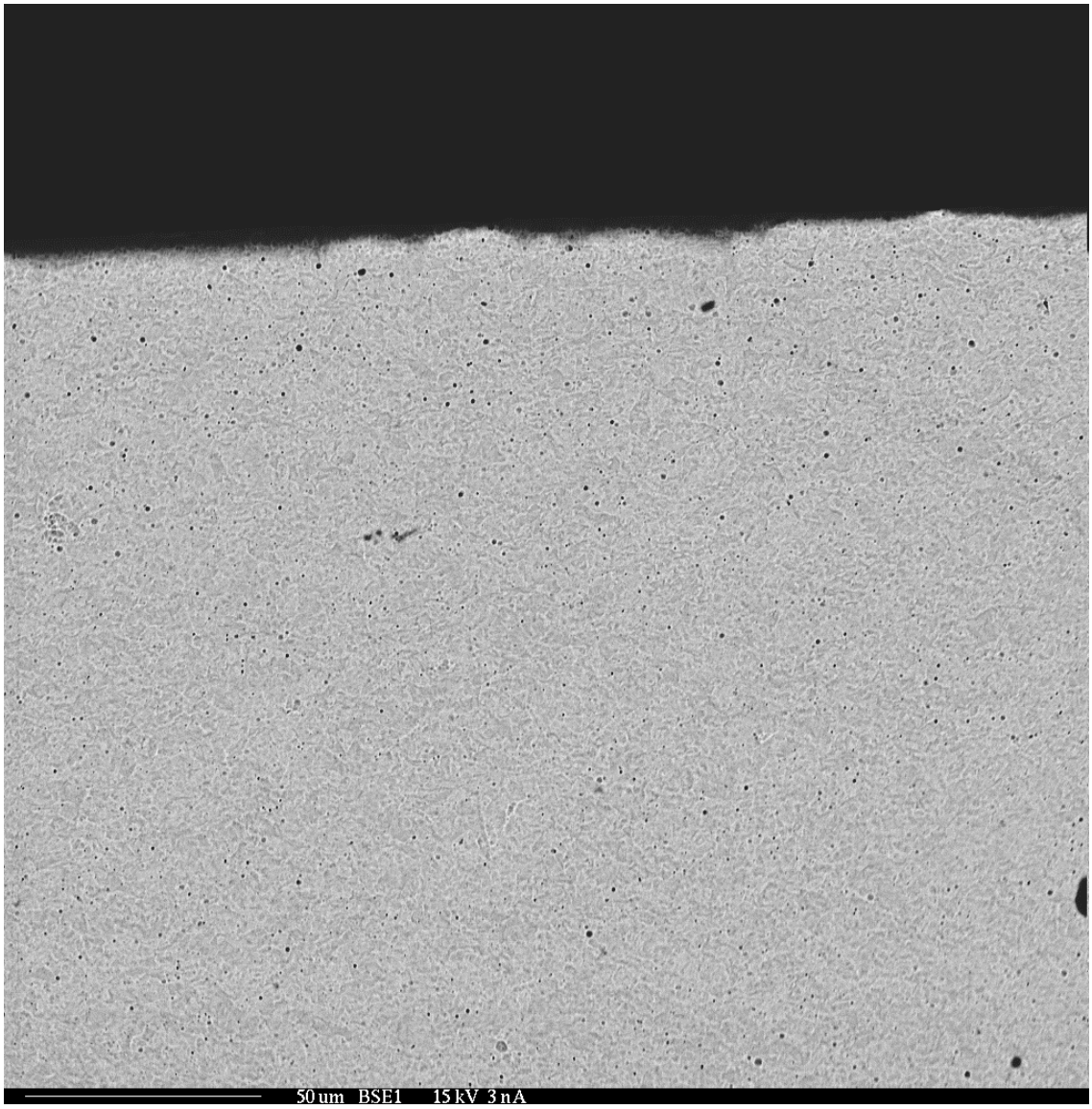

Figure 45 BSE image of Experiment M1-30, outer surface, which was conducted for 3 hours with a charge of 0.5 A/cm^2 in a ~120°C boiling bath. Small pores are observed. No rim structure is observed.

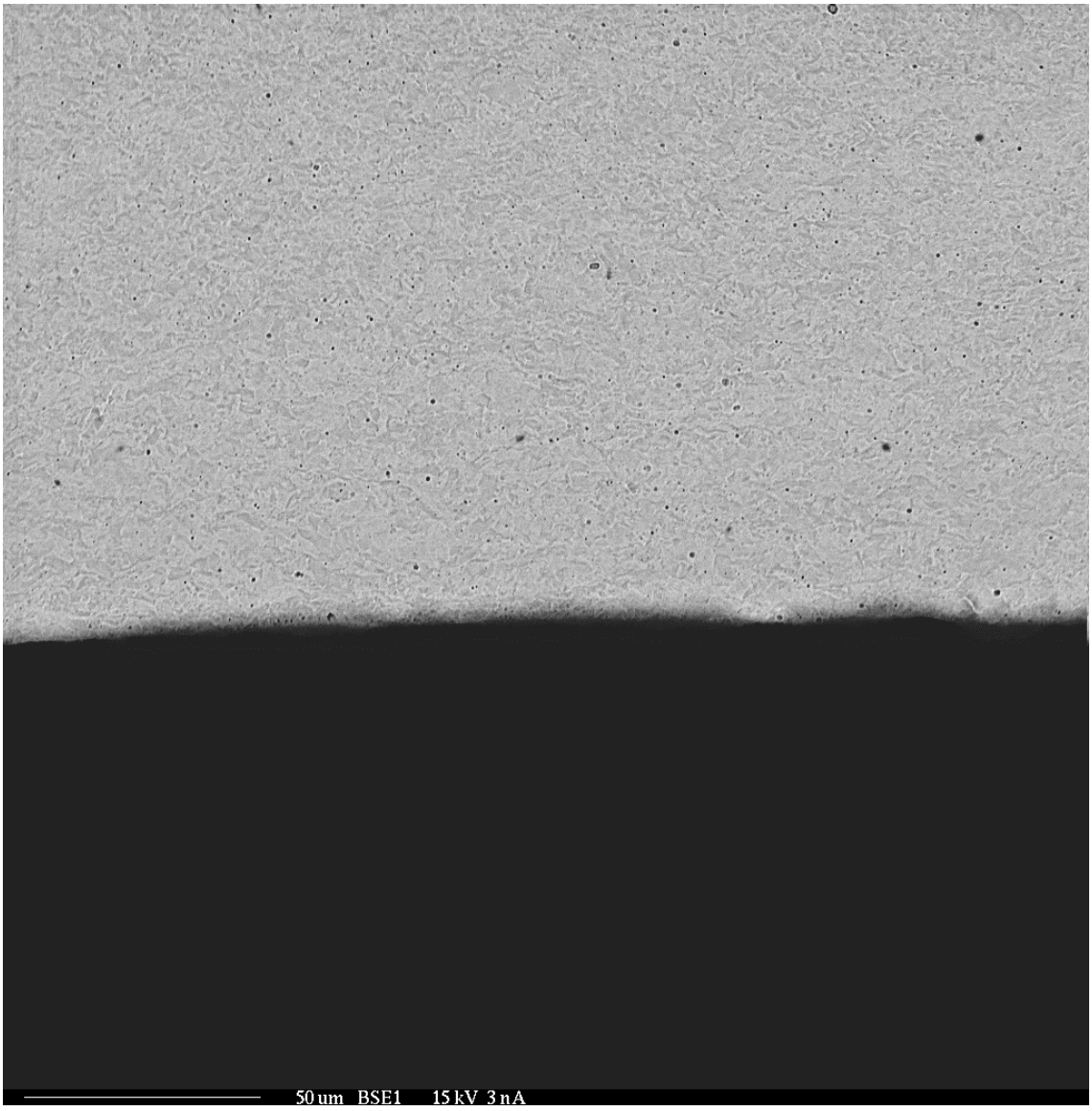

Figure 46 BSE image of ID from Experiment M1-30 showing small pores and sparse porosity.

While the imaging of experiment M1-30 failed to show a hydride rim, the good etch revealed small pores. Theories for this porosity are discussed in section 5.1.

Table 9 The parameters for the isothermal experiments are found below.

Sample	Experiment Name	Heater Device #1	Solution Temp measured [°C]	Heater Device #2	Heater #2 TEMP [°C]	Amperage [A/cm^2]	Measured Voltage [V]	Std Dev [+/- V]	Charging Time [hours]
1	M2-03	hotplate	90.099	0.69	-------	0.2	1.655	0.299	3
2	M1-06	cartridge	91.08	0.84	-------	0.4	6.609	0.615	2
3	M1-11	cartridge	90.556	0.544	-------	1	8.12	0.973	2.7
4	M1-12	hotplate	90.121	0.678	-------	0.5	5.896	0.191	5.8
5	M1-13	hotplate	124.5397	6.659	-------	0.5	6.163	0.508	6.1
6	M1-14	hotplate	121.778	0.213	-------	0.25	4.963	0.640	2.3

4.2.3 Static Thermal Gradient Insertion of Hydrogen

The experiments using the thermal gradient, M1-20 to M1-25 did not return favorable results as expected. In fact, every single experiment failed to form any hydride rim and hydride fine features were very sparse. This indicated that either hydrogen had not entered the Zircaloy-4 sample, or that the hydrogen which entered had not reached the saturation point necessary to form ZrH platelets. In many samples, the only indication that a reaction had taken place was the increased amount of porosity, in the material. The cause of the increased porosity of the Zircaloy-4 samples has not been identified and theories for the porosity are found in section 5.1.

Experiments M1-20 through M1-25 were initiated with bath temperatures of ~120°C and the thermal gradient was established before activating the system current. Table 10 shows the experiment matrix for M1-20 through M1-25. At the end of each experiment, the charge was turned off and the sample was allowed to cool. In experiments M1-20 to M1-22 the cooling was accomplished by turning off the hotplate and the cartridge heater and allowing natural convection to reduce the system temperature. In other experiments, M1-23 to M1-25, a slower cooling process was used. This slow cooling process was set to be -1°C per; A. Motta reported that hydrides are more likely to form with a slow cooling rate. [6]

Table 10 Experimental parameters for M1-20 through M1-25.

Sample	Experiment Name	Solution Temp measured [°C]	Heater #2 TEMP [°C]	Programmed Amperage [A/cm^2]	Measured Amperage [A/cm^2]	Charging Time Goal [hours]	Charging Time Actual [hours]	"Slow" cooling?
7	M1-20	126.771 +/- 5.983	190*	0.5	0.494 +/- 0.007	48	16.6	n
8	M1-21	120.157 +/- 0.610	259.43 +/- 1.48	0.5	0.493 +/- 2.732E-13	12	10.2	n
9	M1-22	121.871 +/- 1.290	247.14 +/- 0.602	0.5	0.485 +/- 4.181E-13	72	70.1	n
10	M1-23	117.328 +/- 0.438	199.584 +/- 3.134	1	0.993 +/- 1.916E-13	24	2.2	y
11	M1-24	119.774 +/- 1.454	205.001 +/- 2.120	0.5	0.485 +/- 9.03E-14	24	24	y
12	M1-25	117.983 +/- 0.546	342.447 +/- 6.764	0.5	0.489 +/- 2.537E-13	24	8	y

*The cartridge heater was controlled by a separate device, Thermal Solutions Temperature Control Unit, which required the Thermocouple input located inside of the cartridge heater. No temperature information was recorded but notes from the lab indicate that, while the target temperature was 200°C, the cartridge heater only reached 190°C

Experiment M1-20 was conducted using a temperature controller, Thermal Solutions Model: EZ-Zone PM which required the thermocouple input from the cartridge heater and did not permit recording of the temperature. Over the course of the experiment as H_2O boiled off and was electrochemically separated into H_2 and O_2, which escaped the system. This reduction in H_2O resulted in a solution that contained more H_2SO_4 relative to H_20 and, with its higher boiling point, H_2SO_4 was capable of retaining more energy before boiling. Thus, while the bath was brought to a boil at ~120°C initially, the solution temperature would gradually increase over time. Overall, the temperature of the system was 126.771 +/- 5.983 °C. The experiment ran for 16.6 hours at 0.494 +/- 0.007 A/cm^2 before the circuit was broken due to failure of the zirconium anode wire.

This was the first experiment to use the Al_2O_3 sample holder with the Viton caps and the aluminum sleeve. All subsequent experiments would use this same sample holder though the aluminum sleeve would be replaced or reused depending on the condition of the sleeve after a given experiment. If H_2SO_4 reached the aluminum sleeve because the Viton caps were not sealed tightly to the sample, the aluminum would corrode and expand. This expansion, when it occurred, made it very difficult to remove the sample from the Al_2O_3 sample holder and a hammer and chisel where needed to dislodge the sample and aluminum sleeve.

From experiment M1-20 through the last experiment M1-36, no hydride rims would develop. The failure to develop hydride rims may be related to the use of Viton and aluminum and is discussed in section 5.1.

Figures 47 to 49 illustrate the SEM imaging of sample M1-20. These results showed fine hydride features throughout the material, which were similar to those of the

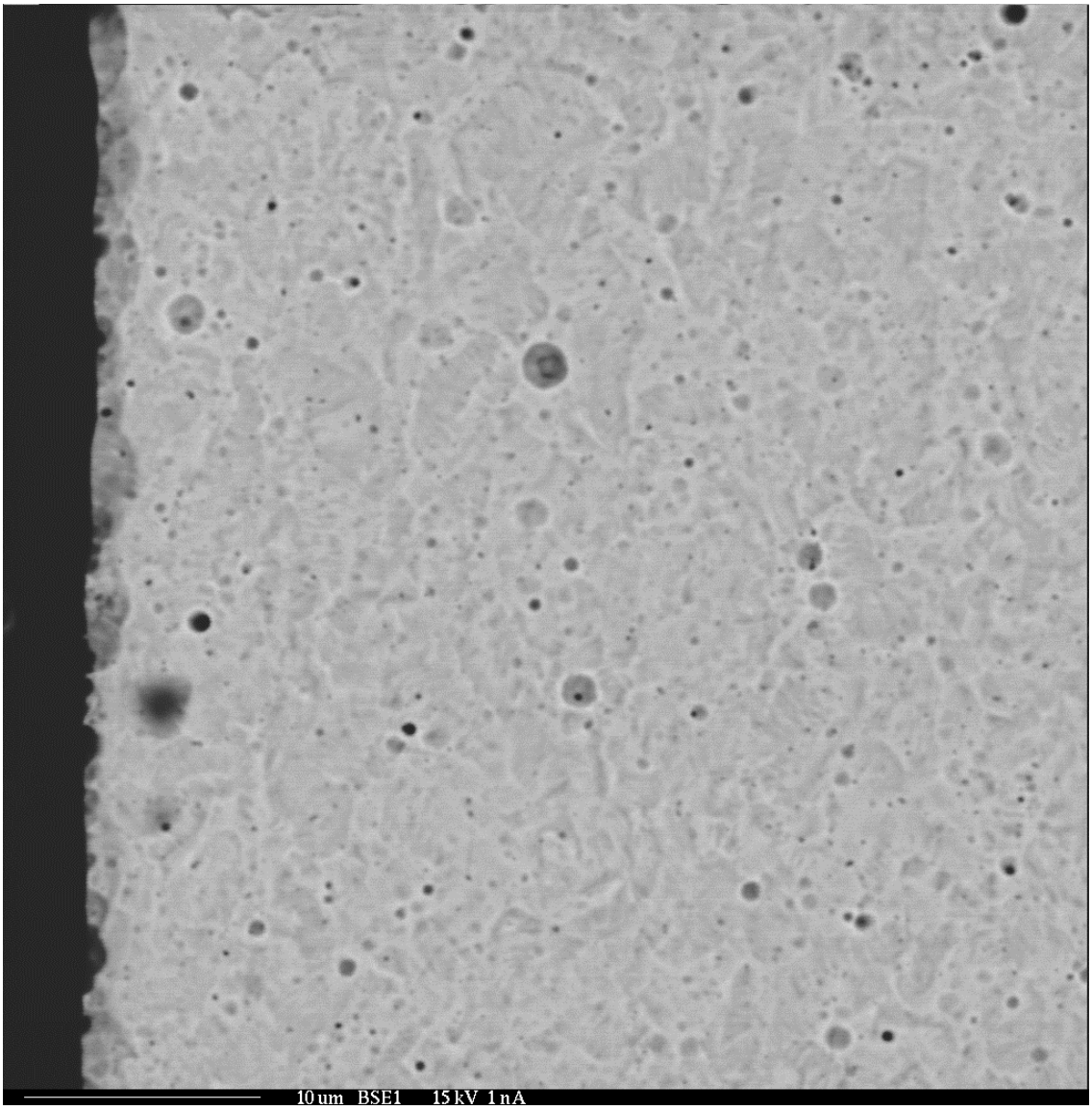

Figure 47 BSE image of experiment M1-20 outer surface with no rim formation, large pores, and higher porosity. This experiment was charged for 16.6 hours at 0.494 +/- 0.007 A/cm^2 with a bath temperature of 126.771 +/- 5.983 °C and a static cartridge heater temperature ~190°C.

control R1. At the same time, visual inspection revealed that pores had also developed which were larger than those in R1.

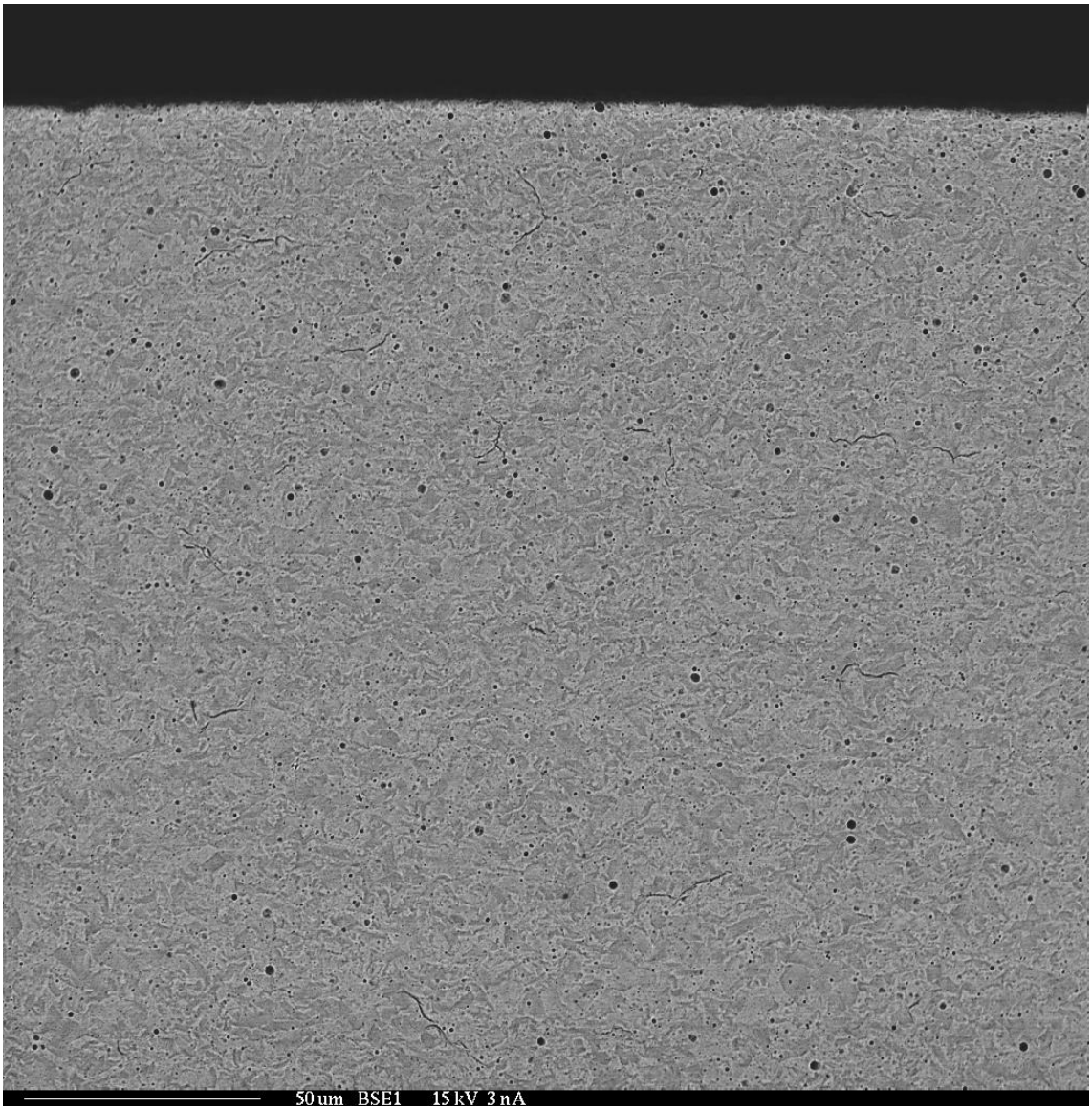

Figure 48 BSE image of experiment M1-20 illustrating fine hydride features and increased porosity on the outer surface.

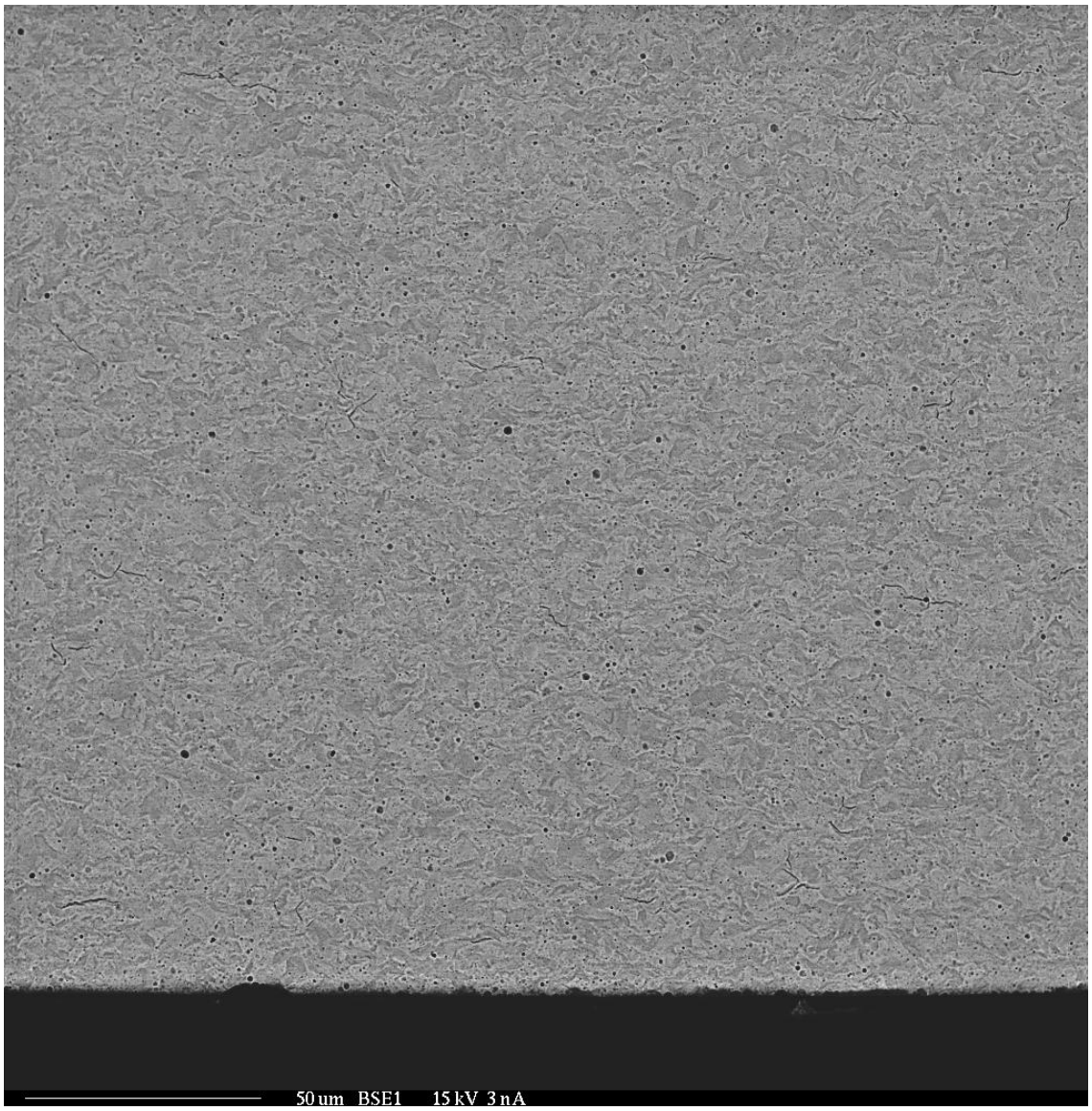

Figure 49 BSE image of experiment M1-20 illustrating a relatively lower porosity in the inner surface, compared to the outer surface, along with other fine hydride features.

Experiment M1-21 was conducted using a variac, STACO ENERGY Model 3PN1010B, which allowed analogue control of the cartridge heater while the thermocouple T2 reading the cartridge heater temperature was recorded with the

LABVIEW L2.vi program. Starting with this experiment, the rest of the experiments M1-22 to M1-25 and M1-30 to M1-36, ran with the same equipment and software configuration. The temperature of the system was 120.157 +/- 0.610 °C while the cartridge heater was kept at 259.43 +/- 1.48 °C. The experiment ran for 10.2 hours at 0.493 +/- 2.7321E-13 A/cm^2 before the zirconium anode wire failed and the circuit was broken. This experiment was imaged with the microprobe. Results mirrored those of M1-20 and no significant differences were noted.

Experiment M1-22 was conducted with an solution temperature of 121.871 +/- 1.29 °C while the cartridge heater was kept at 247.14 +/- 0.602 °C. The experiment ran for 70.1 hours at 0.485 +/- 4.181E-13 A/cm^2 before being shut down normally. This was the longest experimental run conducted and yet no hydride rim was formed. In the BSE images (Fig. 50 to 52), a very high porosity of small pores was observed along with larger pores.

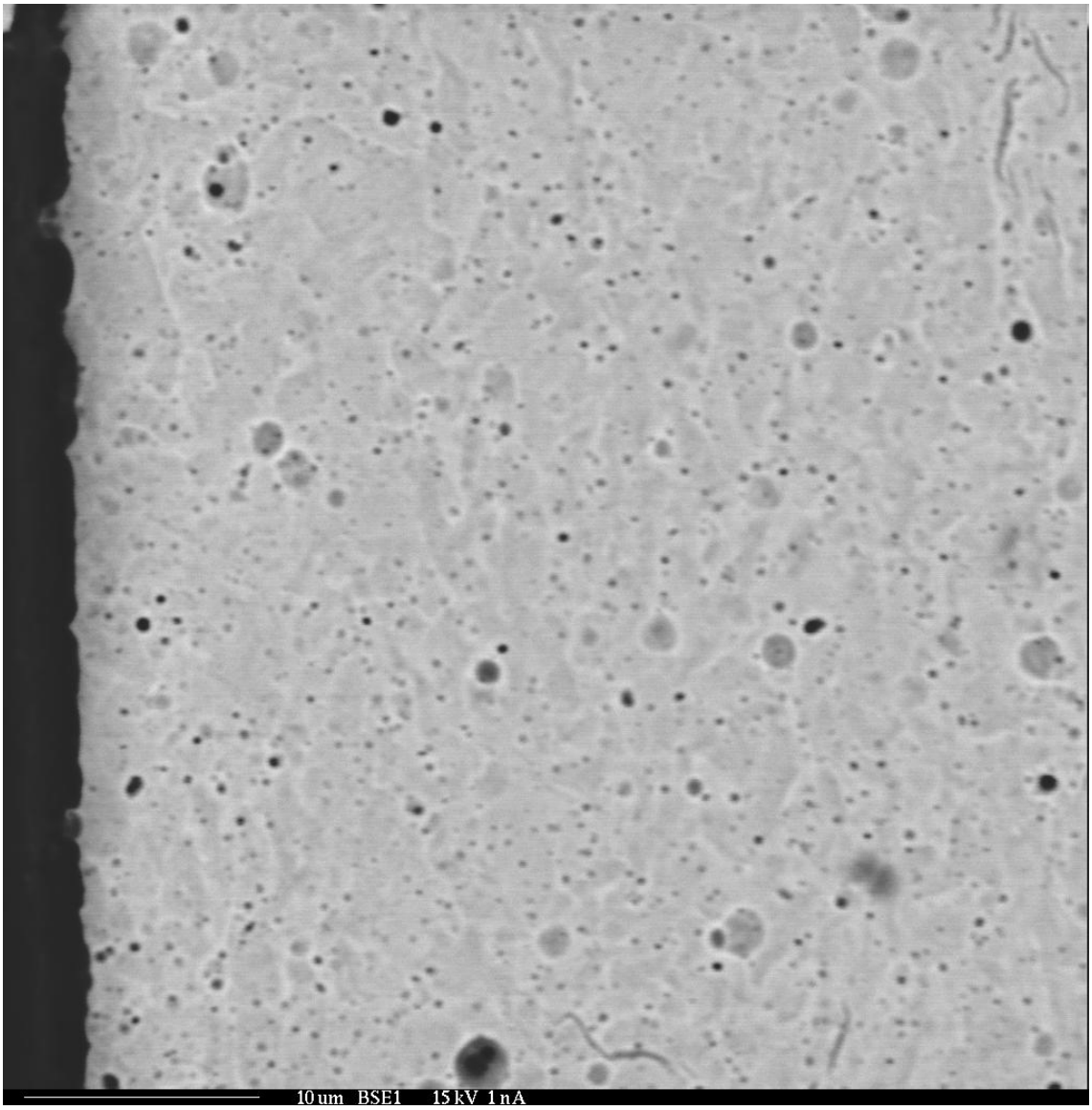

Figure 50 BSE image of Experiment M1-22 conducted at 121.871 +/- 1.29 °C while the cartridge heater was kept at 247.14 +/- 0.602 °C. The experiment ran for 70.1 hours at 0.485 +/- 4.181E-13 A/cm^2. The porosity of small pores was extremely high and the large pores were still evident. Fine hydride features were observed, but no hydride rim or other major features were detected.

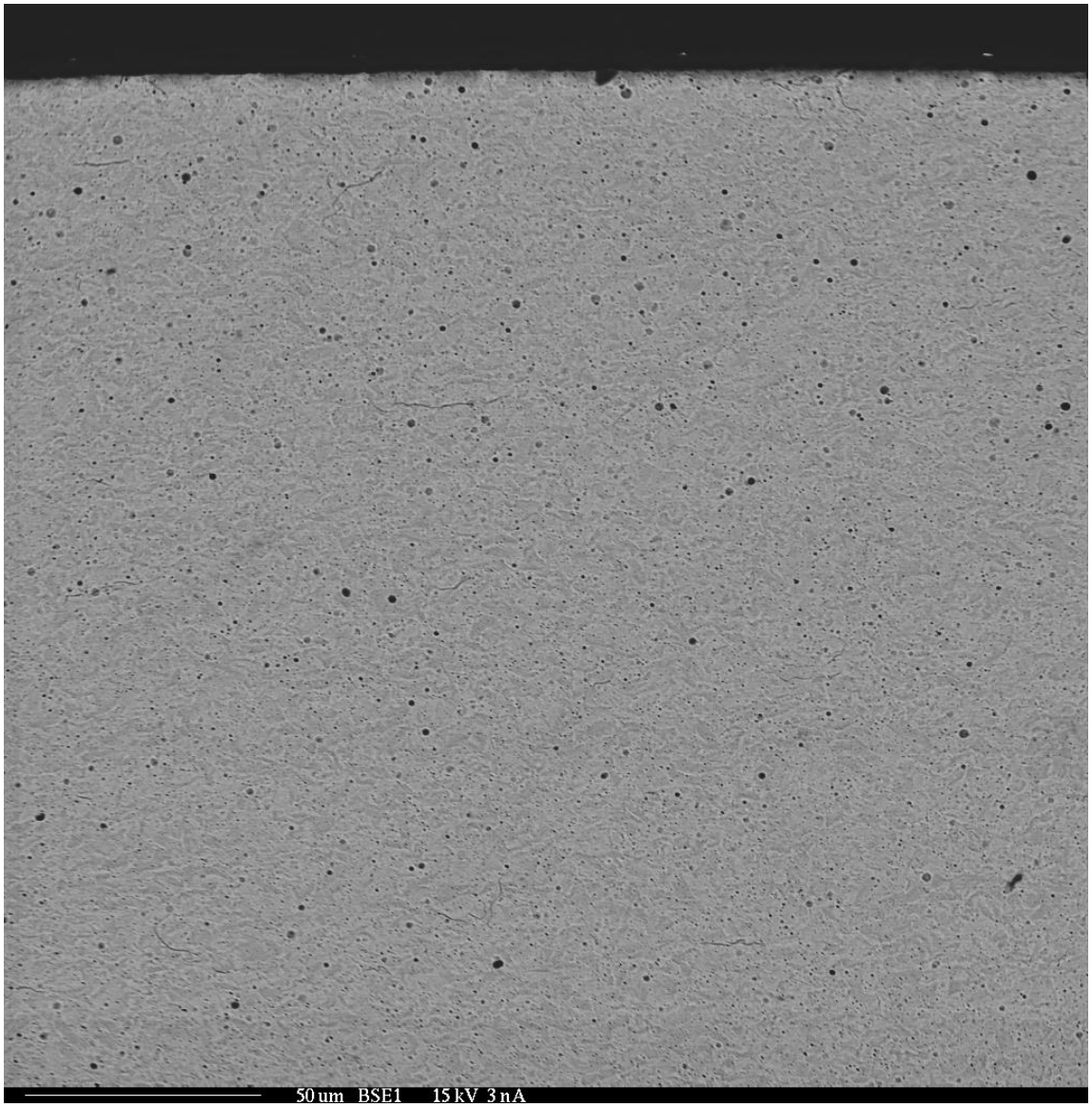

Figure 51 BSE image of experiment M1-22 outer surface with increase porosity and no hydride rim.

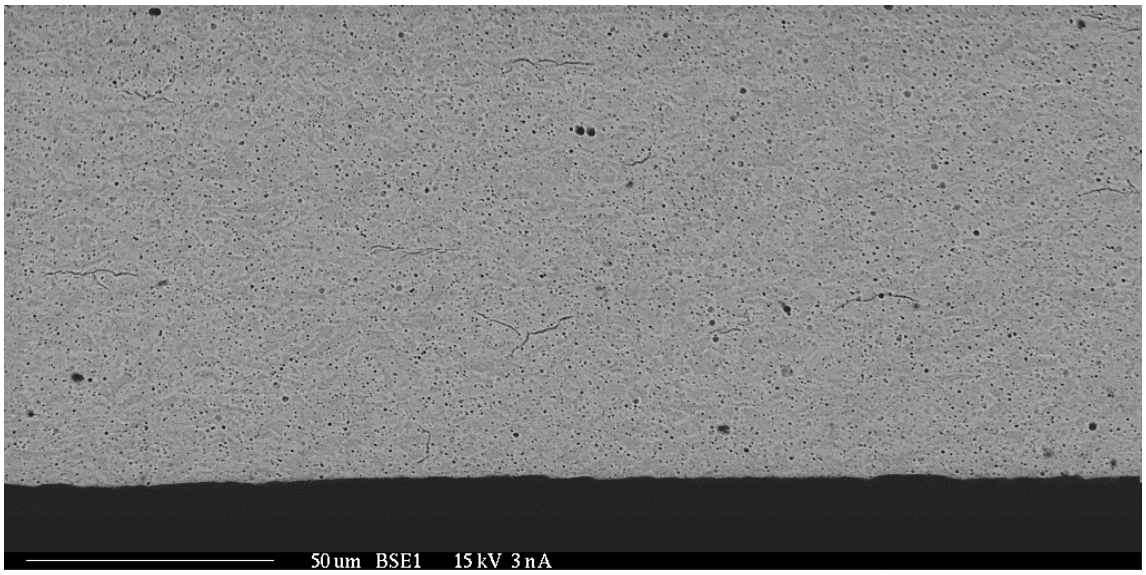

Figure 52 BSE image of experiment M1-22 inner surface with fine hydride features and increased porosity.

During experiment M1-23 the sample was charged at ~1 A/cm^2. For the given size of the sample, this resulted in a ~5.62 A current passing through the surface of the sample which was double that of other experiments. This was the largest charge used in any experiment and was intended to create a dense population of hydrogen at the surface of the sample in order to speed up hydrogen uptake. The experiment was conducted with a solution temperature of 117.328 +/- 0.438 °C and a cartridge temperature of 199.584 +/- 3.134 °C for 2.2 hours before the circuit was broken due to failure of the zirconium anode wire. When the sample came out of the experiment, a significant reduction in mass was evident as seen in Fig. 53 and Fig. 54 and recorded in Table 8. BSE images (Fig 55 and Fig. 56) show that no major hydride formations developed. From this experiment it was determined that the system would experience physical

reductions of material if the charge were increased to a high level and experiments following M1-23 were conducted with currents of less than 2.5 A overall.

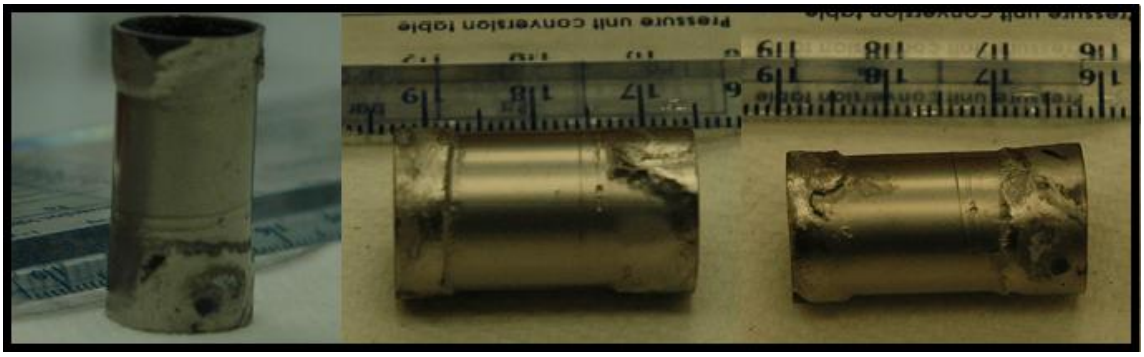

Figure 53 The sample from experiment M1-23 underwent a 1A/cm2 charge which resulted in a breakdown of the material due to the cumulative ~5.62 A which flowed throught the circuit. This experiment ended when the zirconium anode wire failed.

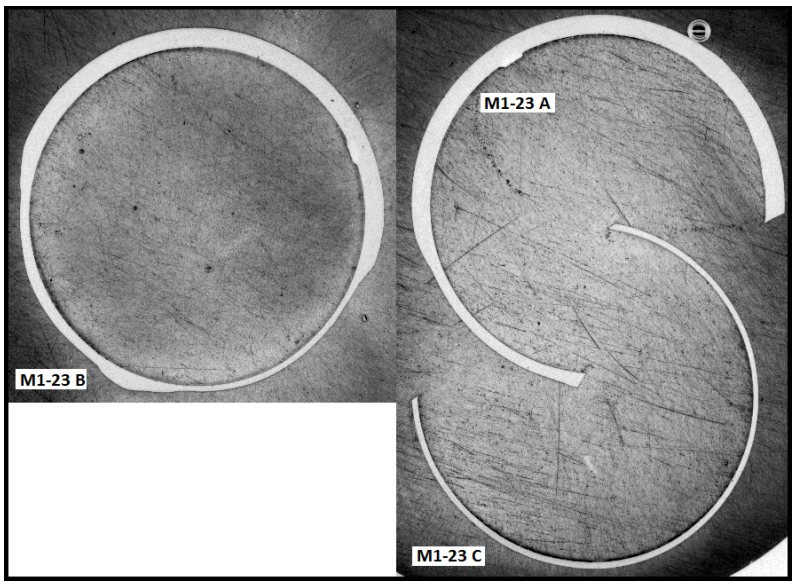

Figure 54 Epoxy mounted samples from experiment M1-23 illustrate the reduction in mass across the sample. The thicker ends were covered by the Viton caps and the thinnest center slice was exposed to the bath.

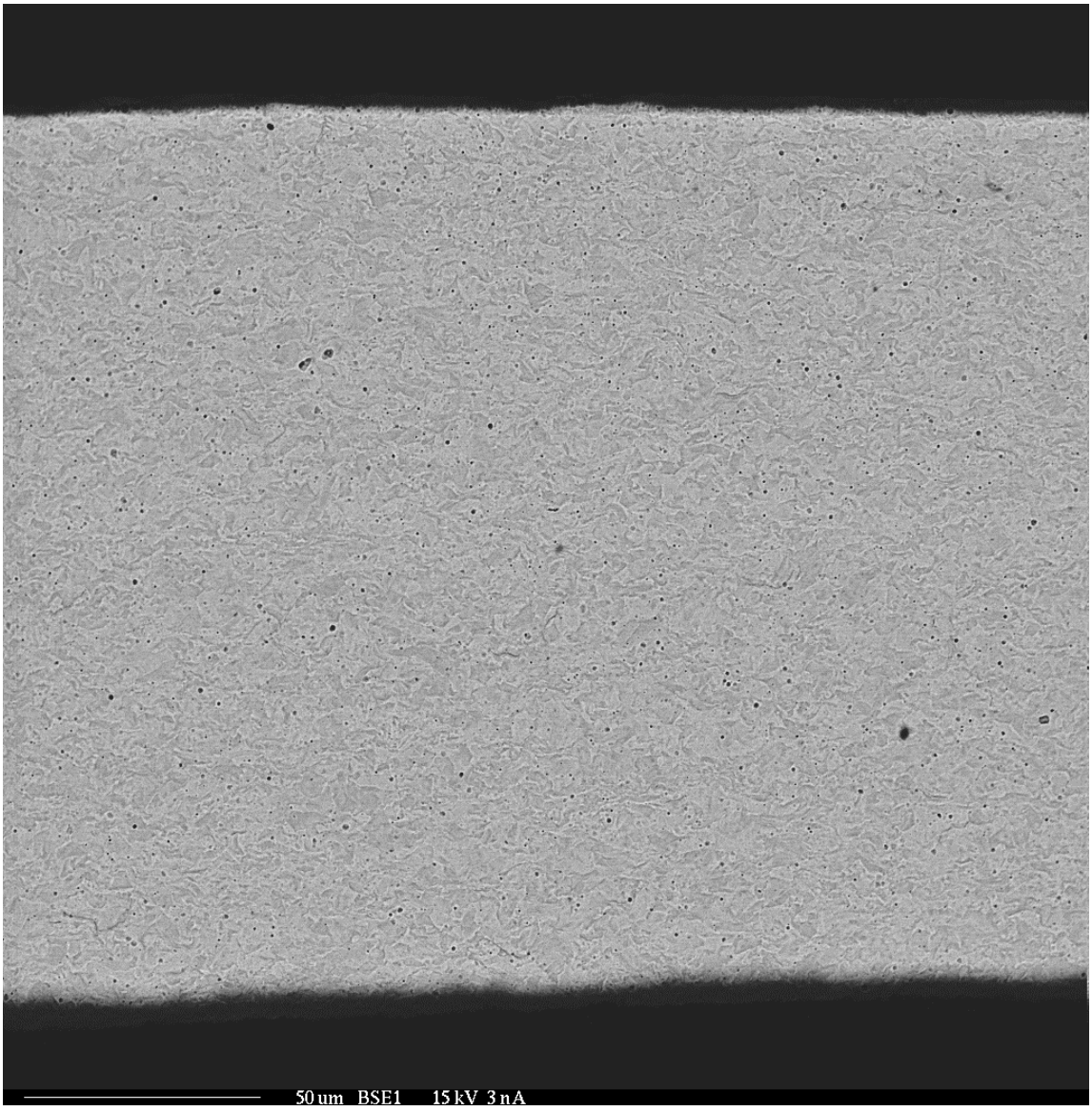

Figure 55 BSE image of M1-23 C section which was charged at 1 A/cm^2 for 2.2 hours. No major hydride formations were observed.

The following images (Fig 56 to Fig 58) illustrate results representative of the experiments M1-20 and M1-25 with the exception of M1-23 already noted. Figure 56 illustrates the increased porosity and Fig. 57 and Fig. 58 illustrate the general gradient which is noted by inspection. There were no significantly discernible rims or other

hydride formations visible in the SEM images. Fine features of zirconium hydride platelets were visible in various samples, similar to those present in the control sample (Figs. 32 to 33), but these did not constitute a significant morphological formation. For

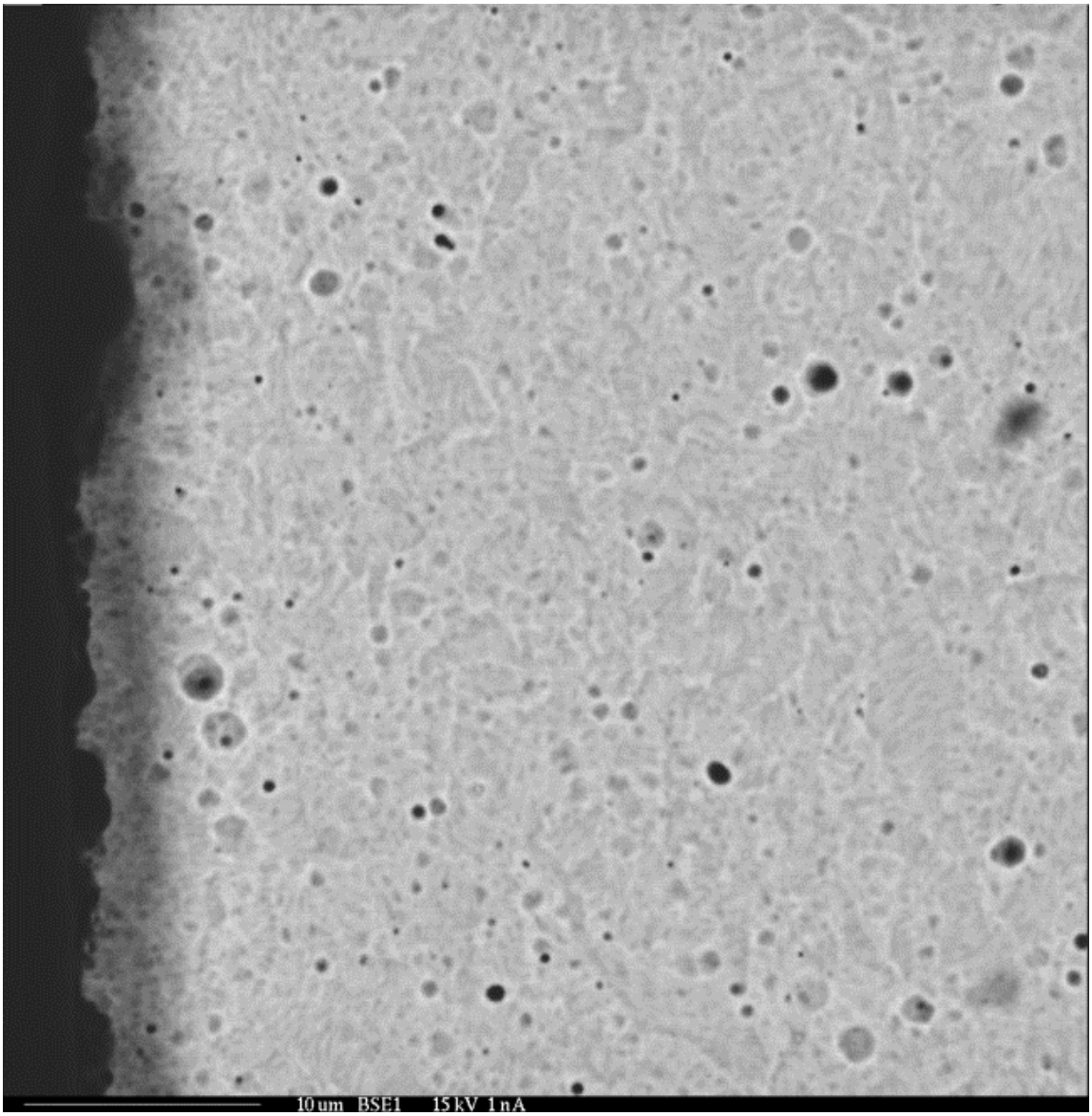

Figure 56 BSE image of a sample, from M1-25, illustrating increased porosity (etched out with acid bath) and the absence of the hydride rim. The darkening affect on the edge is a shadow due to rounding at the edge.

these experiments, which utilized a static thermal gradient, when the cartridge heater applied heat to the inside of the sample greater than the heat of the bath, the hydride rim did not form and the porosity of the sample increased.

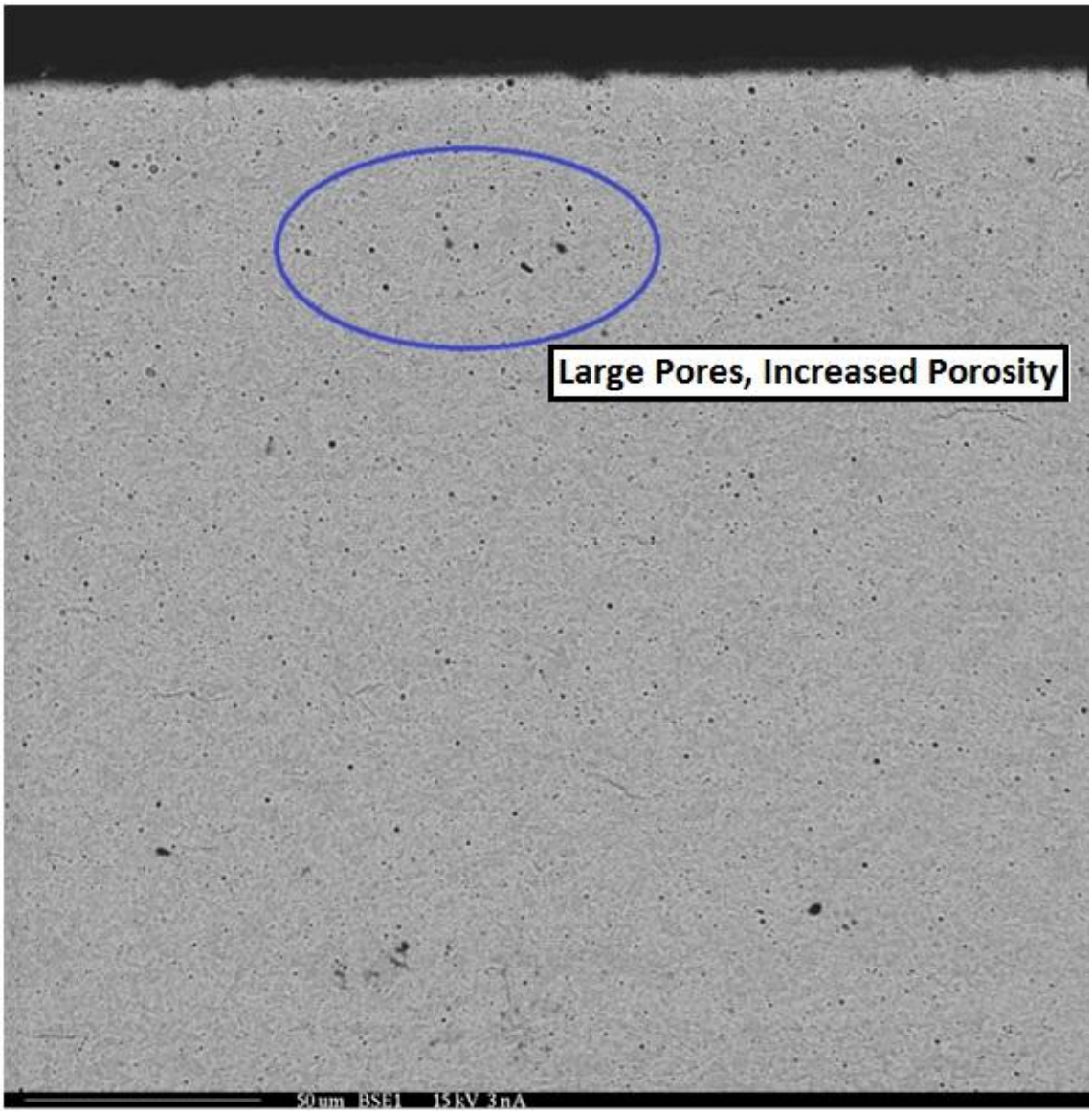

Figure 57 Large pores and an increased porosity were evident near the outer diameter in Experiment M1-25.

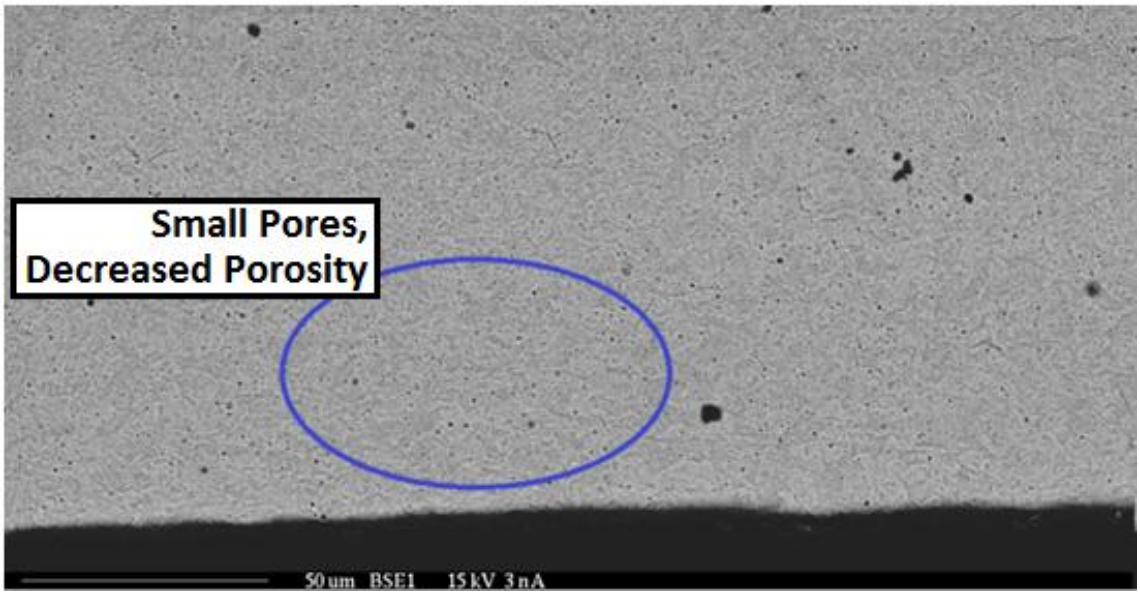

Figure 58 Small Pores with a decreased porosity, relative to the outer diameter, were observed near the inner diameter in Experiment M1-25.

4.2.4 Dynamic Thermal Gradient Insertion of Hydrogen

Experiments M1-31 through M1-36 involved starting up the experiment and running at ~120 °C for 1 to 3 hours while applying a charge. The idea was that this initial process would start the formation of a hydride rim. Then, after a given period of time, the temperature of the cartridge heater was increased and the system was allowed to continue charging. It was anticipated that this would draw hydrides which had formed at the rim, into the body of the sample. All of the results however developed the same way as experiments M1-20 through M1-25. There were very few notable hydride features in these samples and in some cases a slight mass reduction was observed. Table 11 shows the parameters for experiments M1-30 to M1-36. BSE images of

Table 11 Experimental parameters for M1-30 through M1-36

Sample	Experiment Name	Solution Temp Target [°C]	Heater #2 TEMP [°C]	Heater time on **	Amperage [A/cm^2]	Measured Amperage [A/cm^2]	Charging Time Goal [hours]	Charging Time Actual [hours]	"Slow" cooling?
13	M1-30	120.92 +/- 0.188	121.627 +/- 0.220	0	0.5	0.479 +/- 0.002	3	3:02	y
14	M1-31	118.758 +/- 0.175	220.624 +/- 1.950	2 hrs after t0	0.5	0.479 +/- 0.001	3	3:00	y
15	M1-32	120.71 +/- 0.377	181.926 +/- 0.697	1 hr after t0	0.5	0.481 +/- 0.002	3	3:00	y
16	M1-33	119.039 +/- 0.106	150.898 +/- 0.179	1 hr after t0	0.5	0.491 +/- 0.001	3	2:59:53	y
17	M1-34	119.031 +/- 8.36	294.588 +/- 2.049	2.5 hr after t0	0.5	0.483 +/- 0.002	8	8:08:53	y
18	M1-35	121.451 +/- 0.994	155.685 +/- 0.412	3 hr after t0	0.3	0.281 +/- 0.001	12	26:35:00	y
19	M1-36	123.647 +/- 1.731	182.298 +/- 1.032	3 hr after t0	0.3	0.282 +/- 0.005	24	44:21:00	y

**(starting from t0) example - 180 1hr (cartridge heater to 180 at t0 + 1hr and stays that way until changed or until experiment ends.)

M1-3x experiments resembled those of Figure 56 to 58 with no major hydride formations observed in any of the M1-3x experiments.

4.2.5 BSE Imaging of Zirconium Hydride from Vapor Diffusion

Three samples from A. Parkinson's vapor diffusion where sectioned, polished, etched, and imaged using the same Cameca electron microprobe. The parameters for experiment 89, 91, and 93 are given in Table 12. The results of the imagines are shown in Fig. 59 and 60. A clear gradient is evident in these samples.

Table 12 Parameters from Parkinson experiment. [22]

Experiment Number	% Hydrogen Used	Flow rate at end of experiment (SCFH)	Pressure (+H2O)	Temp (°C)	Time (hrs)	sample mass (g)	actual % if all hydride	mass increase (g)
89	5	3	25	537	1	3.5392	7.421688	0.0057
91	5	3	25	487	1	3.5441	3.900751	0.003
93	5	3	25	477	2	3.543	61.52094	0.0473

4.3 Variation in Image Quality

It is important to note that the image quality was affected based on the quality of the polishing on the sample and on the acid etch process. While there were obvious differences in quality which would obstruct fine feature recognition, the major features sought in these experiments could be identified rather easily across a wide tolerance of etching results. Figures 60 to 62 illustrate several etch attempts on the same sample in

approximately the same location. While some images show sharp, fine features, all three of the images show the major features.

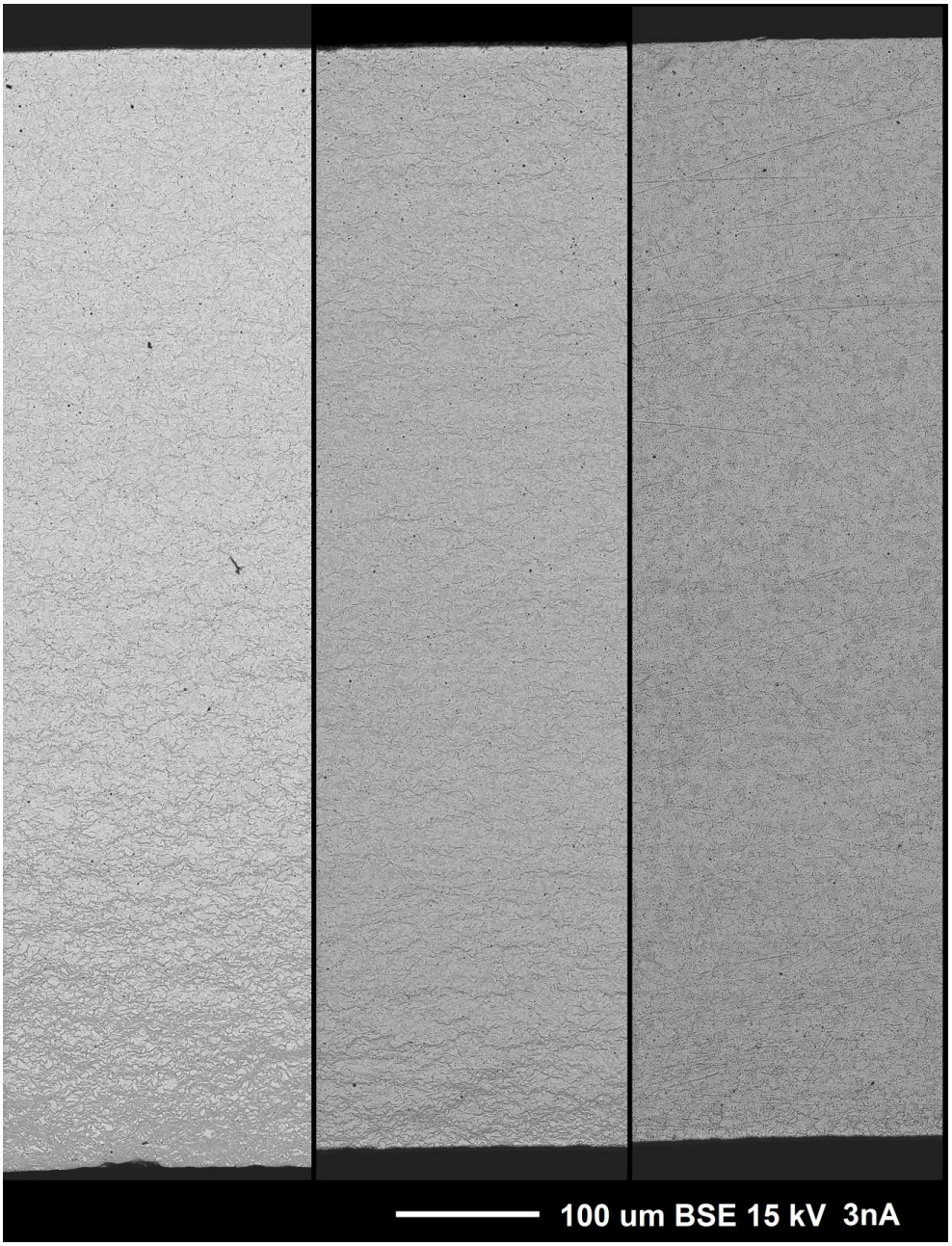

Figure 59 Vaporous diffusion samples from Parkinson Experiment 93, 91, and 89 respectively.

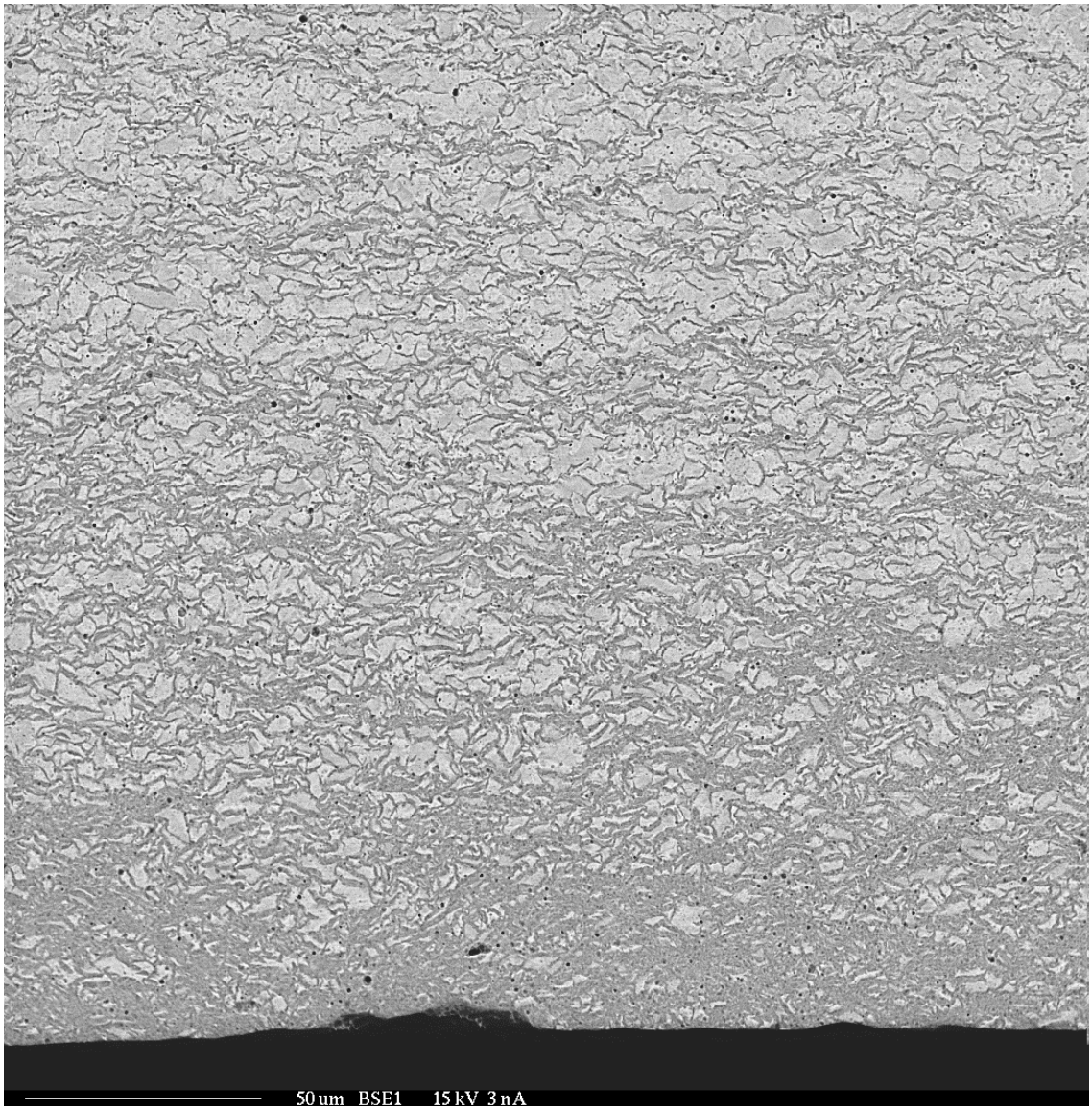

Figure 60 SEM image for sample A1-3 (Parkinson Experiment 93) which was subjected to vapor diffusion. Lower edge correlates to ID of Zricaloy-4 tube.

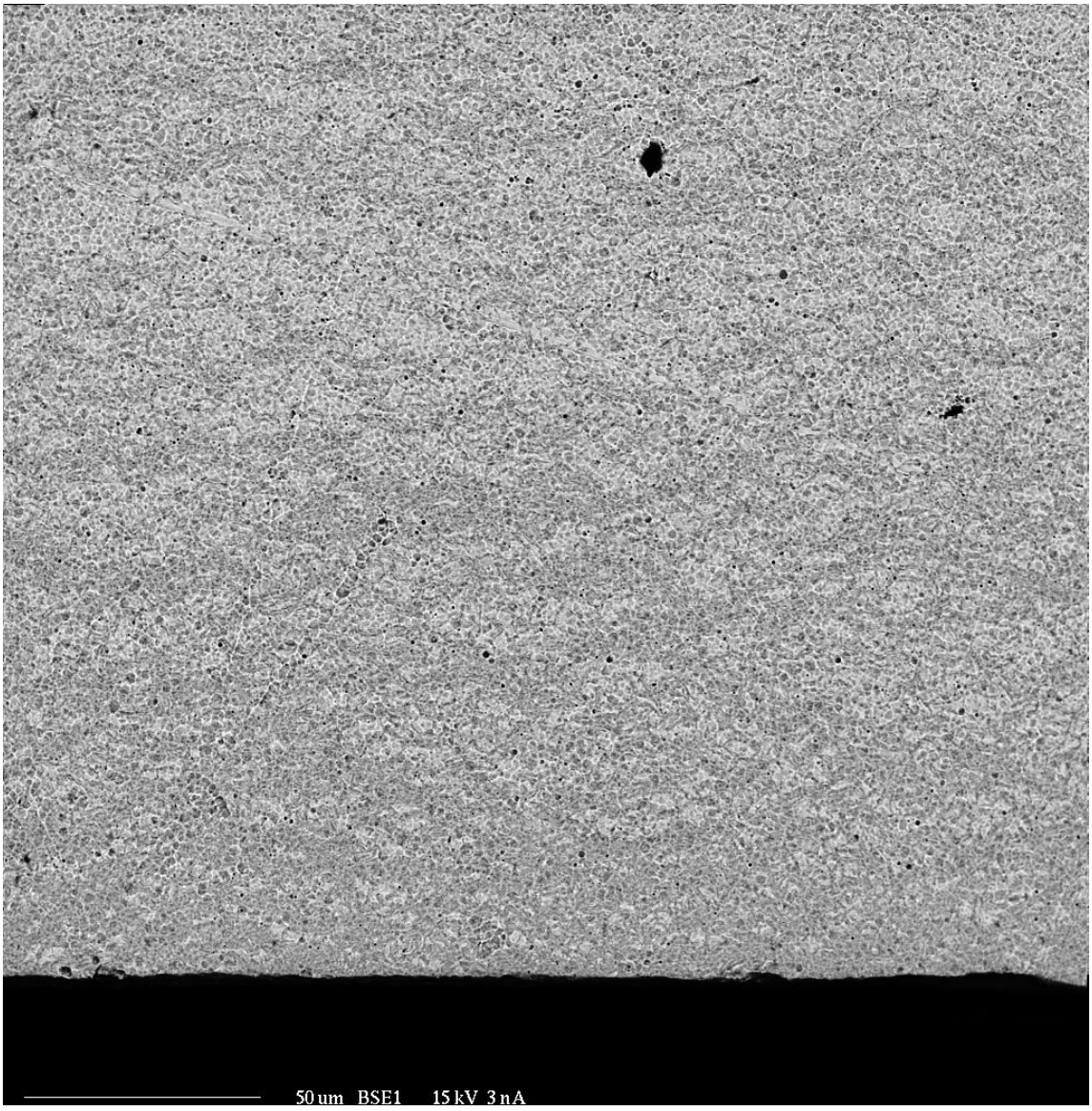

Figure 61 Alternate etch for experiment 93. Features are not as clear, but are still distinguishable.

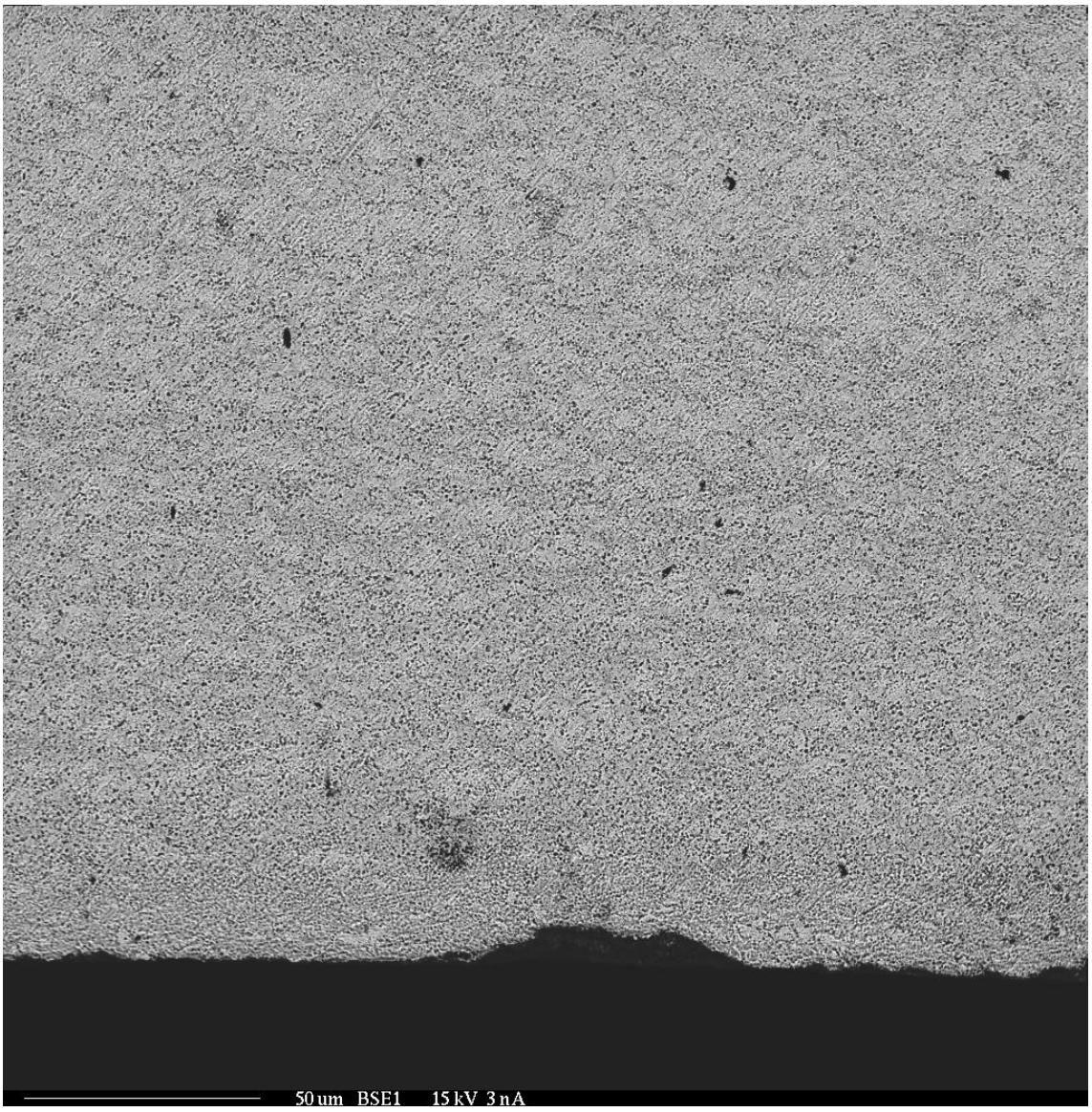

Figure 62 A third etch for experiment 93. This light (t≈5 seconds) etch still shows the major hydride formations.

CHAPTER V

DISCUSSION

5.1 Principle observation on the ECH-TG System Evolution

The ECH-TG system underwent a number of adjustments and upgrades from the beginning of this project to the end. Early experimentation required developing several versions of counter electrodes and sample holders. Initial use of a bronze electrode resulted in an electroplating of the anode and required a complete redesign of the electrode after the first experiment. This failure, while requiring a counter electrode re-design, did serve a valuable role in eliminating Method 2 as an experimental procedure. The desired path for the hydrogen in the Method 2 procedure would have resulted in electroplating of the sample. However, the copper material which dissolved in solution reformed on top of the anode. This observation indicated that hydrogen would not flow through the sample and instead would just flow to the anode through the solution. These results lead to the tabling of the Method 2 procedure in favor of working with Method 1, (Section 4.1).

A graphite electrode was assembled in order to replace the bronze electrode. Use of a graphite electrode resulted in carbon dissolving into the electrolytic bath. While this made it challenging to see the experiment, the electrolytic circuit was closed and early experiments could be conducted. At the same time, the Boron Nitride sample holders were machined and used for experiments M1-11 to M1-13/M1-14. Two sample holders made of BN survived two experiments a piece before breaking down in the solution.

Before breaking down however, the ECH-TG system in this configuration produced the only successful hydride rim formations.

The next change to the system for experiments M1-20 to M1-25 involved obtaining a Pt electrode and using al Al_2O_3 sample holder. These two changes in and of themselves should have resulted in similar results as those of the system just prior to their use. However at the same time that the Al_2O_3 sample holder was brought into use, an aluminum sleeve was also used to support the thermal transfer from the cartridge heater to the Zircaloy-4 sample. This, along with the introduction of viton caps intended to inhibit solution penetration to the inner surface of the Zircaloy-4 sample, somehow provided a pathway for hydrogen to flow around or flow through the Zircaloy-4 sample without forming major hydride features. Experiments M1-20 to M1-25 and M1-30 to M1-36 all have this major system change in common. Future work should focus on eliminating the aluminum sleeve and viton initially to see if hydride rims can be formed with the Pt electrode and the Al_2O_3 sample holder. Once this is accomplished, the viton caps can be added back into the system to attempt to seal the inner surface from electrolyte solution.

Experiment M1-23 attempted a high current per area (1 A/cm^2) charge and saw a 50.32% reduction in mass. It was also determined that charge, and specifically a relatively large current >5 A would result in a mass reduction of the Zircaloy-4 samples. This observation lead to a procedural adjustment which kept all successive currents below 4 A and preferentially around 2.5 A.

A slow cooling process of 1 °C per minute was implemented for experiments starting with M1-23 in an attempt to capture some of this hydrogen in the zirconium matrix. However the results showed no discernible difference between samples which where fast cooled versus those that were slow cooled. It is still advisable to continue the slow cooling process as literature indicates that the correct phase of hydride will only form with slow cooling. [2]

The presence of enlarged pores in experiments M1-20 to M1-25 and M1-30 to M1-36 was initially mistaken to be the remnants of H_2 bubbles in the matrix. While it is now believed that there was little to no hydrogen present in the Zircaloy-4 samples to manipulate, at the time, experiments were designed to manipulate these mis-diagnosed bubble formations This resulted in a largely mis-directed effort which was compounded by long lead times to use the microprobe for sample imaging. These long lead times meant the results were not available for faster analysis and what could have been a faster recognition of the absence of H_2 bubbles and a correct interpretation of pore formation. This lag in data analysis resulted in entire batches of experiments being conducted which provided little new information. At the end of experimentation however, samples from M1-13 and experiment 93 from A. Parkinson's work were viewed under a high-powered optical microscope. It was determined that the major hydride formations in these samples could be seen with the microscope. This means that future work does not need to wait long periods for microprobe time to determine the results of an experimental procedure. This discovery will save time and allow more rapid development of the system for future work.

The pores are now believed to be due to a general reduction of the Zircaloy-4 material in concert with the hydriding of the material and oxidation effects. It will be important to future work to study why these pores form and understand how to impede their growth because they will contribute to weakening the sample.

5.2 Comparison of experiments

5.2.1 Isothermal Insertion of Hydrogen via Electrolytic Process

Hydride rims were easily formed under isothermal conditions at both ~90 °C (Experiment M1-11 and M1-12) and ~120 °C (Experiment M1-13) . One of the key findings of the M1-13 experiment was the formation of the hydride rim in a boiling bath. With the use of a hotplate to generate the boiling temperatures, the bottom surface of the pyrex beaker served as the main point of liquid vaporization. The bubbles then traveled upward and while they would pass near to the sample and come in contact with the sample surface, the sample outer surface was still in direct contact with the liquid. This direct contact with the liquid would allow a very dense concentration of hydrogen to interface with the Zircaloy-4 sample. In comparison, when the experiments with thermal gradients where conducted, the surface at which the liquid vaporization would occur was on the outer surface of the Zircaloy-4 sample. This would then result in a very thin layer of vapor developing between the Zircaloy-4 sample and the liquid bath. This vapor layer would exhibit a much lower density of molecules and therefore contain a much smaller density of hydrogen when compared with direct liquid to sample contact. While this

bubbling surface phenomenon may have contributed to a lack of hydride formations when the thermal gradient was activated, it still does not explain the lack of a rim formation in experiment M1-30, which was heated with only the hotplate and yet still did not develop a rim structure.

It was then considered that the thermal gradient present in experiments M1-20 to M1-25 and M1-31 to M1-36, was somehow dissolving hydrides or contributing to an alternate path for the hydrogen. This theory however did not make sense in the light that the zirconium hydride reaction is energetically favorable and that the dissolution of ZrH_2 is 900+ °C. The maximum cartridge heater temperature was ~350°C and so it could not have dissolved the hydrides.

With the temperature variables of boiling and thermal gradient eliminated, time was then considered as a possible factor to inhibiting rim development. If experiments with shorter charge times were not picking up enough hydrogen to form major hydride formations, then perhaps a longer time was needed. This however did not make sense in the light that M1-11, M1-12, and M1-13 experiments, which developed rims, where all conducted under 10 hours. Experiments M1-22, M1-24 and M1-35 and M1-36 where conducted for 70.2, 24, 26, and 44 hours respectively and yet did not form a rim. It must be taken into consideration however that the charge calculation for the system was based only on the visible surface area of the sample. If the charge was based on the mass of the sample, then some of the later experiments, including the longest run ones, would have required a higher charge.

Finally, it was considered that the one constant that changed from experiment M1-13 to M1-20 and beyond, was the sample holder. The components of Viton, aluminum and Al_2O_3 were all different from the Boron Nitride sample which was used in experiments M1-11, M1-12, and M1-13. It is theorized that one, or some combination of, these new materials used for the last sample holder contributed to an alternate path for the hydrogen and inhibited zirconium hydride formation. Of particular concern was the aluminum sleeve when it was realized that the electric potential of Al could be stronger than that of Zr. The aluminum sleeve used for experiments M1-20 to M1-25 and M1-30 to M1-36 may have served as a sink for the hydrogen. While the analysis was not completed here, it is hypothesized that differences in electric potential would have resulted in preferential absorption of hydrogen by the aluminum sleeve before the Zirconium started absorbing hydrogen.

5.2.2 Thermal Gradient Insertion of Hydrogen via Electrolytic Process

The use of the thermal gradient did not generate the expected results. It is theorized that problems with the aluminum sleeve have clouded the effects the thermal gradient would have on the hydride rim.

Generally however, the system worked as designed. It was possible to keep the OD at one temperature and increase the temperature at the ID of the sample. Future work involving a parametric study can examine smaller thermal gradients in an effort to identify methods of encouraging hydride movement in the Zricaloy-4 samples.

5.2.3 Insertion of Hydrogen via Vapor Diffusion

Vapor diffusion developed a clear gradient in the three sample analyzed from A. Parkinson's work. These gradients however formed on the inner surface and dissipated towards the outer surface. Further analysis suggests that there were two possibilities for this "reversed" gradient.

For the vapor diffusion method, A. Parkinson passed a hydrogen and argon mixture over the Zircaloy-4 tube. When the tube was oriented horizontally (Fig. 11) for apparatus diagram, and the corresponding flow was down the axis of the tube, very little hydrogen pickup was recorded. When the same experiment was performed with the tube standing vertically, and thus the flow moved around the outside of the tube, a larger hydrogen pickup was evident. In this second configuration, it is apparent that the hydrogen gas was stationary on the inner surface, relative to the flowing gas on the outer diameter. This may have allowed for a more rapid intrusion of hydrogen into the inner diameter.

The other explanation for the larger hydride presence at the ID versus the OD was explained in the sample preparation of the vapor diffusion samples. Instead of pickling the outside diameter, A. Parkinson put the whole sample in without any pre-treatment. With this lack of pickling, the outer surface could have been exposed to any number of contaminants that would have inhibited hydride up-take.

In either case, it will be important for future work to re-assemble the vapor diffusion device and to process samples which have been pickled to provide a uniform data point from which to start experimentation.

CHAPTER VI

SUMMARY AND CONCLUSIONS

6.1 Summary

This project was successful in developing an electrolytic system to form major zirconium hydride formations in Zircaloy-4 samples. Specifically, the proof-of-concept experiments were able to replicate the hydride rim previously reported in literature.[13]. The rims ranged from 8.690 +/- 0.982 μm to 12.365 +/- 0.635 μm. The Labview L2.vi program developed for this system along with the various computer controlled components permit relatively easy control of the ECH-TG system and will serve as a stable foundation for future work.

Hydride rims can be formed with an isothermal electrolytic process. Using a vapor diffusion method, a gradient of hydrides can be developed in Zircaloy-4 samples. The system was not successful in producing a gradient formed with the electrolytic solution by itself. However, literature has shown that creating hydride rims and the annealing in a furnace, at 300-400 °C for 20 minutes to 2 hours, will result in a distribution of the hydrides into the material. This last annealing step was not performed for this project, but could be undertaken in future work.

Complications with the aluminum sleeve used with the Al_2O_3 sample holder seem to have clouded the results of experiments including the thermal gradient. While this research was not able to prove one way or the other whether the thermal gradient will in fact move zirconium hydrides, simple adjustments can be made to eliminate the

aluminum sleeve and test for the affect. By using a large Al_2O_3 sample holder and mounting the sample in place with a thin viton o-ring, the system will be similar to the system designs which produced hydride rims.

The initial follow-up experiments would focus on creating the hydride rim with the viton caps in an isothermal condition. The same experiment would then be run with the cartridge heater initialized and set at a temperature 5 degrees above the boiling acid temperature. 5 degree incremental increases would be used for a total of 10 experiments where the cartridge heater would finally be placed 50 °C above the temperature of the bath.

While this researcher relied on an electron microprobe to see the formations, The very last micro-probe session with two well-etched samples revealed that an optical microscope could be used to see the same formations. It is essential that a good polish and etch technique be used. When done correctly, the hydride formations will be revealed so that the future researcher does not need to wait for a micro-probe session to analyze experimental results. This will tremendously speed up the analysis of experiments and give future researchers the ability to modify experiment parameters on an almost daily basis versus the weekly or bi-weekly basis by this researcher.

Future Work would include:

- Determine if the Aluminum sleeve affected hydride formation.
- Quantify rim thickness as a function of temperature and charge.
- Form rims and then initiate 5°C changes in thermal gradient.
- Expand LABVIEW to control Cartridge Heater for better automation

- Ensure epoxy curing does not cause remodeling of hydrides.
- Restart vaporous diffusion device and determine how to get gradient on OD.
- Perform IGF or VHE and XRD to quantify amount of hydride and phase.

6.2 Conclusions

Successful creation of the zirconium hydrides was evident in the rim formations of early experiments. Subsequent attempts to move the crust formations further into the material where considered unsuccessful, but possible hurdles to this success have been noted and a solution is probable. “Pumping,” the system by running multiple cycles of charging and thermal gradients with cool down periods was not attempted in this work. Future research could look at this technique in concert with the developed process and find possible success. Additionally, furnace annealing electrolytically charged samples was not undertaken either. Late literature review indicated that hydride formations may develop in these samples with heating to 400 °C and subsequent furnace cooling. While this work succeeded in producing an electrolytic system, further work is needed to apply the thermal gradient properly across the samples in the continued research to form zirconium hydrides similar to those found in nuclear reactor UNF. With a steady supply of zirconium hydrided cladding, extensive research can be launched to understand long term affects on UNF storage and help make important decisions for permanent fuel storage and recycling options.

REFERENCES

[1] U.S. NRC. “Fact Sheet on Dry Cask Storage of Spent Nuclear Fuel” March 2012. http://www.nrc.gov/reading-rm/doc-collections/fact-sheets/dry-cask-storage.html

[2] Lemaignan, C. and Motta, A. T. 2006. Zirconium Alloys in Nuclear Applications. Materials Science and Technology. WILEY-VCH.

[3] DOE-HDBK-1017/2-93 1993, DOE Fund. Handb., Mat. Sci, V 2 of 2, U.S. pp. 12, 24

[4] J.B. Bai, C. Prioul, D. Francois, Metall. Mater. Trans. 25A (1994) 1185.

[5] Y. Kim, S. Ahn, Y. Cheong. “Precipitation of crack tip hydrides in zirconium alloys.” Journal of Alloys and Compounds 429 (2007) 221–226.

[6] A. Motta. “Hydride Formation and Testing using in-situ Synchrotron Radiation” Presented Nov 2011. Las Vegas, NV DOE meeting on Nuclear Fuel Cladding.

[7] L. H. Hamilton, B. Scowcroft et al. Report to Sec. of Energy S. Chu: “Blue Ribbon Commission on America’s Nuclear Future.” Jan. 26, 2012.

[8] D. B. Rigby. Report: “Evaluation of the Technical Basis for Extended Dry Storage and Transportation of Used Nuclear Fuel.” NWTRB Dec 2010

[9] A. J. Parkison, S. M. McDeavitt, Metall. Mater. Trans. 42A (2011) 192

[10] U.S. NRC. NUREG-1350, Volume 23 “Information Digest” 2011-2012

[11] B. Hanson “Gap Analysis to Support Extended Storage of Used Nuclear Fuel” NWTRB Fall 2011 Board Meeting. Sept. 13, 2011.

[12] R. Attermo, A. Sietnieks, Electrochim. Acta 14 (1969) 21.

[13] J.T. John, P.K. De, H.S. Gadiyar, High temperature cathodic charging of hydrogen in zirconium alloys and iron and nickel base alloys, BARC-1544, 1991.

[14] Y. Choi, J. Mater. Sci. Lett. 16 (1997) 66.

[15] S. Yamanaka, K. Yoshioka, M. Uno, M. Katsur, H. Anada, T. Matsuda, S. Kobayashi, J. Alloys Compounds 293-295 (1999)23.

[16] Ansto Replacement Research Reactor Progect SAR "Chapter 5.9 Reactor Materials." Document: RRRP-7225-EBEAN-002-REV0-Ch5(f).doc Nov 2004.

[17] ATI Wah Chang. Reactor Grade Zirconium Alloys for Nuclear Waste Disposal. Technical Data Sheet. http://www.atimetals.com/businesses/business-units/wahchang/products/Documents/Zr%20nuke%20waste%20disposal.pdf Accessed 6/4/2012.

[18] D. L. Douglass, The Metallurgy of Zirconium, Vienna, Austria. International Atomic Energy Agency. 1971.

[19] EPRI Industry Spent Fuel Storage Handbook 1021048 Final Report, July 2010

[20] Delayed Hydride Cracking in Zirconium Alloys in Pressure Tube Nuclear Reactors. IAEA-TECDOC-1410 Oct 2004, IAEA

[21] D.T. Kraemer. Establishing Methods for Recycling Spent Zircaloy Cladding Using a Hydride-Dehydride Processing Route. M.S. Thesis, Purdue University, West Lafayette, IN. 2005.

[22] A. Parkinson. Hydride Production in Zircaloy-4 as a Function of Time and Temperature. M.S. Thesis, Texas A&M University, College Station. 2008.

APPENDIX A: SYSTEM DESIGN (COMPONENTS and LABVIEW DIAGRAM)

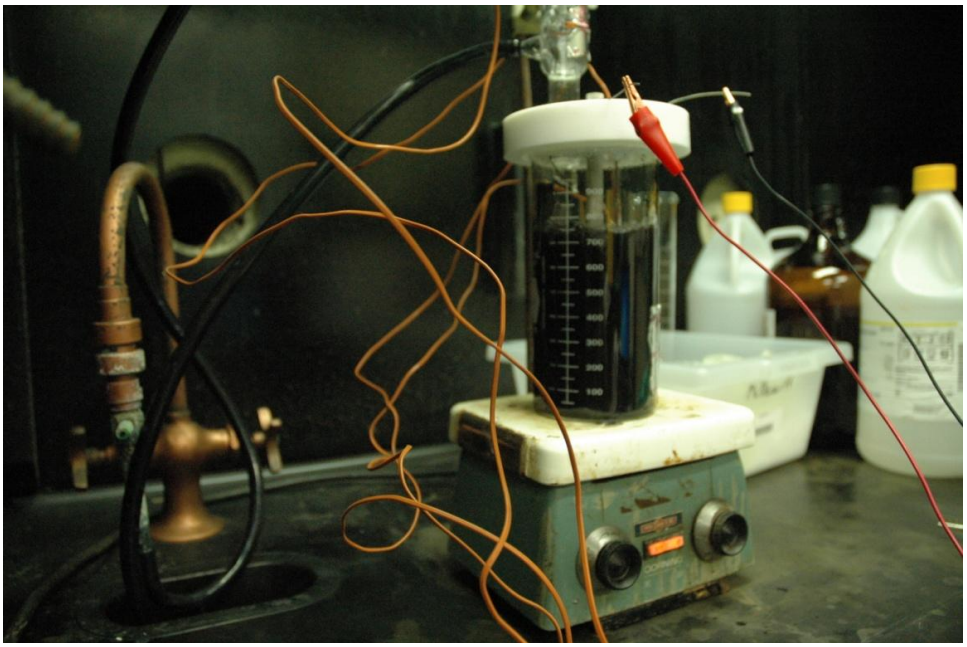

Figure A - 1: This image is from an experiment running with the graphite electrode on the original analog hotplate with the boron nitride sample holder

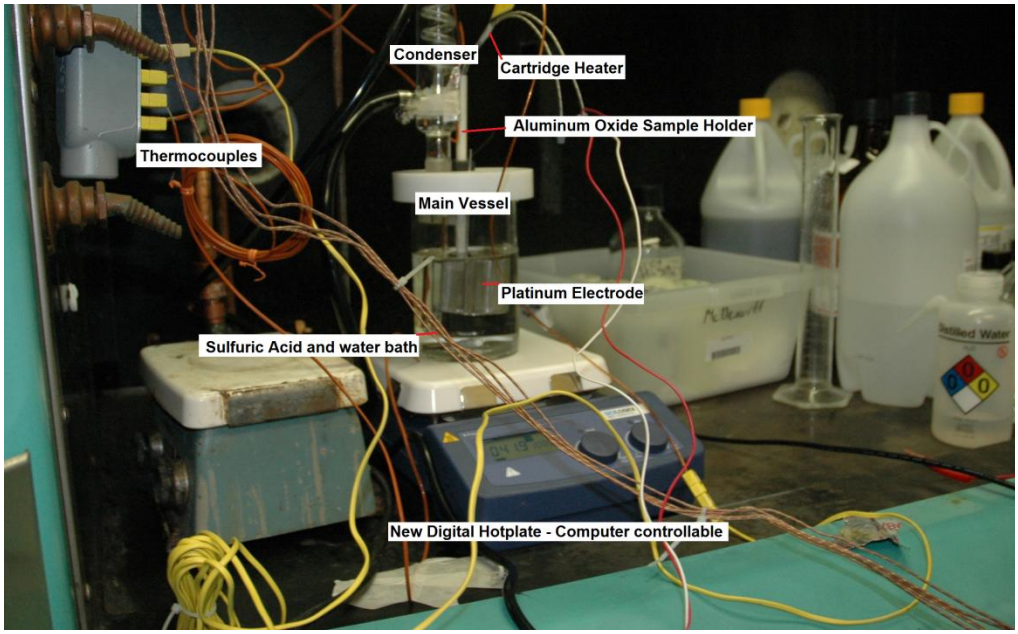

Figure A - 2: This is the current design and setup as of March 25th, 2012.

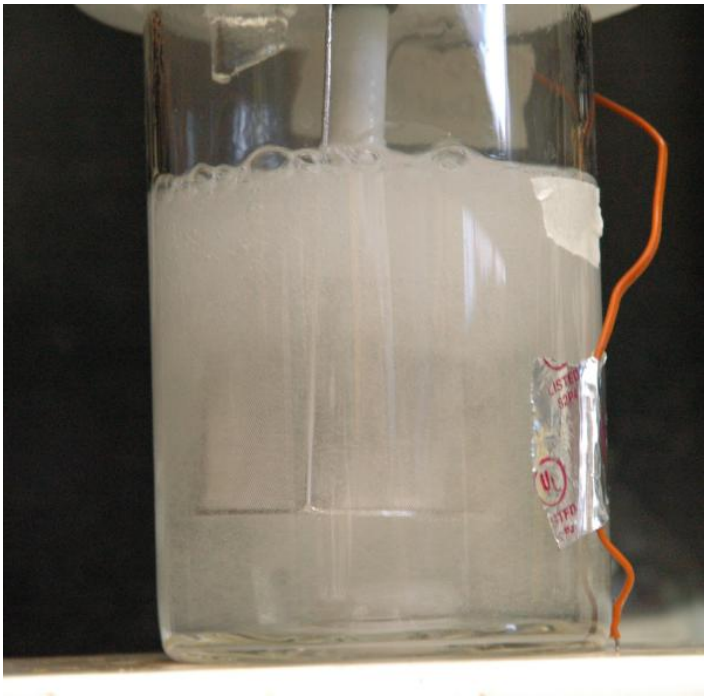

Figure A - 3: Image of current system while running.

Figure A - 4: These are Zircaloy-4 0.5” tall samples before and after charging with original system.

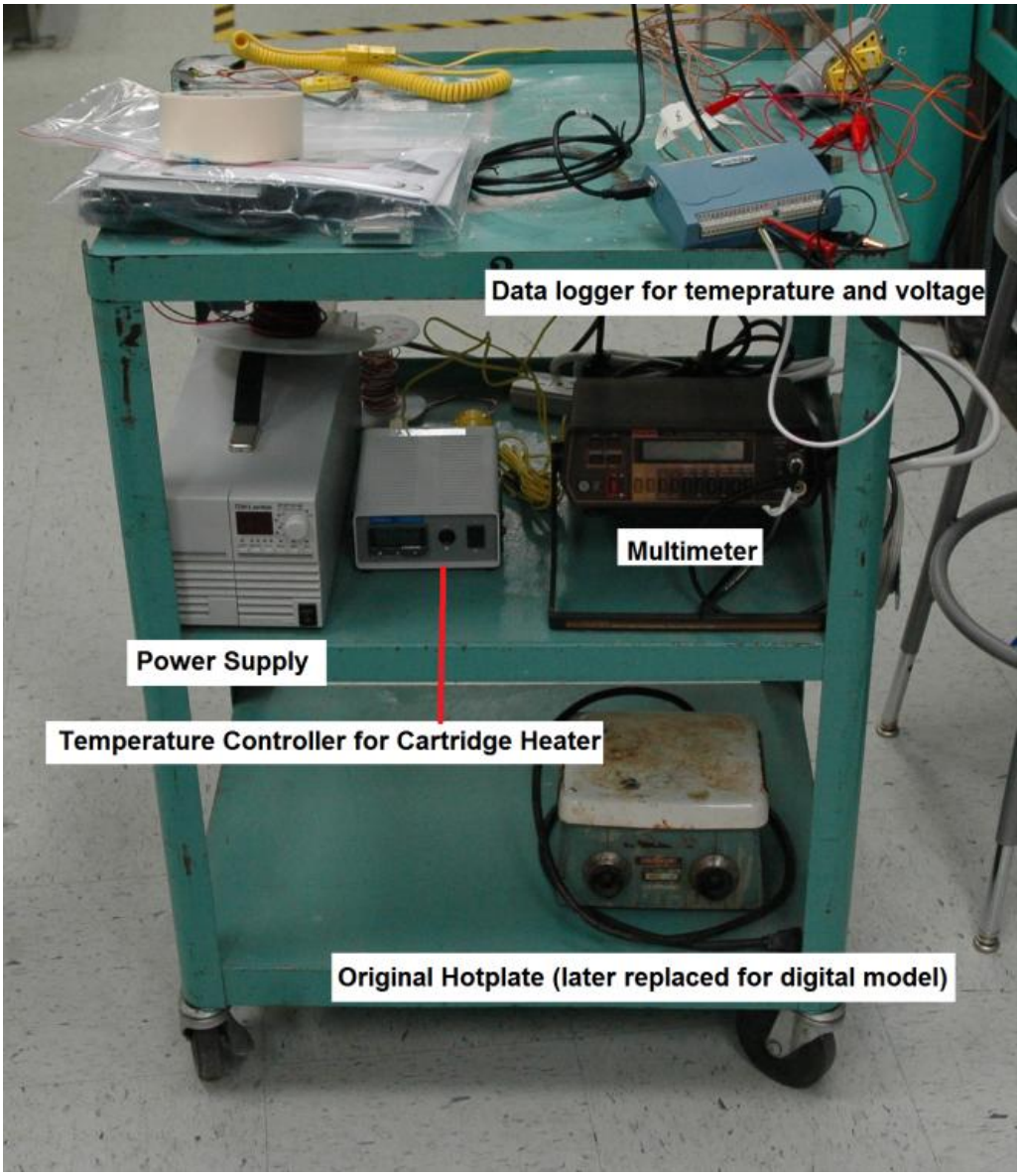

Figure A - 5: This is the "mobile workstation" used for this experiment. It allows transportation between laboratories and the graduate office where programming of the components takes place. As the system is finalized a more permanent electronic cabinet will be use

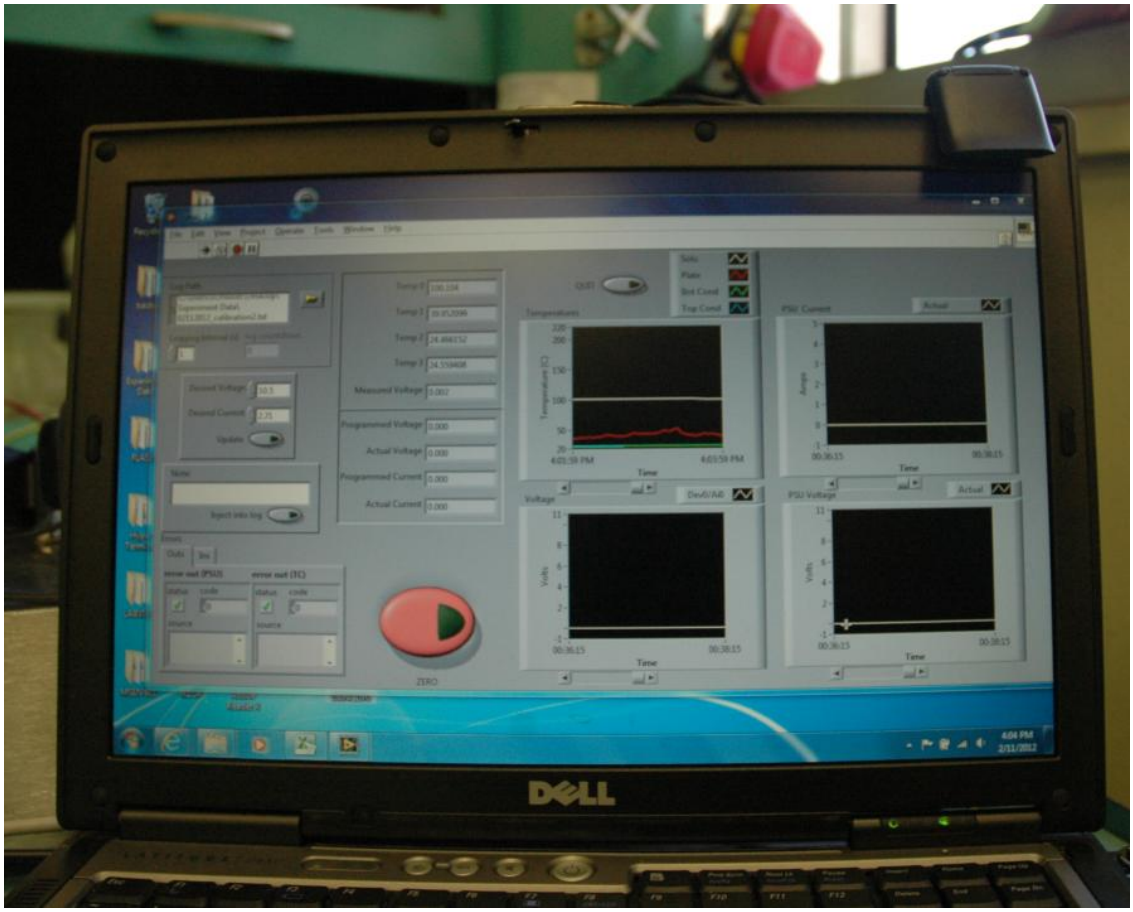

Figure A - 6: This is the NI Labview window which controls the experiment. Temperatures, expected voltage, actual voltage, current, and control to the power supply are built into the system. Remote control of the hotplate and the cartridge heater are currently being

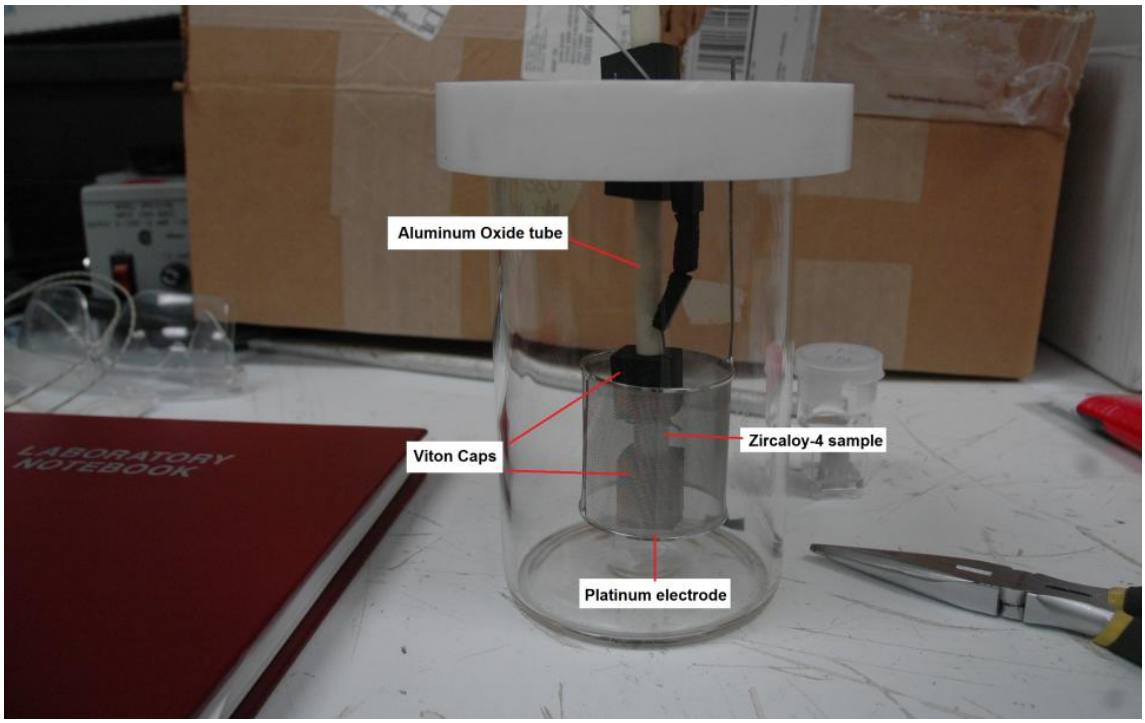

Figure A - 7: This is the newest design with the Aluminum Oxide sample holder, the Viton Caps (to prevent solution from getting to the inner diameter of the sample), and the Pt electrode. The caps will be re-developed to cover less of the sample in future versions.

A List of the Primary components, schematics, and sources procurement are listed below.

Components and dimensions:
Physical Devices:

STIRRING HOTPLATE:
SCILOGEX MS7-H550-Pro 7x7 LCD Digital Hotplate Stirrer

DAQ: OMEGA OM-USB-TC-AI
8 Channel Thermocouple/Voltage Input USB Data Acquisition Module

VARIAC: STACO ENERGY Model 3PN1010B

USB TO RS232 CABLES

THERMOCOUPLES

THERMOCOUPLE ARRAY

CARTRIDGE HEATER 1 – 4” WATLOW

CARTRIDGET HEATER 2 – 1 ½ inch DALTON Electric Watt-Flex

USB CAMERA – LOGITECHs

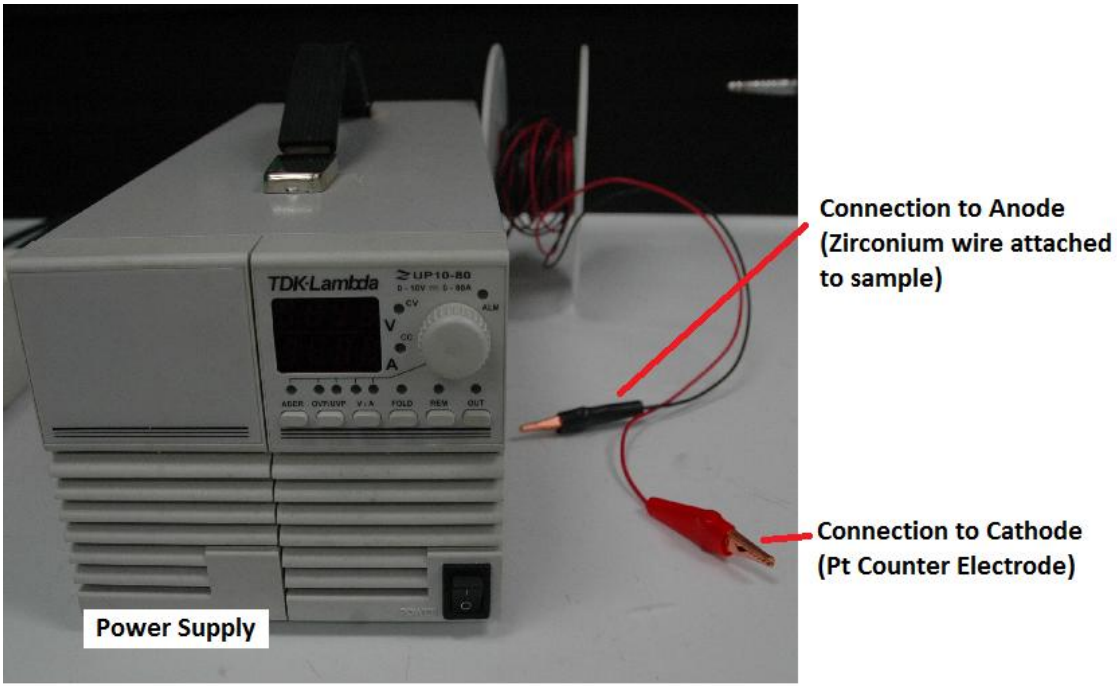

Power Supply:
TDK-Lambda ZUP 10-80

Assembly Components:

Platinum Electrode:
Premier Lab Supply
1982 S.W. Hayworth Avenue
Port St. Lucie, Florida 34953 USA
Phone (772)-873-1700
Frame: Pt/Ir 3%, Mesh 100% Pt
Cylinder Dia: 50mm; Height 50mm Overall Height 150mm; Stem Dia: 1.5
Approximate Weight: 24 grams

Pyrex glass vessel:
Custom made at Texas A&M University: Chemistry Department: Glass Shop by Bill Merka.

Dimensions:
Sample Holder #1

Sample Holder #2

Sample Holder #3

ANODE WIRE

VITON O-RINGS
VITON CAPS
BRONZE ELECTRODE
GRAPHITE ELECTRODE

Software:
SOLIDWORKS
NI LABVIEW
DRAGON STIRSOFT
TRACERDAQ

APPENDIX B: INITIAL TEST MATRIX

This is the original experiment matrix with Method 1 and Method 2. Only two of the following experiments (M1-06 and M2-03) where completed. Subsequent experiments required alterations to the procedure and resulted in the next group of experiments starting with M1-11 as illustrated in Table 7 of the Thesis.

Sample - Experiment Name	Scheduled procedure date	Pickled	Method 1	Temp Cart Heater [C]	Amperage [A/cm^2]	Method 2	Amperage [A/cm^2]	Charging Time [hours]
1 - (RAW)	1/5/2012							
2 - (Etched only)	1/5/2012							
3 - M1-01	1/8/2012	X	X	0	0.2			2
4 - M1-02	1/10/2012	X	X	300	0.2			2
5 - M1-03	1/10/2012	X	X	400	0.2			2
6 - M1-04	1/11/2012	X	X	500	0.2			2
7 - M1-05	1/12/2012	X	X	600	0.2			2
8 - M1-06	1/8/2012	X	X	0	0.4			2
9 - M1-07	1/10/2012	X	X	300	0.4			2
10 - M1-08	1/11/2012	X	X	400	0.4			2
11 - M1-09	1/11/2012	X	X	500	0.4			2
12 - M1-10	1/12/2012	X	X	600	0.4			2
13 - M2-01	1/5/2012	X				X	0.2	0.5
14 - M2-02	1/5/2012	X				X	0.2	1
15 - M2-03	1/5/2012	X				X	0.2	2
16 - M2-04	1/9/2012	X				X	0.2	3
17 - M2-05	1/9/2012	X				X	0.2	4
18 - M2-06	1/6/2012	X				X	0.4	0.5
19 - M2-07	1/6/2012	X				X	0.4	1
20 - M2-08	1/6/2012	X				X	0.4	2
21 - M2-09	1/7/2012	X				X	0.4	3
22 - M2-10	1/7/2012	X				X	0.4	4

APPENDIX C: SAMPLE PREPARATION MANUAL

This guide for sample preparation was prepared courtesy of Ryan Brito. Unless otherwise notes, this was the procedure used to prepare samples.

Zirconium Hydride Sample Preparation

Instructions for preparing a zirconium sample for SEM imaging of hydrides formed in the alloy.

These instructions will instruct you how to cut, clean, mount, polish, and etch a zirconium sample to observe the formation of hydrides in the alloy. You must be properly trained to use the diamond saw and polisher before beginning. You should also be familiar with basic lab safety. You should review the MSDS sheets for the chemicals used and the PSA before starting.

Cutting the Sample

Safety

- Wear goggles when operating the diamond saw.
- Do not attempt to remove samples or diamond saw while the motor is running.
- Use the shield when operating the saw to block excess oil and sample debris.

Materials

- ☐ Sample
- ☐ Diamond Saw
- ☐ Oil
- ☐ Paper Towels

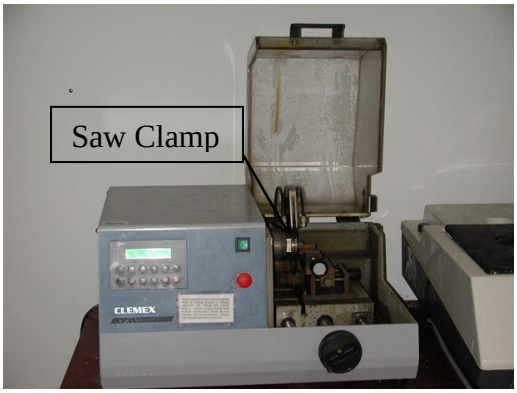

Recommended Settings

120 RPM

Procedure

1. Unscrew the saw clamp and insert the diamond saw between the pads.
2. Check that the oil level reaches the bottom of the blade. Oil must lubricate the blade to prevent heating during the cut.
3. Mount the sample in the holder at the desired cut length. Ensure the cut is close to the holder to prevent snapping the sample rather than cutting.
4. Turn the machine on and set to 120 RPM.
5. Lift the sample from the blade surface.
6. Turn on the motor and then place the sample on the blade. The weight of the holder will keep the sample in contact with the blade.
7. Close the shield during the cut.
8. When the cut is almost complete, lift the shield and remove the sample from the blade surface just before the cut is finished.
9. Turn off the machine, remove the sample and diamond blade from the motor, and clean the set-up.

Mounting the Sample

Safety

- Wear gloves and goggles throughout the procedure.
- Methanol and ethanol are volatile and flammable, so no open flames should be present. Consult MSDS Sheets for more safety information.

Materials

- ☐ Ethanol
- ☐ Methanol
- ☐ 2 Beakers
- ☐ Cut Sample
- ☐ Forceps
- ☐ Kim-Wipes
- ☐ Epoxy Resin
- ☐ Epoxy Hardener
- ☐ Scale
- ☐ 2 Styrofoam Cups
- ☐ Wooden Mixer
- ☐ Epoxy Mold
- ☐ Permanent Marker

Procedure

Cleaning the Sample

1. Pour a small amount of ethanol into a beaker and a small amount of methanol into the other beaker.
2. Using the forceps, place the sample in the ethanol. Leave immersed for approximately 30 seconds.
3. Remove the sample from the ethanol and allow to air dry.
4. Immerse the sample in the methanol using the forceps and leave for 30 seconds.
5. Remove the sample from the methanol and allow to air dry on a Kim-Wipe.

Preparing the Epoxy

6. Tare the scale with one of the Styrofoam cups.

   TIP: Mix epoxy with 5 parts resin to 1 part hardener by mass. To minimize chemical waste, calculate the amount needed before mixing.

7. Directly pour the desired mass of epoxy hardener into the Styrofoam cup.
8. Repeat steps 6 and 7 for the epoxy resin.
9. Slowing pour the epoxy resin from one Styrofoam cup down the wooden mixer into the cup with the epoxy hardener.
10. Mix the epoxy well for five minutes.

    TIP: To minimize the introduction of bubbles to the mixture, stir slowly and deliberately. Tilting the cup slightly helps but do not rotate the wooden mixer or vigorously scrape the sides of the Styrofoam cup.

11. Allow the epoxy to settle for a few minutes.

Mounting the Sample

12. Label each epoxy mold with the permanent marker to identify the samples being mounted.
13. Place the sample in the middle of the mold ensuring the cut side faces down and touches the bottom of the mold. Use a sample holder if necessary.
14. Slowly pour the epoxy down the wooden mixer into the mold. Do not move the sample or allow air bubbles to form around the sample.
15. Let the epoxy cure overnight.
16. Excess epoxy mix can be disposed of in the trash, but ethanol and methanol need to be disposed of in their respective waste containers. Clean the workspace as necessary.

Polishing the Sample

Materials

- ☐ Mounted Sample
- ☐ Grit Papers/Pads
- ☐ 6 µm Grit Paste
- ☐ 1 µm Grit Paste
- ☐ Green Lube
- ☐ Colloidal Silica Paste

Recommended Settings

RPM	150
Direction	Complimentary
Force	4 N
Stage RPM	150

Procedure

1. Turn on the polisher and use the settings above.
2. Wash off the stage to help to remove the grit papers.
3. Place the 180-grit paper on the stage and press out any air bubbles.
4. Wet the surface with water for lubrication.
5. Place mounted samples into the sample holder noting which sample is in which port.
6. Start the polisher and periodically check the samples stopping the polisher when the sample surface is exposed.
7. Repeat steps 3-6 for the 400, 800, and 1200-grit papers.

   TIP: Note the direction, density, and depth of the scratches for each paper. Only when the scratches are uniform on the sample can you move to the next highest grit paper. By the end of the 1200-grit paper, no scratches should be visible by eye.

8. Clean stage and holder with water to remove any particles from the grit papers or sample.
9. Place the 6 µm grit pad on the stage and lubricate with the 6 µm grit paste and green lube.
10. Turn off the water source for the polisher.
11. Polish the sample for 10 minutes lubricating the pad with paste and green lube every 2 minutes.
12. Repeat steps 8-11 for the 1 µm pad and paste and the 0.05 µm pad and colloidal silica.
13. Clean the stage, holder, and sample well after use.

Etching the Sample

Safety

- Hydrofluoric acid can cause severe burns that may not be immediately painful or apparent. Hydrofluoric acid penetrates the skin and decalcifies bones leading to death. Seek medical attention for any exposure. See the MSDS sheet for more information.
- Nitric acid can cause severe burns and irritate the eyes and respiratory system. See the MSDS sheet for more information
- Hydrogen peroxide is a very hazardous irritant. See the MSDS sheet for more information.
- The following safety measures must be taken to protect against the above chemicals:
    - All work handling the chemicals must be done within a fume hood.
    - Goggles, nitrile gloves, acid-resistant gloves, a face shield, lab coat, and full apron must be worn when handling the chemicals.
    - After handling the chemicals, the gloves must be washed before touching anything outside of the fume hood.

Materials

- ☐ Hydrogen Peroxide (30%)
- ☐ Nitric Acid (70%)
- ☐ Hydrofluoric Acid (49%)
- ☐ Cotton Balls
- ☐ Tongs
- ☐ Plastic Beaker
- ☐ Large Plastic Tub
- ☐ Tubing for Sink
- ☐ Methanol
- ☐ Ultrasonic Bath

Procedure

1. To make the etchant, add 25 mL of the hydrogen peroxide, 25 mL of the nitric acid, and 8 drops of hydrofluoric acid to the plastic beaker.
2. Attach the tubing to the faucet of the sink let it run continuously into the plastic tub.
3. Using the tongs, saturate the cotton ball in the etchant and rub over the sample for 10 seconds.
4. Immediately dunk the sample into the tub of water and leave submerged for several minutes.
5. Clean the fume hood and materials and dispose of the remaining etchant.
6. Clean the gloves and remove the samples from the tub.
7. Prepare an ultrasonic methanol bath.
8. Clean the samples by submerging in the methanol bath for several minutes.
9. Allow the samples to air dry.